**Universidade do Minho**
Escola de Medicina

Raquel Gonçalves Correia

# Role of Nucleus Accumbens Direct and Indirect Pathways in Anxiety- and Depressive-Like Behaviors

julho de 2020

Role of Nucleus Accumbens Direct and Indirect Pathways in Anxiety- and Depressive-Like Behaviors
Raquel Gonçalves Correia
UMinho | 2020

Universidade do Minho
Escola de Medicina

Raquel Gonçalves Correia

# Role of Nucleus Accumbens Direct and Indirect Pathways in Anxiety- and Depressive-Like Behaviors

Dissertação de Mestrado
Mestrado em Ciências da Saúde

Trabalho realizado sob a orientação de
**Doutora Carina Isabel Soares da Cunha**
e
**Doutora Ana João Gomes Rodrigues**

julho de 2020

## Agradecimentos

À Doutora Ana João Rodrigues, minha orientadora, pela oportunidade que me deu em desenvolver a minha tese de mestrado na sua equipa. Quero agradecer por toda a dedicação, por todo o conhecimento transmitido. Foi sem dúvida um ano cheio de aprendizagens em várias vertentes.

À Doutora Carina Cunha, minha coorientadora, por ter aceitado orientar-me durante este ano de tese, mesmo à distância de um oceano. Provaste-me que mesmo longe é possível acompanhar de perto todo o trabalho desenvolvido ao longo deste ano. Obrigada por todo o teu empenho e ajuda!

Às minhas colegas de equipa, Verónica e Bárbara, por todo o apoio que me deram no laboratório. O meu crescimento a nível profissional também se deve a vocês, sem dúvida alguma.

À Carolina, Sara, Rogério e Susana, por me terem acolhido em Braga e por serem a companhia de eleição para os momentos de descontração nos almoços, fins de tarde e até jantares, por mais que o tempo fosse escasso.

Ao Rogério e à Susana, por terem sido muitas vezes a minha companhia em trabalhos de bancada menos animadores. Obrigada por espalharem alegria e positivismo!

Um agradecimento especial à Susana por ter vivido tão intensamente comigo esta aventura de entregar uma tese em plena Pandemia.

À Patrícia, Inês e Maria que mesmo estando a quilómetros de distância, estiveram sempre perto! Não serão esquecidas as simples mensagens de apoio e comemorações de pequenas vitórias!

Aos meus pais por permitirem o meu crescimento a nível académico e por toda a paciência que tiveram comigo nos maiores momentos de stress.

À minha irmã Vera, por ouvir os meus desabafos intermináveis, mesmo que por vezes a disposição fosse pouca.

O trabalho apresentado nesta tese foi realizado no Instituto de Investigação em Ciências da Vida e Saúde (ICVS) da Universidade do Minho. Este trabalho foi financiado pela Fundação Bial 30/2016; e financiado pelo Fundo Europeu de Desenvolvimento Regional (FEDER), no âmbito dos projetos POCI-01-0145-FEDER-016428 (MEDPERSYST) e PTDC/MED-NEU/29071/2017 (REWSTRESS), através do COMPETE 2020 e pelos fundos nacionais, através da Fundação para a Ciência e Tecnologia (FCT) – projeto UIDB/50026/2020; e pelos projetos NORTE-01-0145-FEDER-000013 e NORTE-01-0145-FEDER-000023, suportados pelo Programa Operacional Regional do Norte Portugal (NORTE 2020), no âmbito do Acordo de Parceria PORTUGAL 2020; e Plataforma de Microscopia Científica do ICVS, membro da infraestrutura nacional *PPBI - Portuguese Platform of Bioimaging* (PPBI-POCI-01-0145-FEDER-022122); por fundos nacionais, através da Fundação para a Ciência e Tecnologia (FCT).

## STATEMENT OF INTEGRITY

I hereby declare having conducted this academic work with integrity. I confirm that I have not used plagiarism or any form of undue use of information or falsification of results along the process leading to its elaboration.

I further declare that I have fully acknowledged the Code of Ethical Conduct of the University of Minho.

## O papel das vias direta e indireta do núcleo accumbens em comportamentos do tipo ansioso e depressivo


### Resumo

Evidências sugerem que a ansiedade e depressão estão associadas a alterações no circuito de recompensa do cérebro. O núcleo accumbens (NAc) é um componente-chave deste circuito, sendo responsável pela motivação, reforço e recompensa. Aproximadamente 95% dos neurónios do NAc são neurónios espinhosos médios (MSNs), que expressam o recetor de dopamina D1 (D1-MSNs) ou o recetor de dopamina D2 (D2-MSNs). Os D1-MSNs projetam diretamente para a área tegmental ventral (VTA), formando a via direta do circuito de recompensa, enquanto a via indireta compreende D1- e D2-MSNs que projetam indiretamente para o VTA através do pálido ventral (VP). Notavelmente, pacientes com depressão e ansiedade apresentam uma disfunção robusta do NAc, no entanto, não é claro se essa disfunção é seletiva para as vias direta ou indireta, ou ambas.

Neste estudo, analisámos o papel dos D1- e D2-MSNs em comportamentos de *ansiedade e depressão*, manipulando optogeneticamente estes neurónios durante tarefas comportamentais. Além disso, realizámos gravações eletrofisiológicas *in vivo* combinadas com optogenética a fim de perceber o efeito funcional da ativação específica de D1- e D2-MSNs.

Os resultados mostram que a ativação optogenética de D1-MSNs para o VP modula a *ansiedade* e a *depressão*, uma vez que a sua ativação causou um fenótipo ansioso no teste de *light/dark box* e um fenótipo depressivo no *forced swim test* (FST). A ativação das projeções de D1-MSNs para o VTA parece causar um fenótipo ansioso medido no *light/dark box*, no entanto, não tem impacto no comportamento do tipo depressivo.

A ativação optogenética das projeções de D2-MSNs para o VP induz um fenótipo ansioso, medido pelo *elevated plus maze* (EPM) e *novelty suppressed feeding* (NSF); no entanto, não tem impacto no comportamento do tipo depressivo, medido pelo FST, *tail suspension test* (TST) e *sweet drive test* (SDT).

Os registos eletrofisiológicos revelaram uma diminuição geral da atividade neuronal no VP e VTA durante a estimulação dos terminais de D1- ou D2-MSNs.

Os nossos resultados sugerem um papel diferencial das vias direta e indireta no comportamento *ansioso* e *depressivo*, o que é de extrema importância para entender os mecanismos fisiopatológicos subjacentes a estes distúrbios. O nosso estudo destaca que são necessários mais estudos para aprofundar o conhecimento sobre a contribuição de D1- e D2-MSNs em fenótipos *ansiosos* e *depressivos*, que, a longo prazo, podem ser importantes para o desenvolvimento de abordagens terapêuticas mais direcionadas.



**Palavras-chave:** ansiedade, área ventral tegmental, depressão, núcleo accumbens, pálido ventral

## Role of Nucleus Accumbens Direct and Indirect Pathways in Anxiety- and Depressive-Like Behaviors


### Abstract

Increasing evidence suggests that mental disorders, like anxiety and depression, are associated with functional alterations in the brain reward circuit. The nucleus accumbens (NAc) is a core brain region of the reward circuit, and it is important for motivation, reinforcement, and reward. About 95% of NAc neurons are medium spiny neurons (MSNs), which express either dopamine receptor D1 (D1-MSNs) or dopamine receptor D2 (D2-MSNs). D1-MSNs project directly to the ventral tegmental area (VTA), forming the direct pathway of the reward circuit, while the indirect pathway comprises both D1- and D2-MSNs that project indirectly to the VTA through the ventral pallidum (VP). Remarkably, patients with depression and anxiety present robust NAc dysfunction; however, it is unclear if this impairment is selective for the direct or indirect pathways, or both.

In the present work, we studied the role of D1- and D2-MSNs in anxiety- and depressive-like behaviors, by optogenetically manipulating these neurons during behavioral tasks. Moreover, we performed *in vivo* electrophysiological recordings combined with optogenetics to understand the functional outcome of specific activation of D1- and D2-MSNs.

Our results show that optogenetic activation of D1-MSNs-to-VP modulates anxiety and depressive-like behaviors, since it triggered an anxious-phenotype in the light/dark box test, and a depressive-like phenotype in the forced swim test (FST). Similarly, activation of D1-MSNs-to-VTA neurons seems to cause an anxious-phenotype measured in the light/dark box; but it has no impact on depressive-like behavior.

Optogenetic activation of D2-MSNs-to-VP neurons induces an anxious-phenotype, measured by the elevated plus maze (EPM) and novelty suppressed feeding test (NSF); however, it has no impact on depressive-like behavior, measured by FST, tail suspension test (TST) and sweet drive test (SDT).

Electrophysiological recordings revealed a general decrease of the neuronal activity in the VP and VTA during stimulation of D1- and D2-MSN terminals.

Our results suggest a differential role of direct and indirect pathways in anxiety- and depressive-like behaviors. These results show that D1- and D2-MSNs play distinct roles in anxious and depressive phenotypes, which is of utmost importance to better understand the pathophysiological mechanisms underlying these disorders. Our study highlights that further studies are needed to deepen our knowledge on the contribution of D1- and D2-MSNs in anxious and depressive phenotypes, that in a long range can be important for the development of targeted therapeutic approaches.



**Keywords:** anxiety, depression, nucleus accumbens, ventral pallidum, ventral tegmental area

## Contents

## Abbreviations

A2A: adenosine 2A

AAV: adeno-associated virus

ACh: acetylcholine

ANOVA: analysis of variance

AP: anteroposterior

Amy: amygdala

bp: base pairs

BNST: bed nucleus of stria terminalis

ChR2: channelrhodopsin 2

CIN: cholinergic interneuron

CMS: chronic mild stress

CR: calretinin

CSDS: chronic social defeat stress

D1-MSN: medium spiny neuron expressing dopamine receptor D1

D2-MSN: medium spiny neuron expressing dopamine receptor D2

D1R (Drd1 or D1): dopamine receptor D1

D2R (Drd2 or D2): dopamine receptor D2

DA: dopamine

DBS: deep brain stimulation

DGAV: Direção-Geral de Alimentação e Veterinária

DIO: double-floxed inverted open reading frame

dlVP: dorsolateral ventral pallidum

DNA: deoxyribonucleic acid

DSM: Diagnostic and Statistical Manual of Mental Disorders

DV: dorsoventral

EPM: elevated plus maze

eYFP: enhanced yellow fluorescent protein

FBS: fetal bovine serum

FELASA: Federation for Laboratory Animal Science Associations

fMRI: functional magnetic resonance imaging

FS: fast-spiking interneuron

FST: forced swim test

GABA: gamma-aminobutyric acid

GFP: green fluorescent protein

Hippo: hippocampus

ICVS: Instituto de Investigação em Ciências da Vida e Saúde/Life and Health Sciences Research Institute

IF: immunofluorescence

LCN: lipocalin

LH: lateral hypothalamus

LHb: lateral habenula

LTS: low threshold spiking

MC4R: melanocortin 4 receptor

ML: mediolateral

mPFC: medial prefrontal cortex

MSN: GABAergic medium-sized densely spiny neuron

NAc: nucleus accumbens

NAcc: nucleus accumbens core

nAChR: nicotinic acetylcholine receptor

NAcmSh: nucleus accumbens medial shell

NAcs: nucleus accumbens shell

NOS: nitric oxide synthase

NPY: neuropeptide Y

NSF: novelty suppressed feeding

OF: open field

PBS: phosphate buffered saline

PBS-T: phosphate buffered saline with 0.3% triton x-100

pCIN: putative cholinergic interneuron

PCR: polymerase chain reaction

pDAergic: putative dopaminergic neuron

PFA: paraformaldehyde

PFC: prefrontal cortex

pFS: putative fast-spiking interneuron

pGABAergic: putative GABAergic neuron

pMSN: putative medium-sized densely spiny neuron

PV: parvalbumin

SDT: sweet drive test

SEM: standard error of the mean

SN: substantia nigra

SOM: somatostatin

SPT: sucrose preference test

TST: tail suspension test

vmVP: ventromedial ventral pallidum

VP: ventral pallidum

VTA: ventral tegmental area

YFP: yellow fluorescent protein

# Chapter 1 – Introduction

## 1. Introduction

Mental disorders affect around 971 million people worldwide[1]. According to the Diagnostic and Statistical Manual of Mental Disorders (DSM-5®) "A mental disorder is a syndrome characterized by clinically significant disturbance in an individual's cognition, emotion regulation, or behavior that reflects a dysfunction in the psychological, biological, or developmental processes underlying mental functioning. Mental disorders are usually associated with significant distress or disability in social, occupational, or other important activities..."[2].

Increasing evidence have shown that alterations in brain regions of the reward circuit are implicated in neuropsychiatric disorders such as depression and anxiety[3]. For example, deep brain stimulation (DBS) to the nucleus accumbens (NAc) of patients suffering from treatment-resistant depression causes antidepressant and anxiolytic effects[4]. Furthermore, depression is characterized by reduced responses to rewarding events[5] and exaggerated responses to aversive ones[6], thus hinting to a relevant role played by the reward circuit in the emergence of both depressive and anxiety symptoms.

In the following sections, we offer a simplified overview of the reward circuit. We will focus on the NAc inputs and outputs, particularly in medium spiny neurons (MSNs) expressing either dopamine receptor D1 (D1-MSNs) or dopamine receptor D2 (D2-MSNs). To finalize, we will summarize the findings about the role of NAc sub-circuits in depression and anxiety.

### 1.1. The brain reward circuit

The reward circuit is a complex network of brain regions and neurotransmitters that evolved to respond to natural rewards, such as sex and food, and that are evolutionarily essential for survival, reproduction, and health[7]. In a very simplistic manner, reward processing occurs through dopamine (DA) projections from the ventral tegmental area (VTA) to the NAc, amygdala, prefrontal cortex (PFC)[7,8], and hippocampus, though other brain regions are also involved[9,10] (**Figure 1**). DA projections from the VTA to NAc are often considered the core of the reward circuit[8] (**Figure 1**), being responsible for the perception and valuing of rewards and the initiation of their consumption, although these same regions also respond to aversive stimuli[11–13].

The dopamine system plays a major role in movement and mood, which are crucial to reward function and motivation[8,14]. VTA DA neurons present two different patterns of firing activity, which differently influences behaviors: while low-frequency tonic firing (or pacemaker activity) is associated with motivation[15,16], phasic firing of DA neurons mainly encodes reward prediction[17,18].

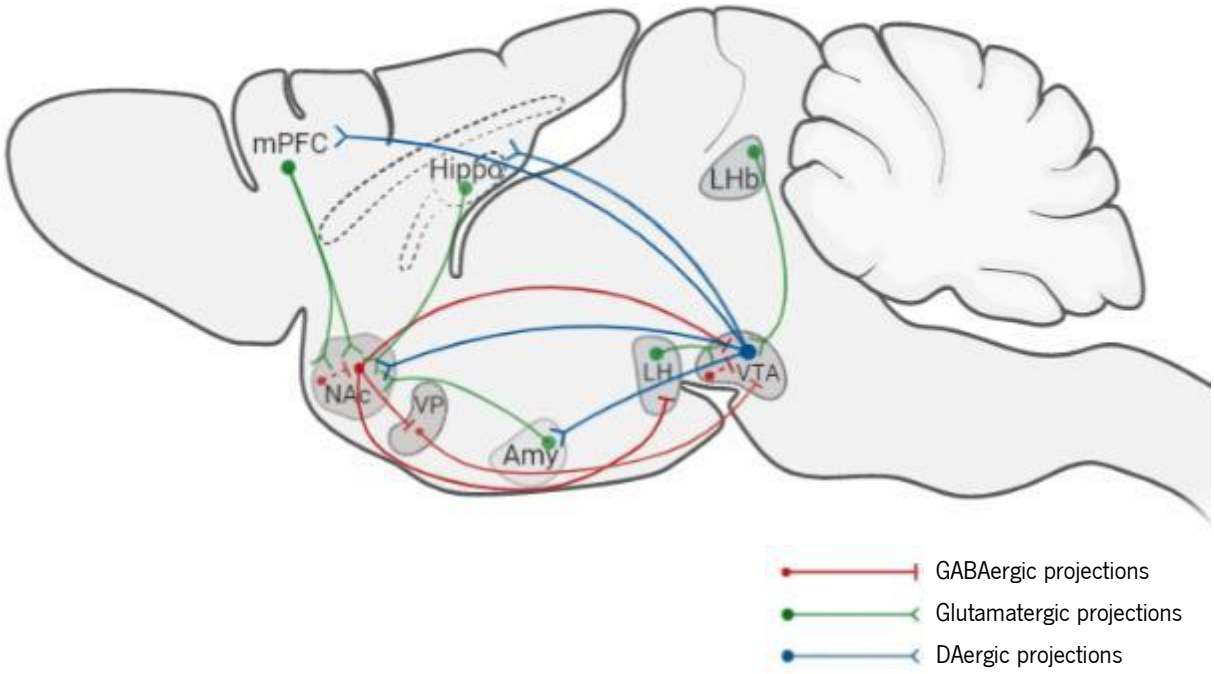


**Figure 1. The rodent brain reward circuit.** A simplified schematic of the major dopaminergic (in blue), glutamatergic (in green), and GABAergic (in red) projections of the reward circuit. Dopaminergic projections from the VTA to the NAc are the principal connections of the reward circuit. The NAc sends GABAergic projections to the VTA through D1-MSNs via the direct pathway, or through D1- and D2-MSNs that project to the VP via the indirect pathway. The NAc receives glutamatergic monosynaptic inputs from the mPFC, hippocampus, and amygdala, among other regions. The VTA receives glutamatergic inputs from the amygdala, lateral habenula, and lateral hypothalamus, among others. (The scheme was adapted from Russo and Nestler, 2013[10]).

*GABA: gamma-aminobutyric acid; VTA: ventral tegmental area; NAc: nucleus accumbens; D1-MSNs: medium spiny neurons expressing dopamine receptor D1; D2-MSNs: medium spiny neurons expressing dopamine receptor D2; VP: ventral pallidum; mPFC: medial prefrontal cortex; Hippo: hippocampus; Amy: amygdala; LHb: lateral habenula; LH: lateral hypothalamus.*

## 1.2. The ventral striatum – nucleus accumbens (NAc)

### 1.2.1. Neuroanatomy

The NAc is part of the basal ganglia and is sub-divided into core (NAcc) and shell (NAcs)[19,20] sub-regions. These two compartments can be discerned by various histochemical, electrophysiological, connectional, and cellular criteria[21]. On the molecular level, calbindin[19,22,23], enkephalin[24] and $GABA_A$ receptors[25] are preferentially located at the NAcc, while substance P[23], calretinin[23], DA[26], serotonin[26] and serotonin receptors[27] are preferentially located at the NAcs. Besides that, the levels of Fos-like immunoreactivity in response to antipsychotics such as haloperidol and clozapine are increased in the NAcs, suggesting this subregion as a potential target site for antipsychotic drug action[28–32].

The NAc is involved in motor, emotional and motivational processes[33] and its subdivisions can exert opposing effects on motivated behaviors[34]. The NAcc seems to play a crucial role in spatial learning[35], responses to motivational stimuli[36,37], conditioned responses[38–40] and impulsive choices[41]. On the other hand, the NAcs is thought to mediate the reinforcing properties of novelty[36], rewarding substances[42], drug relapse[43,44] and feeding behavior[45].

The NAc receives excitatory (glutamatergic) projections from prelimbic and infralimbic cortices (and others)[10,46–48], as well as amygdala, hippocampus[10,49], thalamus[47], and VTA[50] which form interconnections with each other (**Figure 1**). The rostral half of the NAc receives inputs from the prelimbic area, whereas the caudal half of the NAc receives inputs from the frontal cortical area[51]. Entorhinal and perirhinal cortices project to the ventral part of the NAc[51]. NAcc and NAcs receive inputs from different areas. For example, dorsal peduncular and infralimbic cortex project to the medial shell, whereas the dorsal prelimbic, anterior cingulate and perirhinal project to the core[52]. Additionally, the NAc also receives GABAergic and cholinergic projections from local axon collaterals and striatal interneurons[53,54].

The NAc exerts its function, mainly through GABAergic projections to VTA and VP[34,55–58], although it also projects to other brain regions such as the amygdala, bed nucleus of stria terminalis, sublenticular substantia innominata, lateral hypothalamus, thalamus and globus pallidus[59–62] (**Figure 1**). Although both NAc sub-divisions possess the same cellular composition, their output patterns are different.

NAc neurons that project to the VTA preferentially target GABAergic interneurons[63], which leads to lateral disinhibition of VTA DA neurons[34,64,65]. Specifically, NAc medial shell innervates GABAergic and dopaminergic neurons of the medial VTA, while NAc lateral shell innervates GABAergic neurons of the lateral VTA[34] (**Figure 2a**).

NAcc neurons project preferentially to the dorsolateral VP (dlVP), while NAcs neurons project to the ventromedial VP (vmVP)[55–57] (**Figure 2b**). NAc GABAergic neurons also project to GABAergic VP neurons, which will send GABAergic signals to downstream targets, namely DA neurons of the VTA[66–70]. VP GABAergic neurons, along with NAc afferents are implicated in discriminating stimulus conditions of reward, consumption, working memory, and mediation of reward-motivated behaviors[71].

### 1.2.2. NAc neuronal subtypes

About 95% of NAc neurons are GABAergic medium spiny neurons (MSNs)[72] (**Figure 1**). MSNs are constituted by two neuronal subpopulations that express different dopamine receptors[72], and regulate motivated behaviors[10,73,74]. MSNs that express dopamine receptor D1 (D1-MSNs), substance P and dynorphin, project to VP and VTA, while MSNs that express dopamine receptor D2 (D2-MSNs), adenosine 2A (A2A) receptor and enkephalin project exclusively to VP[56] (**Figure 2**). D1-MSNs that project directly from the NAc to the VTA form the direct pathway (**Figure 2a**), while the indirect pathway comprises both D1- and D2-MSNs that project to the VP[56,64,75,76] (**Figure 2b**). Interestingly, D1-MSNs that project to VP seem to originate from D1-MSN-VTA projecting neurons since the majority of D1-MSNs collateralize between these two brain regions[73].

The remaining 5% of NAc neurons are interneurons[77] that play a crucial role in controlling MSN excitability, affecting behavior outcome[78–82].

The most abundant interneurons are GABAergic in nature (3-4%) that are divided into two major populations[80]: neuropeptide Y (NPY)-, somatostatin (SOM)-, and nitric oxide synthase (NOS)-containing interneurons, known as low threshold spiking (LTS) interneurons[83,84]; and parvalbumin-containing (PV) interneurons, also known as fast-spiking (FS) interneurons[85]. Other subtypes of interneurons have been discovered in the dorsal striatum[79]; however, their presence in the NAc remains unclear. Despite the division of GABAergic interneurons in different populations, their principal role consists in monosynaptic inhibition of MSNs through feedforward inhibition[86–88].

Another type of interneurons are the cholinergic interneurons (CIN) (0.5-1%)[89] that are involved in the modulation of the direct and indirect pathways[90,91]. Activation or inhibition of these interneurons leads to a decrease or increase of the electrophysiological activity of MSNs, respectively[90]. Specific stimulation of CINs causes dopamine release in a β2 nicotinic acetylcholine (ACh) receptor (nAChR)-dependent manner[92]. Also, CINs receive inhibitory GABAergic inputs from MSNs and dopaminergic inputs from the VTA[93]. *In vivo*, CINs are tonically active and their activity is paused when animals are exposed to a conditioning stimulus[90].

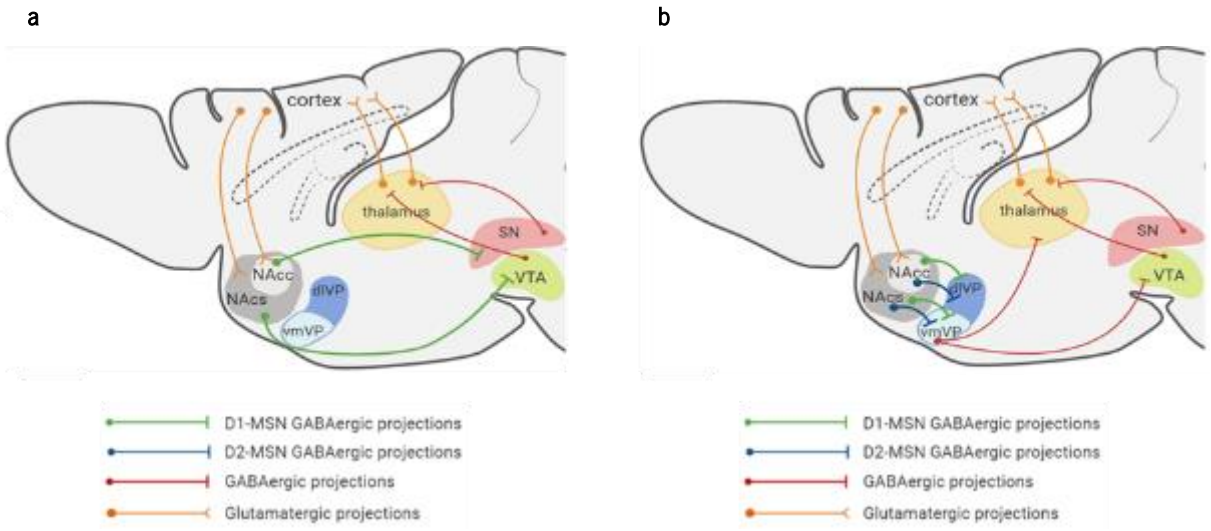


**Figure 2. The direct and indirect pathways of the reward circuit. (a)** In the ventral striatum, the direct pathway comprises NAc projections to the SN/VTA and from there to the mediodorsal thalamus. The direct NAc innervation of the SN/VTA is exclusively mediated by D1-MSNs. **(b)** The indirect pathway projects to the VP before reaching the output nuclei. The NAcc projects to the dlVP and the NAcs projects to the vmVP. The dlVP projects to the SN, whereas the vmVP projects to VTA. Both D1- and D2-MSNs compose the indirect pathway. (The scheme was adapted from Soares-Cunha *et al.*, 2016[94]).
*NAc: nucleus accumbens; SN: substantia nigra; VTA: ventral tegmental area; D1-MSNs: medium spiny neurons containing dopamine receptor D1; VP: ventral pallidum; NAcc: NAc core; dlVP: dorsolateral VP; NAcs: NAc shell; vmVP: ventromedial VP; D2-MSNs: medium spiny neurons containing dopamine receptor D2.*

### 1.3. Role of D1- and D2-MSNs in reward and aversion

Several studies have suggested opposing roles for the direct and indirect pathways of the basal ganglia[95–97]. It has been proposed that the direct pathway mediates positive reinforcement and reward while the indirect pathway mediates transient punishment and aversion[96]. Canonically, D1-MSNs have been described as the ones responsible for positive rewarding events, and D2-MSNs as those responsible for the mediation of aversion[97], however recent data questions this dichotomy[64,74,98]. A study from our team in which optogenetic strategies have been applied to specifically modulate MSN activity has shown that activation of D1-MSNs has a pro-rewarding role since it is sufficient to enhance the motivation to work for food[99]. Other studies indicate that activation of NAc D1-MSNs is sufficient to increase cocaine sensitization and cocaine place preference[100], and inhibition of these neurons suppresses cocaine sensitization[101].

Regarding D2-MSNs, the data available is less concordant to what concerns the role of this MSN subtype in reward and aversion. Lobo and colleagues showed that optogenetic stimulation of NAc D2-MSNs diminished cocaine conditioned place preference[100], suggesting that it could have an aversive role. However, this evidence was contested by a study of Song and colleagues showing that neither acquisition nor expression of cocaine-induced behavioral sensitization was affected by D2-MSNs activation[102]. Moreover, recent studies from our group have shown that optogenetic activation of D2-MSNs during reward-predicting cues strongly increases motivation to work for food[99,103]. In addition, we also showed that both D1- and D2-MSNs can drive reward and aversion, depending on their stimulation pattern[74]. In fact, brief optogenetic stimulation of both MSN subtypes induced positive reinforcement, while prolonged stimulation induced aversion. Furthermore, brief stimulation was associated with increased VTA dopaminergic tone either directly or indirectly via VP[74]. This evidence is in agreement with another study that showed that both D1- and D2-MSN signaling are required in the reinforcing properties of optogenetic activation of VTA-NAc dopaminergic terminals[104]. Finally, others have shown that accumbal D1- and D2-MSN optical activation supports self-stimulation[105].

The fact that the role of NAc MSNs in aversion is less explored than in reward may be because these types of events induce a negative hedonic state that is difficult to evaluate in animals. Thus, avoidance behavior, a core symptom of anxiety, is commonly used as representation of aversion[96].

Studies using avoidance tasks have shown a decrease in the number of conditioning avoidance responses caused by infusions of D1R and D2R antagonists into the NAc[106,107]. These effects could be explained by the contribution of these receptors in early consolidation of aversive memory[108]. Other studies showed positive responses to aversive stimuli of D1- and D2-MSNs within the striatum[109,110]. D1 receptor blockade decreased the expression of conditioned aversive stimuli, suggesting that activation of D1

receptors might contribute to the strengthen of a taste aversive association[109]. Moreover, inactivation of post-synaptic D2 receptors controls aversive learning[110]. Furthermore, our recent published study showed that prolonged stimulation of both D1- and D2-MSNs induces aversion in conditioned place preference and real time place preference tasks[74]. Also, optical stimulation of D2-MSNs was shown to decrease cocaine-conditioning effects[74,100].

### 1.4. Role of D1- and D2-MSNs and downstream targets in depression

Depressive disorders affect around 264 million people worldwide[1]. The Diagnostic and Statistical Manual of Mental Disorders lists a cluster of nine variable symptoms for depression[111]. Anhedonia ("loss of ability to experience pleasure from normally rewarding stimuli, such as food, sex and social interactions"[10]), psychomotor impairment, sleep impairment, loss of appetite, loss of weight, and retraction from social interaction are some of the symptoms that can be evaluated in rodents[111]. Rodent depression models that are based on exposure to stress are fundamental in the study of depressive-like phenotypes. The chronic social defeat stress (CSDS) and chronic mild stress (CMS) are the most used models to induce depressive-like behaviors in rodents[10,112]. Mice exposed to CSDS develop social avoidance, anhedonia, metabolic syndrome, and anxiety-like behaviors, whereas mice exposed to CMS develop anhedonia, deficits in grooming, and compromised immune function[10].

Given that there is no specificity in the symptoms for depression, different circuits or components of a particular circuit may regulate discrete depressive-like phenotypes[113,114]. Since anhedonia, assessed as a lack of pleasure, loss of appetite and motivation towards everyday positive rewards are common symptoms of depression, it is not surprising that the deregulation of the reward circuit has been shown to be implicated in the mediation of depressive-like behaviors[3,5,114–117].

The NAc also demonstrates a critical role in depression symptomatology such as anhedonia and loss of motivation towards natural rewards[10,115,116,118]. For example, in humans suffering from depression, deep brain stimulation (DBS) of this brain region leads to a relief of anhedonic symptoms[4,119,120]. Also, patients with major depression reveal a higher availability of D2/3 receptor in the ventral striatum[121]. Human depressive patients exhibit reduced activity and volume of the NAc[122], which was also confirmed in a study using mice[123]. Furthermore, Lim and co-workers showed, in a study using chronic restraint stress, that activation of melanocortin 4 receptors (MC4Rs) decreases the strength of excitatory synapses on D1-MSNs, and that blocking MC4Rs prevents stress-induced anhedonia. Thus, these anhedonic outcomes might be mediated by specific change in excitatory synaptic transmission onto D1-MSNs[118].

Optogenetic manipulation of NAc MSNs in animals exposed to social stress shows an opposing role of MSN subtypes in depressive-like behaviors[124,125]. Indeed, stimulation of D1-MSNs leads to a decrease of depressive-like phenotype while stimulation of D2-MSNs leads to an increase of depressive-like phenotype[124,125]. A recent study that comes in line with these findings, identified the activity of D1-MSNs as a predictive marker of depression susceptibility since, before stress induction, D1-MSN activity and calcium transients increased during social interaction[126]. Although D1- and D2-MSNs play different roles, there are similarities between the anatomical projections of these neurons[64,76]. Therefore, the cell type differences are prevenient from efferent circuit disparities[113].

Optogenetic manipulations of the VTA dopaminergic neurons result in distinct alterations in depressive-like behaviors, depending on the type of stress protocol used. While phasic activation of VTA DA neurons in animals exposed to social defeat stress causes an increase in the depressive-like phenotype[117], phasic activation of the same neurons in animals exposed to CMS leads to a reduction in the depressive-like phenotype[114], thus demonstrating that distinct depression models might result in opposing VTA functional impairments.

The VP is also involved in depression. A study of Knowland and colleagues[76] showed that increased activity of VP PV neurons is a hallmark of depressive-like behavior. VP PV neurons that project to the VTA convey exclusively inhibitory signals to GABAergic neurons and mostly excitatory inputs to DAergic neurons, and in susceptible animals, encode for social avoidance. This symptom can be reversed by optogenetically silencing these neurons. This suggests a selectively stronger synaptic connection between VP PV neurons and VTA neurons in susceptible animals. In fact, VP PV neurons that project to the VTA receive increased excitatory inputs. In addition, one may also consider that VP GABAergic innervation of the VTA GABAergic neurons may be increased in susceptible animals, leading to disinhibition of VTA DA neurons, which comes in line with the described hyperactivity of VTA DA neurons in some animal models of depression[117,127].

These data suggest that distinct circuits involving the NAc, VP, and VTA can mediate different facets of depressive-like behavior and can display distinct cellular adaptations as well[113]. Thus, it remains unclear if NAc D1-MSNs-to-VTA neurons or NAc D1-MSNs-to-VP and D2-MSNs-to-VP neurons are selectively necessary to produce depressive phenotypes, or if synchronization between the neuronal activity of these two downstream areas is necessary[113].

### 1.5. Role of D1- and D2-MSNs and downstream targets in anxiety

Anxiety disorders affect around 284 million people worldwide[1]. Anxiety is a psychological state that, in some circumstances, can be beneficial[128]. Daily stressful events can induce anxiety-like behaviors[129,130]. It is important to refer that anxiety produces behavioral responses such as increased vigilance, freezing, hypoactivity and suppressed food consumption. In rodents, anxiety-like behaviors are characterized as those elicited by aversive stimuli[131]. Thus, avoidance is a core feature of anxiety[132,133]. Dopamine levels are altered upon prolonged exposure to stress, and it has been show that these are highly correlated with this disorder[128,134–137]. Indeed, animals exposed to CMS develop anxiety-like phenotype[112] and display a decrease in VTA dopamine neuronal activity[68]. Furthermore, several brain regions such as the bed nucleus of stria terminalis (BNST)[138–142], hippocampus[143], amygdala[143], PFC[143,144], NAc[133,144–146], VP[68,147], and VTA[68] are involved in anxiety[141,148], which is indicative of a close relation between the reward circuit and anxiety[68,146].

Although quite different, anxiety and depression exhibit a high level of comorbidity[149]. Indeed, patients with major depression reveal a higher availability of D2/3 receptor in the ventral striatum which is associated with comorbid anxiety symptoms[121].

NAcc DBS with high-frequency stimulation is capable of reducing anxiety levels in naïve rats[144]. Accordingly, studies in humans using NAc DBS show amelioration of anxiety symptoms[4,120]. Furthermore, a functional magnetic resonance imaging (fMRI) study highlighted a role for the NAc in avoidance and anxiety behaviors[133]. In fact, active avoidance leads to increased activation of the NAc that was associated with high levels of anxiety. On the other hand, passive avoidance leads to decreased activity of this brain region, but the anxiety levels remained high. Another study in humans suffering from social anxiety disorder demonstrated a reduced neuronal activity in the ventral striatum, measured in the fMRI[150].

Several studies have shown larger NAc volume in patients suffering from anxiety[151,152], and more recently, a study showed that NAc volume may be a predictor for anxiety improvement using cognitive-behavioral therapy and selective serotonin reuptake inhibitor treatment[153].

Pharmacological studies have shown the involvement of the VP in anxiety-like behavior[147,154,155]. For example, microinjection of neurotensin[155] and substance P[147,154] in the VP revealed an anxiolytic effect. Also, a study in monkeys showed that the VP plays a central role in controlling aversive behaviors during delayed response tasks, being related to anxiety[156].

VTA also plays a role in anxiety-like behavior. A pharmacological study showed an increase in anxiety-like behavior when rats receive VTA infusion of an acetylcholinesterase inhibitor or muscarinic receptor agonist[157], pinpointing a novel role for VTA cholinergic neurons in mediating responses to stress and anxiety. Moreover, optogenetic activation of VTA GABAergic neurons was found to induce anxiety-like

behavior[158], suggesting that over-excitation of GABAergic VTA neurons may underlie diseases related to anxiety. Also, a human study suggested a critical role for VTA in anxiety disorders. In a fear generalization task, that involves the presentation of a conditioned stimulus or generalization stimuli, fMRI revealed that patients with generalized anxiety disorder showed increased and less discriminating VTA reactivity to generalization stimuli, a symptom that was positively associated with trait anxiety[159].

Despite the increasing evidence of the involvement of several neuronal circuits in anxiety disorders[141,148], the involvement of brain regions of the reward circuit, and in particular the role of the direct and indirect pathways of the basal ganglia, remains poorly understood.

# Chapter 2 – Objectives

## 2. Objectives

In this dissertation we intended to dissect the role of NAc-to-VP and NAc-to-VTA inputs in anxiety- and depressive-like symptoms.

The main objectives of the present dissertation were:

1) Assess the role of D1- and D2-MSNs in anxiety- and depressive-like behaviors using optogenetic manipulation during behavioral tasks;

2) Test the functional outcome of specific activation of D1- and D2-MSNs in VP and VTA using *in vivo* electrophysiological recordings combined with optogenetics.

# Chapter 3 – Materials and Methods

## 3. Materials and Methods

### 3.1. Animals

One D1-cre (line EY262, Gensat.org) or D2-cre (line ER44, Gensat.org) heterozygous transgenic male mouse was mated with two wild-type C57/Bl6 females with 8 weeks of age (**Figure 3a**). Progeny were separated according to transgenic line and gender, and were housed in groups of a maximum of 6 animals per cage, according to the type of the homecage used (type 2L).

All animals were maintained under standard laboratory conditions (12h light/dark cycle with lights on at 08:00h, ambient temperature of 22°C ± 1°C and 60% relative humidity) with standard diet and water *ad libitum*). All behavioral experiments were performed during the light period of the light/dark cycle.

Health monitoring was performed according to FELASA guidelines. All procedures were conducted according to European Union Regulations (Directive 2010/63/EU). Animal facilities and experimenters were certified by the Portuguese regulatory entity, Direção-Geral de Alimentação e Veterinária (DGAV). All protocols were approved by the Ethics Committee of the Life and Health Sciences Research Institute and by DGAV (protocol #19074, dated of 30/08/2016).

### 3.2. Genotyping

Male progeny produced were genotyped at post-natal day 21, by PCR. DNA was isolated from tail biopsy using Citogene DNA isolation kit (Citomed, Lisbon, Portugal). In a single PCR genotyping tube, the primers Drd1a F1 (5'-GCTATGGAGATGCTCCTGATGGAA-3') and CreGS R1 (5'-CGGCAAACGGACAGAAGCATT-3') were used to amplify the D1-cre transgene (340 bp), and the primers Drd2 (32108) F1 (5'-GTGCGTCAGCATTTGGAGCAA-3') and CreGS R1 (5'-CGGCAAACGGACAGAAGCATT-3') were used to amplify the D2-cre transgene (700 bp). An internal control gene (lipocalin, 500 bp) was used in the PCR (LCN_1 (5'- GTC CTT CTC ACT TTG ACA GAA GTC AGG -3') and LCN_2 (5'- CAC ATC TCA TGC TGC TCA GAT AGC CAC -3')). Heterozygous mice were differentiated from the wild-type mice by the presence of two amplified DNA products corresponding to the internal control gene and the transgene. Gels were visualized with GEL DOC EZ imager (Bio-Rad, Hercules, CA, USA) and analyzed with the Image Lab 4.1 (Bio-Rad, Hercules, CA, USA).

### 3.3. Constructs, virus injection, and cannula implantation for optogenetic manipulation

Cre-inducible AAV5/EF1a-DIO-hChR2(H134R)-eYFP and AAV5/EF1a-DIO-eYFP viruses were obtained directly from the UNC Gene Therapy Center (University of North Carolina, NC, USA) (**Figure 3b**). AAV5 vectors titers were 3.7–6 × $10^{12}$ viral molecules/ml as determined by dot blot.

D1-cre (line EY262, Gensat.org) and D2-cre (line ER44, Gensat.org) heterozygous transgenic male mice with 8 weeks of age were submitted to stereotaxic surgeries. Mice were anesthetized with 75 mg $kg^{-1}$ ketamine (Imalgene, Merial, Lyon, France) plus 1 mg $kg^{-1}$ medetomidine (Dorbene, Cymedica, Horovice, Czech Republic). 500nl of the specific virus used for optogenetic excitation (ChR2) or as control (YFP) was unilaterally injected in the NAc of D1- and D2-cre mice (stereotaxic coordinates from bregma[160]: +1.3mm anteroposterior (AP), +0.9mm mediolateral (ML), and -4.0mm dorsoventral (DV)) using an 30-gauge needle Hamilton syringe (Hamilton Company, Reno, NV, USA), at a rate of 100nl $min^{-1}$. After injection, the syringe was left in place for 5 minutes to allow diffusion (**Figure 3c**, **d** and **e**). An optic fiber (200μm core fiber optic; Thorlabs, Newton, NJ, USA) with 2.5 mm stainless steel ferrule (Thorlabs, Newton, NJ, USA) was implanted in the VP (for D1- and D2-cre mice (**Figure 4a** and **b**); stereotaxic coordinates from bregma[160]: -0.1mm AP, +1.6mm ML, -3.9mm DV) or in the VTA (for D1-cre mice (**Figure 4c**); stereotaxic coordinates from bregma[160]: -3.2mm AP, +0.5mm ML, -4.5mm DV) and was secured to the skull with dental cement (C&B kit, Sun Medical, Shiga, Japan). Animals were removed from the stereotaxic frame, sutured, given an anesthetic reversal – 1mg $kg^{-1}$ atipamezole (Antisedan) and let to recover for three weeks before initiation of the behavioral procedures. All animals were treated 30 minutes before surgery and 6 hours after surgery with an analgesic – 0.05 mg $kg^{-1}$ buprenorphine (Bupaq, Richter Pharma, Wels, Austria). The same treatment was performed once a day for three consecutive days after surgery. If animals displayed severe loss of body weight a multivitamin supplement would also be administered.

Optogenetic manipulation was performed using 5mW of blue light generated by a 473 nm DPSS laser (CNI Laser, Changchun, China) delivered to mice through fiberoptic patch cords (0.22 NA, 200 μm diameter; Thorlabs, Newton, NJ, USA) that were attached to the implanted ferrule. Laser output and pulsed light were controlled by a pulse generator (Master-8; AMPI, New Ulm, MN, USA). The stimulation was performed for 3 minutes, with 25 ms pulses at 20 Hz.

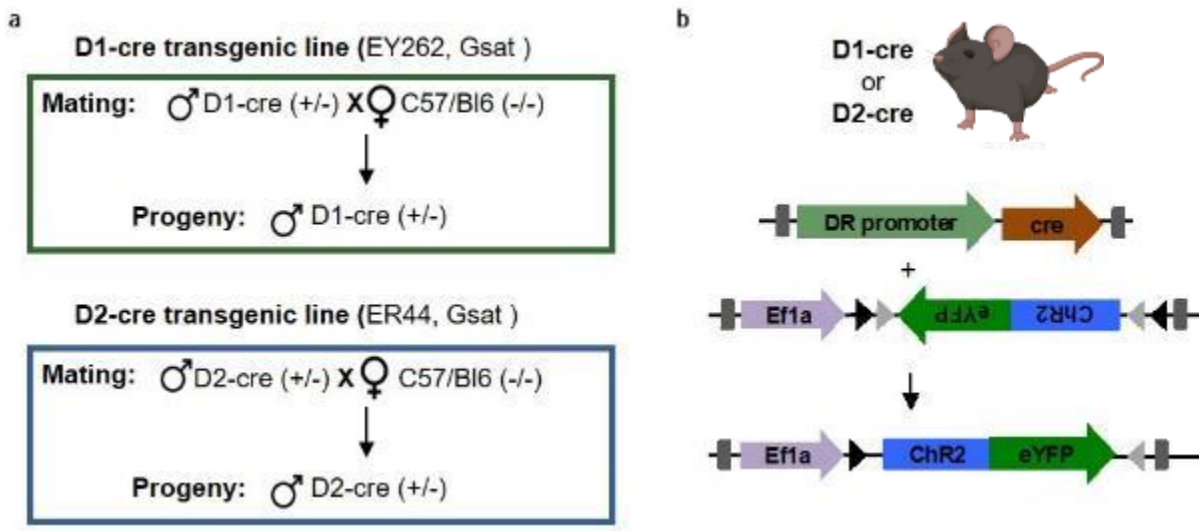


**Figure 3. Colony management.** (**a**) Generation of specific D1- and D2-cre transgenic lines. D1-cre heterozygous (+/-) transgenic male mice (EY262, Gensat) or D2-cre heterozygous (+/-) transgenic male mice (ER44, Gensat) were mated with wild-type (-/-) C57BL/6J female mice. The progeny was genotyped and heterozygous D1-cre and D2-cre transgenic male mice were used. (**b**) Strategy used for optogenetic activation of D1- and D2-MSNs in the VP or VTA of D1- or D2-cre mice. An adeno-associated virus (AAV5) carrying a plasmid construct with cre-dependent expression of channelrhodopsin (ChR2) in fusion with yellow fluorescent protein (YFP) was injected in the NAc of D1- and D2-cre mice.

## 3.4. Behavioral Assessment

### 3.4.1. Subjects

Transgenic male mice with two to four months of age at the start of the experiment were arbitrarily divided into different groups depending on the transgenic line: D1-VP-ChR2 (n = 8); D1-VP-YFP (n = 8); D1-VTA-ChR2 (n = 7); D1-VTA-YFP (n = 8); D2-VP-ChR2 (n = 10); D2-VP-YFP (n = 9). All behavioral tests were performed blindly. Mice were transferred to the testing rooms 30 minutes before the beginning of each test to allow acclimation.

### 3.4.2. Elevated Plus Maze

The Elevated Plus Maze test (EPM) was performed in accordance to a protocol described by Felix-Ortiz *et al*[61]. The EPM apparatus consisted in a black acrylic plus-shaped platform with two open arms (50.8 x 10.2 cm) and two enclosed arms (50.8 x 10.2 x 40.6 cm) elevated 72.4 cm from the floor (Med Associates Inc., St. Albans, VT, USA).

Individual mice were attached to the fiberoptic patch cable and placed longitudinally in the central platform of the EPM, always facing the same corner. Each session had a duration of 9 minutes, divided in three alternating 3-minute epochs: without laser stimulation, with laser stimulation, and without stimulation (OFF-ON-OFF) (**Figure 5a**). All sessions were recorded by a video camera for posterior analysis.

### 3.4.3. Open Field

The Open Field test (OF) was performed in accordance to a protocol described by Felix-Ortiz *et al*[61]. The open field arena consisted of a square white floor (43.2 cm x 43.2 cm) with four transparent acrylic walls (Med Associates Inc., St. Albans, VT, USA).

Individually mice were attached to the fiberoptic patch cable and placed in the center of the arena, always facing the same wall. Each session had a duration of 15 minutes, divided in three alternating 5-minute epochs: OFF-ON-OFF (**Figure 6a**). Distance traveled, ambulatory time, number of entries and time spent in each zone were measured using an automated video-tracking system (Activity Monitor software; Med Associates Inc., St Albans, VT, USA).

### 3.4.4. Light/Dark Box

The Light/Dark Box test was performed in accordance to a protocol described by Crawley *et al*[62], and Kim *et al*[39]. The Light/Dark Box apparatus consisted of an arena similar to that one used in the open field test (43.2 cm x 43.2 cm), divided half-dark and half-light using an acrylic chamber (Med Associates Inc., St. Albans, VT, USA).

Individual mice were attached to the fiberoptic patch cable and placed in the dark compartment. Each session had a duration of 15 minutes, divided in three alternating 5-minute epochs: OFF-ON-OFF (**Figure 7a**). Distance traveled, ambulatory time, number of entries and time spent in each zone were measured using an automated video-tracking system (Activity Monitor software; Med Associates Inc., St Albans, VT, USA).

### 3.4.5. Novelty Suppressed Feeding

The Novelty Suppressed Feeding test (NSF) was performed in accordance to a protocol described by Felix-Ortiz *et al*[61]. The apparatus used for the test was similar to the open field arena with the floor covered with clean corn cob bedding. One familiar food pellet (Mucedola 4RF21-GLP) weighing approximately 6 g was placed on the center of the arena.

After 18 hours of food deprivation with water *ad* libitum, individual mice were attached to the fiberoptic patch cable and placed in one corner of the arena. The latency to reach the food pellet as well as the latency to begin a feeding episode was manually recorded. The task ended when the mice first fed or after 10 min without consuming the food pellet (**Figure 8a**). Immediately after testing, mice were removed from the arena and placed into their homecage to measure food consumption. Pre-weighted food was placed on the floor of the homecage and was weighted 5, 10 and 30 min after the animal was placed in

the homecage. The task was repeated twice on different days for each mouse, counterbalanced for laser stimulation session (ON) or no stimulation session (OFF). In the session with laser stimulation, the stimulation was performed for all the period until the animal first fed, with 25 ms pulses at 20 Hz.

### 3.4.6. Forced Swim Test

The Forced Swim Test (FST) was performed in accordance to a protocol described by Can *et al*[63]. The apparatus consisted of a transparent cylindrical tank (50 cm height x 20 cm diameters) filled with warm water (23 – 25 °C) 15 cm from the bottom so the mice are not able to reach the bottom of the tank.

Individual mice were attached to the fiberoptic patch cable and carefully placed in the water. Each session had a duration of 9 minutes, divided in three alternating 3-minute epochs: OFF-ON-OFF (**Figure 9a**). All sessions were recorded by a video camera for posterior analysis.

### 3.4.7. Tail Suspension Test

The Tail Suspension Test (TST) was performed in accordance to a protocol described by Tye *et al*[14]. Individual mice were attached to the fiberoptic patch cable and its tail was secured by one strip of duct tape 2 cm from the base of the tail, so the mice are not able to climb during the test. Each session had a duration of 9 minutes, divided in three alternating 3-minute epochs: OFF-ON-OFF (**Figure 10a**). All sessions were recorded by a video camera for posterior analysis.

### 3.4.8. Sweet Drive Test

The Sweet Drive Test (SDT) was performed in accordance to a protocol described by Mateus-Pinheiro *et al*[64]*.* The SDT apparatus consisted in a black acrylic enclosed arena (82 x 44 x 30 cm) divided by transparent walls that defined 3 separated compartments: a middle chamber (20 x 44 x 30 cm), a right chamber and a left chamber (31 x 44 x 30 cm).

Mice were pre-habituated to sweet pellets (Cheerios®, Nestlé) in two different days, 2 weeks before the test. Mice were habituated to the SDT apparatus one day before the first trial for 5 minutes.

After 18 hours of food deprivation with water *ad libitum*, individual mice were attached to the fiberoptic patch cable and placed in the middle chamber of the arena. One familiar food pellet (Mucedola 4RF21-GLP) weighing approximately 6 g was placed on the corner of the right chamber, and five Cheerios® weighing approximately 1 g were placed on the corner of the left chamber (**Figure 11a**). Immediately after testing, the food pellet and the Cheerios® were weighed to determine the food consumption and

preference for sweet pellets. Each session had a duration of 8 minutes. The task was repeated twice on different days for each mouse, counterbalanced for laser stimulation (ON) or no stimulation (OFF). The laser stimulation was performed each time the mouse went to the right chamber.

### 3.5. *In vivo* single cell electrophysiology recordings

In order to reduce the generation of new animals for this experiment, transgenic male and female mice, used in a previous study of our group, with approximately 12 months age were used for the *in vivo* electrophysiological recordings. At 8 weeks of age mice were submitted to stereotaxic surgeries as described in section 3.3 but with no cannula implantation.

Mice were anesthetized with 1.75 g $kg^{-1}$ of urethane (Sigma now Merck KGaA, Darmstadt, Germany), divided in 3 doses administered intraperitonially with an interval of 30 min. Mice were placed in the stereotaxic frame (David Kopf Instruments, Tujunga, CA, USA) with nontraumatic ear bars (Stoeling, Wood Dale, IL, USA). A tungsten recording electrode (tip impedance 5-10 Mat 1 kHz) coupled with a fiberoptic patch cable (Thorlabs, Newton, NJ, USA) was placed in the NAc (**Figure 12a**, **d** and **g**; stereotaxic coordinates from bregma[160]: +1.3mm AP, +0.9mm ML, and -3.5 to -4.2mm DV), in the VP (**Figure 13a**, **d** and **g**; stereotaxic coordinates from bregma[160]: -0.12mm AP, +1.6mm ML, -3.5 to -4.0mm DV) and in the VTA (**Figure 14a**, **d** and **g**; stereotaxic coordinates from bregma[160]: -3.2mm AP, +0.5mm ML, -4.0 to -4.8mm DV). A ground screw was placed in the skull to close the circuit allowing signal stabilization. The recordings were performed under a Faraday box to reduce the background. The recordings in D1- and D2-cre mice were alternated in each day.

Single neuron activity was recorded extracellularly, and recordings were amplified and filtered by the Neurolog amplifier (NL900D, Digitimer Ltd, Hertfordshire, UK) (low-pass filter at 500 Hz and high-pass filter at 5 kHz). Spontaneous activity was recorded to establish baseline, for 3 minutes. Laser stimulation was performed using a 5 mW of blue light generated by 473 nm DPSS laser system (CNI Laser, Changchun, China), controlled by a pulse generator (Master-8; AMPI, New Ulm, MN, USA). The stimulation protocol used was the same as in behavioral tests: three alternating 3-minute epochs starting with no laser stimulation (OFF-ON-OFF), with 25 ms pulses at 20 Hz. Data sampling was performed using a CED Micro1401 interface and Spike 2 software (Cambridge Electronic Design, Cambridge, UK).

Firing rate stimulus histograms were calculated for the baseline period, stimulation period and after stimulation period, using a bin size of 1 s. Neurons were considered responsive or non-responsive to the stimulation whether their firing rate varied at least 20% from the baseline period activity[165]. Spike latency

was calculated for each recorded neuron as the time elapsed between the beginning of the laser stimulation and the first spike detected after the beginning of the stimulation.

NAc neurons were classified according to previous descriptions[74,166]. Putative fast-spiking interneurons (pFSs) were identified as those with a baseline firing rate higher than 10 Hz and a waveform half-width less than 100 μs. Tonically active putative cholinergic interneurons (pCINs) were identified as those with a waveform half-width higher than 300 μs. Putative MSNs (pMSNs) were identified as those with baseline firing rate lower than 5 Hz and that do not met the waveform criteria for pCIN or pFS neurons.

VP putative GABAergic neurons (pGABAergic) were identified as those with a baseline firing rate between 0.2 Hz and 18.7 Hz[74,167]. Other non-identified neurons were excluded from the analysis.

VTA neurons were separated into putative dopaminergic (pDAergic) and putative GABAergic (pGABAergic). pDAergic neurons were identified as those with a baseline firing rate lower than 10 Hz and a waveform duration higher than 1.5 ms. pGABAergic neurons were identified as those with baseline firing rate higher than 10 Hz and waveform duration lower than 1.5 ms[74,168]. Other non-identified neurons were excluded from the analysis.

## 3.6. Histological Procedures

### 3.6.1. Immunofluorescence (IF)

Mice were anesthetized and then transcardially perfused with 0.9% saline followed by 4% paraformaldehyde (PFA). Brains were removed, post-fixed in 4% PFA for 24 hours and then rinsed and stored in 30% sucrose at 4 °C until sectioning. Brains were sectioned coronally at a thickness of 40 μm in a vibrating microtome (VT1000S, Leica, Germany) and stored in cryoprotectant solution at -20 °C until use. Sections were washed with PBS/Triton-X100 (0.3%) (PBS-T), treated with citrate buffer 1X to break protein cross-links and expose antigens and epitopes, blocked with PBS-T plus 10% fetal bovine serum (FBS) to inhibit antibodies to bind to non-specific epitopes, and then incubated with the primary antibody goat anti-GFP (1:500, ab6673; Abcam, Cambridge, UK). After washes with PBS-T, sections were incubated with secondary fluorescent antibody donkey Alexa Fluor® 488 anti-goat (1:500, Invitrogen, Carlsbad, CA, USA). All sections were stained with 40,6-diamidino-2-phenylindole (DAPI; 1mg $ml^{-1}$) and mounted using mounting media (Permafluor; Invitrogen, MA, USA). Images were collected and analyzed by confocal microscopy (Olympus FluoViewTMFV3000).

Quantification of GFP infection by IF in each area was performed using ImageJ 1.42 software. For NAc, percentage of area labeled with GFP was calculated dividing the area labeled with GFP by the total area of the NAc, and number of DAPI cells positives for GFP were counted by the “Find Maxima” tool.

For VP and VTA, percentage of area labeled with GFP was calculated by "Analyze Particles" tool. Background of each image was subtracted, and threshold adjusted.

#### 3.6.2. Hematoxylin-eosin staining

After electrophysiological recordings, mice were transcardially perfused with 0.9% saline followed by 4% paraformaldehyde (PFA). Brains were removed, post-fixed in 4% PFA for 24 hours and then rinsed and stored in 30% sucrose at 4 °C until sectioning. Brains were sectioned coronally at a thickness of 40 µm in a vibrating microtome (VT1000S, Leica, Germany). Sections were mounted in microscope slides and left to dry overnight. Hematoxylin-eosin staining was performed, and slides were mounted using mounting media (Entellan® New). Images were collected and analyzed by brightfield microscopy (Olympus Widefield Upright Microscope BX61).

### 3.7. Statistical Analysis

Normality tests (Shapiro-Wilks) were performed for all data analyzed, as well as outlier analysis using the ROUT method, that is based on False discovery rate. When normality assumptions were met, one-way Analysis of Variance (ANOVA) for repeated measures was used to compare before (baseline), during (stimulation) and after stimulation (post-stimulation), and Tukey's post hoc multiple comparisons was used for group differences determination. When normality assumptions were not met Friedman's test was performed, and Dunn's multiple comparison for post hoc analysis. Two-way ANOVA (Mixed Model) for repeated measures was used for comparisons within-between groups (baseline *vs* stimulation *vs* post-stimulation and ChR2 *vs* YFP), and Sidak's post hoc multiple comparisons was used for group differences determination. Statistical analysis was performed with no sphericity assumption and Geisser-Greenhouse's epsilon values were properly reported.

All statistical details of behavioral tasks and electrophysiological recordings are displayed in Table 1. Results are presented as mean ± SEM and were considered statistically significant for $p \leq 0.05$. All statistical analysis was performed using GraphPad (Prism 8.0.2, La Jolla, CA, USA).

# Chapter 4 – Results

# 4. Results

## 4.1. Behavioral assessment with manipulation of D1- and D2-MSNs

Increasing evidence suggests the involvement of NAc, VP and VTA in anxiety[68,146], as well as in depressive disorders[10,76,113,117,118]. To understand the role of each MSN subpopulation in these disorders, we used optogenetics to specifically manipulate NAc D1- or D2-MSN activity during behavior.

D1- and D2-cre mice were injected in the NAc with an AAV5 containing a vector encoding a cre-dependent channelrhodopsin (ChR2; for optical stimulation) or yellow fluorescent protein (YFP; control group) (**Figure 4a**, **b** and **c**). The fiber was placed either in the VTA (D1-cre mice) or in the VP (D1-cre and D2-cre groups).

This approach successfully transfected 60% of NAc cells in D1- and D2-cre mice (**Figure 4d** and **e**; D1-VP-ChR2 73.72±11.94, D1-VP-YFP 58.55±6.86, D1-VTA-ChR2 54.56±11.43, D1-VTA-YFP 58.55±6.86, D2-VP-ChR2 50.74±4.29, D2-VP-YFP 62.67±9.29). Approximately 21% of the VP area was labeled with GFP in D1- and D2-cre mice (**Figure 4f** and **g**; D1-VP-ChR2 21.63±5.29, D1-VP-YFP 21.50±11.32, D2-VP-ChR2 24.49±3.29, D2-VP-YFP 19.78±4.29). Approximately 20% of the VTA area was labeled with GFP in D1-cre mice (**Figure 4h** and **i**; D1-VTA-ChR2 24.39±4.62, D1-VTA-YFP 17.96±6.97).

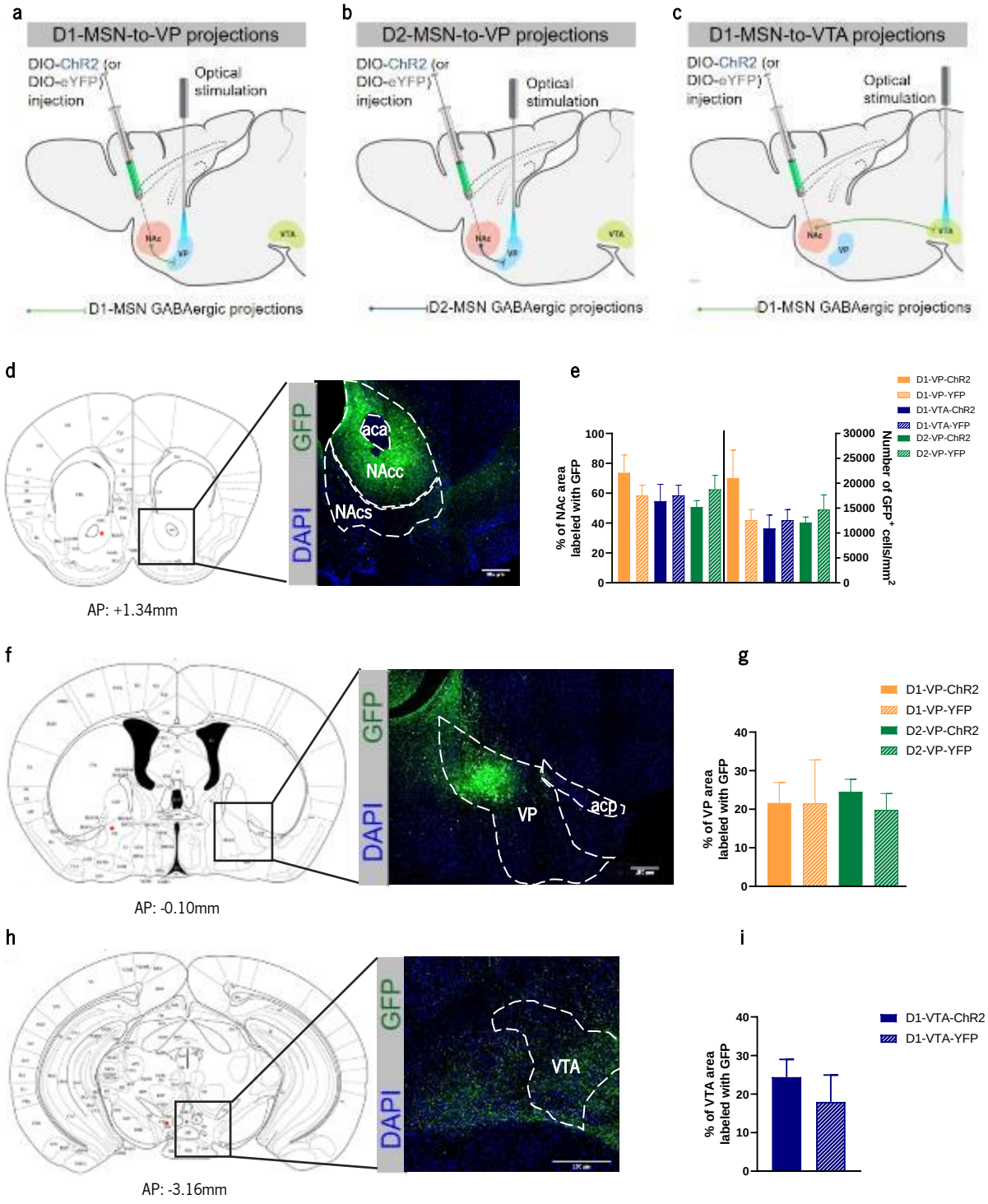


**Figure 4. Stereotaxic surgeries.** (**a**) Stereotaxic surgeries for the study of D1-MSN-to-VP projections: the virus AAV5-EF1a-DIO-ChR2-eYFP (or AAV5-EF1a-DIO-eYFP) was injected in the NAc (stereotaxic coordinates from bregma[160]: AP:+1.3mm; ML: +0.9mm; DV: -4.0mm) of D1-cre mice and an optic fiber was implanted in the VP (stereotaxic coordinates from bregma[160]: AP:-0.1mm; ML: +1.6mm; DV: -3.9mm). (**b**) Stereotaxic surgeries for the study of D2-MSN-to-VP projections: the virus AAV5-EF1a-DIO-ChR2-eYFP (or AAV5-EF1a-DIO-eYFP) was injected in the NAc of D2-cre mice and an optic fiber was implanted in the VP. (**c**) Stereotaxic surgeries for the study of D1-MSN-to-VTA projections: the virus AAV5-EF1a-DIO-ChR2-eYFP (or AAV5-EF1a-DIO-eYFP) was injected in the NAc of D1-cre mice and an optic fiber was implanted in the VTA (stereotaxic coordinates from bregma[160]: AP:-3.2mm; ML: +0.5mm; DV: -4.5mm). (**d**) Representative immunofluorescence image of GFP confirming the injection of the virus in the NAc. Scale bar 250 µm. (**e**) Percentage of NAc area (left Y axis) and number of DAPI cells positive for GFP/mm$^2$ of NAc (right Y axis) infected with virus in each group (D1-VP-ChR2 in orange, D1-VP-YFP in orange and white, D1-VTA-ChR2 in blue, D1-VTA-YFP in blue and white, D2-VP-ChR2 in green and D2-VP-YFP in green and white). (**f**)

Representative immunofluorescence image of GFP confirming the infection of the virus from the NAc to the VP. Scale bar 250 µm. (**g**) Percentage of VP area infected with virus in each group (D1-VP-ChR2 in orange, D1-VP-YFP in orange and white, D2-VP-ChR2 in green and D2-VP-YFP in green and white). (**h**) Representative image immunofluorescence of GFP confirming the infection of the virus from the NAc to the VTA. Scale bar 250 µm. (**i**) Percentage of VTA area infected with virus in each group (D1-VTA-ChR2 in blue and D1-VTA-YFP in blue and white).

### 4.1.1. Alterations in anxiety-like behavior by optogenetic activation of D1- and D2-MSN terminals

To evaluate if stimulation of D1- MSN terminals in the VTA or in the VP, or D2-MSN terminals in the VP were relevant for anxiety-like phenotypes, we stimulated terminals during the EPM (**Figure 5**), OF (**Figure 6**), Light/Dark Box (**Figure 7**) and NSF (**Figure 8**). As a note, all details of the statistical analysis can be found in Table 1 (page 43).

Optogenetic activation of D1-MSN terminals in the VP partially increased the anxiety-like behavior. Stimulation of D1-VP-ChR2 mice did not alter the time or number of entries in the open arms of the EPM (**Figure 5b**, $p = 0.2679$; **Figure 5c**, $p = 0.2557$).

Stimulated mice did not show significant differences in time spent in the center (**Figure 6b**, $p = 0.0370$, post hoc baseline *vs* stimulation $p = 0.6284$), time in ambulation (**Figure 6c**, $p = 0.0598$) or number of entries in the center of the OF arena (**Figure 6d**, $p = 0.0794$). Interestingly, D1-VP-YFP significantly increased the time in ambulation in the center of the arena during the stimulation period, returning to values similar to baseline in the post-stimulation period (**Figure 6c**, $p = 0.0586$, post hoc stimulation *vs* post-stimulation $p = 0.0384$). Importantly, stimulation of D1-VP-ChR2 mice did not change overall locomotion (**Figure 6e**, $p = 0.0991$).

Optogenetic stimulation led to a significant decrease in the distance traveled (**Figure 7b**, $p = 0.0533$, post hoc baseline *vs* stimulation $p = 0.0132$), time spent (**Figure 7c**, $p = 0.4526$, post hoc baseline *vs* stimulation $p = 0.0499$), time spent in ambulation (**Figure 7d**, $p = 0.0051$, post hoc baseline *vs* stimulation $p = 0.0245$, post hoc baseline *vs* post-stimulation $p = 0.0223$) and number of entries (**Figure 7e**, $p = 0.0018$, post hoc baseline *vs* stimulation $p = 0.0172$, post hoc baseline *vs* post-stimulation $p = 0.0266$) in the light zone of the Light/Dark Box. Also, when compared with control group, during the stimulation period, all parameters evaluated in the Light/Dark Box presented lower values for the ChR2 stimulated group (**Figure 7b**, $p = 0.0051$, post hoc ChR2 *vs* YFP $p = 0.0074$; **Figure 7c**, $p = 0.0406$, post hoc ChR2 *vs* YFP $p = 0.0013$; **Figure 7d**, $p = 0.0037$, post hoc ChR2 *vs* YFP $p = 0.0400$; **Figure 7e**, $p = 0.0002$, post hoc ChR2 *vs* YFP $p = 0.0200$). These differences remained statistically significant in the post-stimulation period for distance traveled (**Figure 7b**, $p = 0.0051$, post hoc ChR2 *vs* YFP $p = 0.0450$) and time in ambulation (**Figure 7d**, $p = 0.0037$, post hoc ChR2 *vs* YFP $p = 0.0414$). Importantly, before

stimulation, D1-VP-ChR2 group showed a significantly lower number of entries when compared with control group (**Figure 7e**, $p = 0.0002$, post hoc ChR2 *vs* YFP $p = 0.0401$).

In the NSF, stimulated mice showed a tendency to a higher latency to begin a feeding episode (**Figure 8c**, $p = 0.0233$, post hoc stimulation *vs* no stimulation $p = 0.0567$); however, neither the latency to reach the pellet located at the center of the open arena (**Figure 8b**, $p = 0.3146$) nor the pellet consumption in the home cage (**Figure 8d**, $p = 0.0352$, post hoc stimulation *vs* no stimulation $p = 0.9972$) showed differences between sessions. However, pellet consumption in the control group significantly decreased in the stimulation session (**Figure 8d**, $p = 0.0352$, post hoc stimulation *vs* no stimulation $p = 0.0079$).

Optogenetic activation of D1-MSN terminals in the VTA also showed a partial increase of the anxiety-like behavior. In the EPM, stimulation of D1-VTA-ChR2 mice did not alter the time or number of entries in the open arms (**Figure 5d**, $p = 0.2740$; **Figure 5e**, $p = 0.6733$). Importantly, after stimulation, the number of entries in the open arms for D1-VTA-YFP group increased, being statistically significant when compared with D1-VTA-ChR2 group (**Figure 5e**, $p = 0.0036$, post hoc ChR2 *vs* YFP $p = 0.0213$).

The OF test showed an increase in the time spent (**Figure 6f**, $p = 0.0312$, post hoc baseline *vs* stimulation $p = 0.0413$) and number of entries in the center zone of the OF arena (**Figure 6h**, $p = 0.0040$, post hoc baseline *vs* stimulation $p = 0.0157$, post hoc stimulation *vs* post-stimulation $p = 0.0249$); however, neither the time spent in ambulation in this zone nor the distance traveled were altered by optogenetic stimulation (**Figure 6g**, $p = 0.0143$, post hoc baseline *vs* stimulation $p = 0.4762$; **Figure 6i**, $p = 0.0357$, post hoc baseline *vs* stimulation $p = 0.1572$). It is important to note that the control group showed a tendency for an increase in all parameters measured by the OF (**Figure 6f**, $p = 0.0312$, post hoc baseline *vs* stimulation $p = 0.0788$; **g**, $p = 0.0143$, post hoc baseline *vs* stimulation $p = 0.1670$; **h**, $p = 0.0040$, post hoc baseline *vs* stimulation $p = 0.2816$; and **i**, $p = 0.0357$, post hoc baseline *vs* stimulation $p = 0.1553$).

Contrariwise, in the Light/Dark Box test, D1-VTA-ChR2 mice showed a significant decrease in the time spent in ambulation (**Figure 7h**, $p = 0.0088$, post hoc baseline *vs* stimulation $p = 0.0038$, post hoc baseline *vs* post-stimulation $p = 0.0123$) and in the number of entries in the light zone of the apparatus (**Figure 7i**, $p = 0.0004$, post hoc baseline *vs* stimulation $p = 0.0019$, post hoc baseline *vs* post-stimulation $p = 0.0021$). Importantly, the control group revealed a tendency to decrease the number of entries in the light zone across time (**Figure 7i**). The distance traveled (**Figure 7f**, $p = 0.1994$) and the time spent in the light zone of the Light/Dark box (**Figure 7g**, $p = 0.3565$) were not affected by stimulation.

Regarding NSF, D1-VTA-ChR2 mice had no significant effect neither in the latency to approach the pellet located in the center of the arena nor to initiate consumption of the pellet (**Figure 8e**, $p = 0.3853$; **Figure 8f**, $p = 0.0585$). Interestingly, in the stimulation session, food consumption significantly decreased for the control group (**Figure 8g**, $p = 0.0247$, post hoc stimulation *vs* no stimulation $p = 0.0027$).

Optogenetic activation of D2-MSN terminals in the VP caused a significant increase in anxiety-like behavior. In fact, during the stimulation period, D2-VP-ChR2 mice spent significantly less time in the open arms of the EPM (**Figure 5f**, $p = 0.0052$, post hoc baseline *vs* stimulation $p = 0.0023$, post hoc baseline *vs* post-stimulation $p = 0.0096$) and performed fewer entries in the same arms (**Figure 5g**, $p = 0.0062$, post hoc baseline *vs* stimulation $p = 0.0322$, post hoc baseline *vs* post-stimulation $p = 0.0216$).

Stimulation of D2-VP-ChR2 mice did not alter the time spent in the center of the arena (**Figure 6j**, $p = 0.0395$, post hoc baseline *vs* stimulation $p = 0.1224$), time in ambulation (**Figure 6k**, $p = 0.0613$), number of entries (**Figure 6l**, $p = 0.6244$) or distance traveled (**Figure 6m**, $p = 0.0900$) in the center of the OF, excluding a possible motor effect caused by the stimulation protocol.

Also, the distance traveled (**Figure 7j**, $p < 0.0001$, post hoc baseline *vs* stimulation $p = 0.0368$, post hoc baseline *vs* post-stimulation $p = 0.0249$), as well as the time spent in ambulation in the light compartment of the Light/Dark Box (**Figure 7l**, $p < 0.0001$, post hoc baseline *vs* stimulation $p = 0.0030$, post hoc baseline *vs* post-stimulation $p = 0.0032$) significantly decreased during stimulation period. The time spent in the light zone was not affected by stimulation (**Figure 7k**, $p = 0.1672$). Interestingly, the control group also showed a significant decrease in the distance traveled, time spent in ambulation and number of entries through time (**Figure 7j**, $p < 0.0001$, post hoc baseline *vs* post-stimulation $p = 0.0114$; **Figure 7l**, $p < 0.0001$, post hoc baseline *vs* stimulation $p = 0.0198$, post hoc baseline *vs* post-stimulation $p = 0.0062$; **Figure 7m**, $p = 0.0009$, post hoc baseline *vs* stimulation $p = 0.0423$, post hoc baseline *vs* post-stimulation $p = 0.0294$). Furthermore, the NSF revealed a higher latency to reach the pellet located at the center of the open arena (**Figure 8h**, $p = 0.0030$, post hoc stimulation *vs* no stimulation $p = 0.0022$) and to begin a feeding episode during the stimulation session (**Figure 8i**, $p = 0.1139$, post hoc stimulation *vs* no stimulation $p = 0.0490$). Also, in the stimulation session, D2-VP-ChR2 group showed a significantly higher latency to begin a feeding episode when compared to the D2-VP-YFP group (**Figure 8i**, $p = 0.0856$, post hoc ChR2 *vs* YFP $p = 0.0345$). These effects were not related to anhedonia since pellet consumption was not different between sessions (**Figure 8j**, $p = 0.0174$, post hoc stimulation *vs* no stimulation $p = 0.0697$).

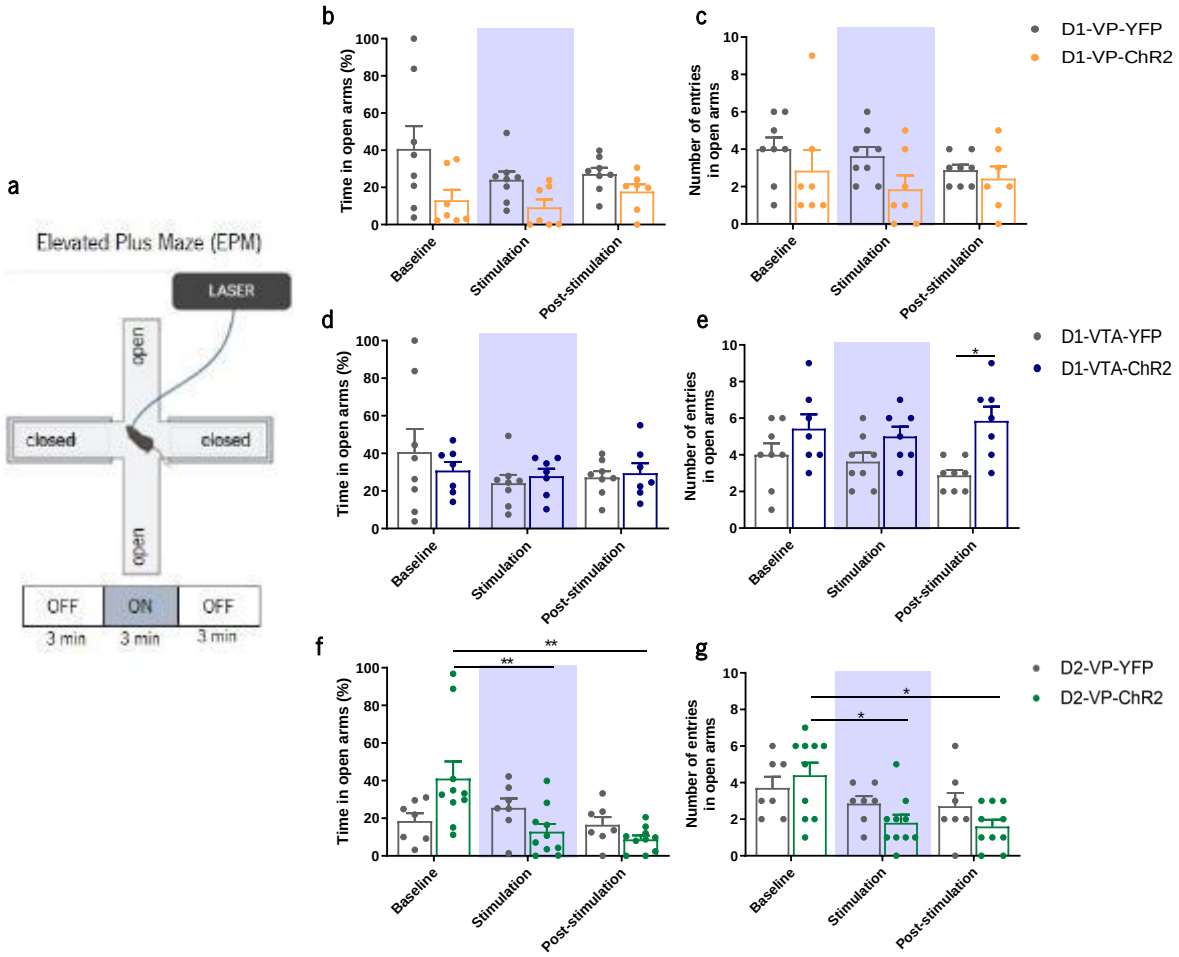


**Figure 5. Anxiety-like behavior assessment - Elevated Plus Maze.** (**a**) Schematic representation of the Elevated Plus Maze (EPM) test with optogenetic stimulation protocol of 3-minute epochs: no stimulation (OFF), laser stimulation (ON), and no stimulation (OFF) (OFF-ON-OFF epochs). (**b**) Percentage of time and (**c**) number of entries in the open arms for D1-VP-YFP (grey; n = 8) and D1-VP-ChR2 (orange; n = 7). (**d**) Percentage of time and (**e**) number of entries in open arms for D1-VTA-YFP (grey; n = 8) and D1-VTA-ChR2 (blue; n = 7). (**f**) Percentage of time and (**g**) number of entries in open arms for D2-VP-YFP (grey; n = 7) and D2-VP-ChR2 (green; n = 10). *p ≤ 0.05, **p ≤ 0.01. Data are represented as mean ± SEM.

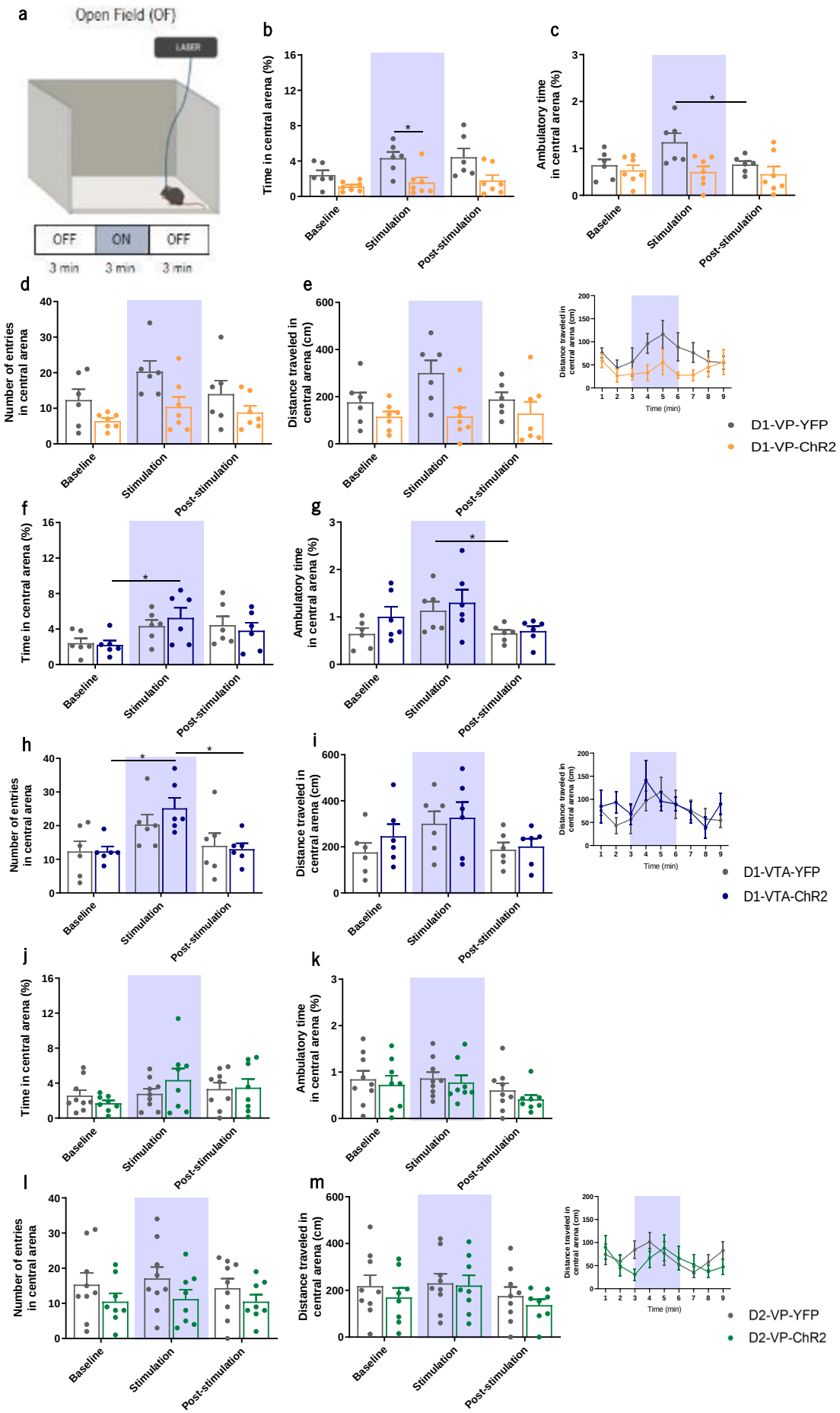
a
Open Field (OF)
LASER
OFF
ON
OFF
3 min
3 min
3 min
b
Time in central arena (%)
Baseline
Stimulation
Post-stimulation
c
Ambulatory time in central arena (%)
d
Number of entries in central arena
e
Distance traveled in central arena (cm)
Time (min)
D1-VP-YFP
D1-VP-ChR2
f
g
h
i
D1-VTA-YFP
D1-VTA-ChR2
j
k
l
m
D2-VP-YFP
D2-VP-ChR2

**Figure 6. Anxiety-like and locomotor behavior assessment - Open Field.** (**a**) Schematic representation of the Open Field (OF) test with optogenetic stimulation protocol of 3-minute epochs: no stimulation (OFF), laser stimulation (ON), and no stimulation (OFF) (OFF-ON-OFF epochs). (**b**) Percentage of time spent, (**c**) percentage of time in ambulation, (**d**) number of entries and (**e**) distance traveled in the center of the arena for D1-VP-YFP (grey; n = 6) and D1-VP-ChR2 (orange; n = 7). (**f**) Percentage of time spent, (**g**) percentage of time in ambulation, (**h**) number of entries and (**i**) distance traveled in the center of the arena for D1-VTA-YFP (grey; n = 6) and D1-VTA-ChR2 (blue; n = 6). (**j**) Percentage of time spent, (**k**) percentage of time in ambulation, (**l**) number of entries and (**m**) distance traveled in in the center of the arena for D2-VP-YFP (grey; n = 9) and D2-VP-ChR2 (green; n = 8). *$p \leq 0.05$. Data are represented as mean ± SEM.

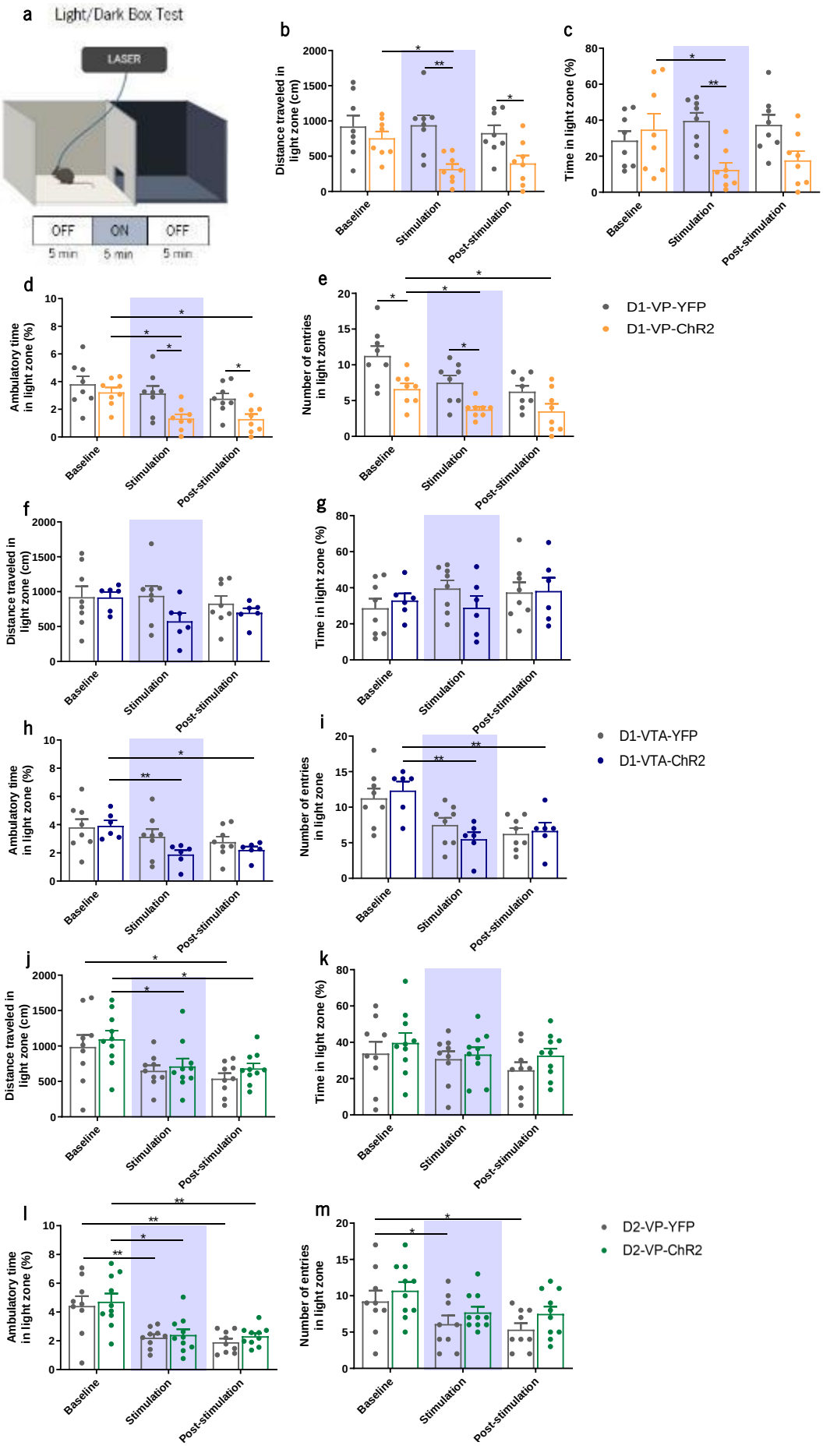
a
Light/Dark Box Test
LASER
OFF
ON
OFF
5 min
5 min
5 min
b
Distance traveled in light zone (cm)
c
Time in light zone (%)
Baseline
Stimulation
Post-stimulation
d
Ambulatory time in light zone (%)
e
Number of entries in light zone
D1-VP-YFP
D1-VP-ChR2
f
Distance traveled in light zone (cm)
g
Time in light zone (%)
h
Ambulatory time in light zone (%)
i
Number of entries in light zone
D1-VTA-YFP
D1-VTA-ChR2
j
Distance traveled in light zone (cm)
k
Time in light zone (%)
l
Ambulatory time in light zone (%)
m
Number of entries in light zone
D2-VP-YFP
D2-VP-ChR2

**Figure 7. Anxiety-like behavior assessment - Light/Dark Box.** (**a**) Schematic representation of the Light/Dark Box test with optogenetic stimulation protocol of 5-minute epochs: no stimulation (OFF), laser stimulation (ON), and no stimulation (OFF) (OFF-ON-OFF epochs). (**b**) Distance traveled, (**c**) percentage of time spent, (**d**) percentage of time in ambulation and (**e**) number of entries in the light zone of the arena for D1-VP-YFP (grey; n = 8) and D1-VP-ChR2 (orange; n = 8). (**f**) Distance traveled, (**g**) percentage of time spent, (**h**) percentage of time in movement and (**i**) number of entries in the light zone of the arena for D1-VTA-YFP (grey; n = 8) and D1-VTA-ChR2 (blue; n = 6). (**j**) Distance traveled, (**k**) percentage of time spent, (**l**) percentage of time in movement and (**m**) number of entries in the light zone of the arena for D2-VP-YFP (grey; n = 9) and D2-VP-ChR2 (green; n = 10). *p ≤ 0.05, **p ≤ 0.01. Data are represented as mean ± SEM.

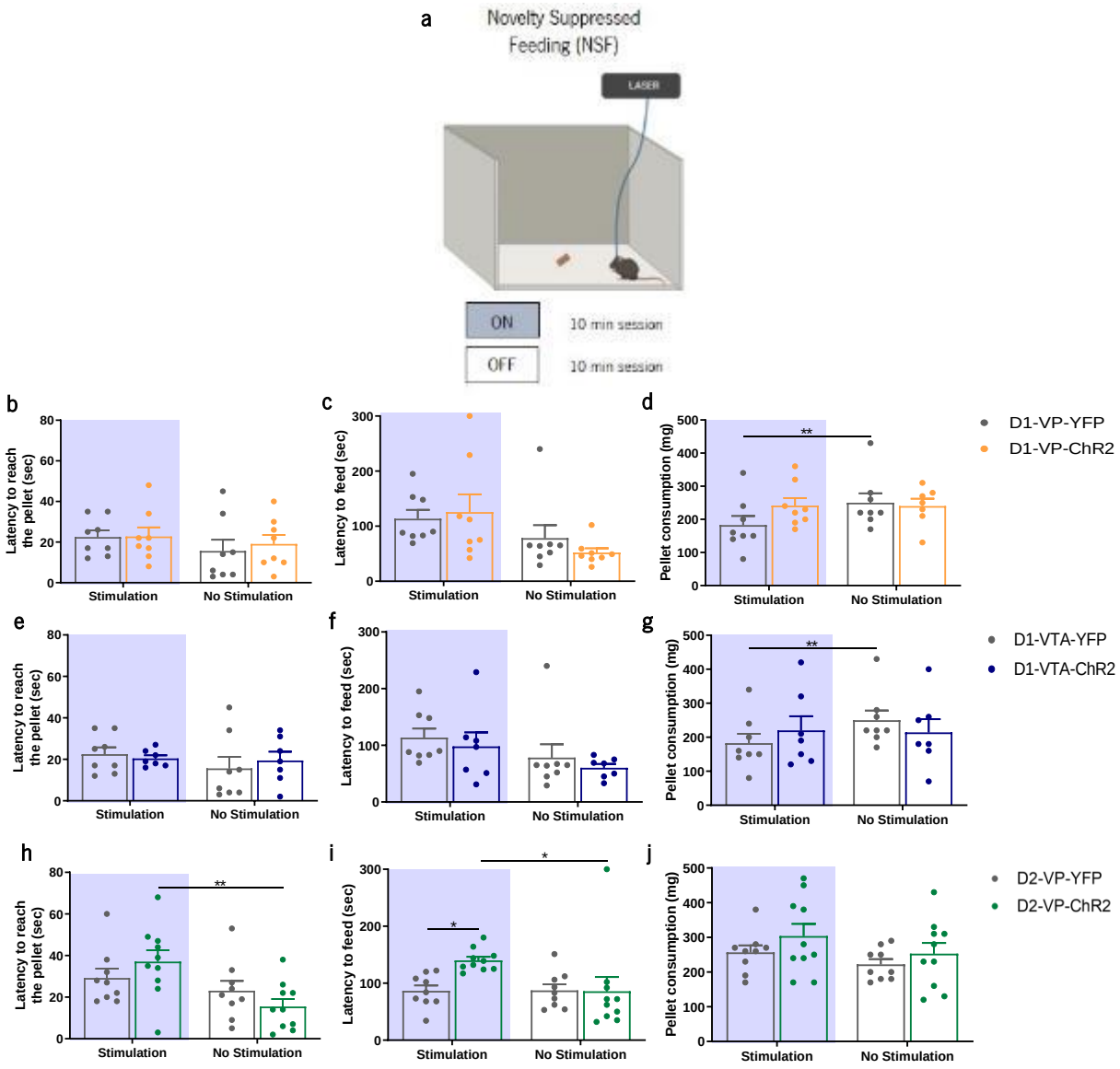


**Figure 8. Anxiety-like behavior assessment - Novelty Suppressed Feeding.** (**a**) Schematic representation of the Novelty Suppressed Feeding (NSF)) test. Optogenetic stimulation was performed until the mouse initiated pellet consumption or at a maximum of 10 minutes in one session (ON). (**b**) Latency for the mouse reach the pellet (in seconds), (**c**) latency for the beginning of a feeding episode (in seconds) and (**d**) food consumption (pellet, milligrams), measured 30 minutes after the end of the feeding episode for D1-VP-YFP (grey; n = 8) and D1-VP-ChR2 (orange; n = 8). (**e**) Latency for the mouse to reach the pellet (in seconds), (**f**) latency for the beginning of a feeding episode (in seconds) and (**g**) food consumption (pellet, milligrams), measured 30 minutes after the end of the feeding episode for D1-VTA-YFP (grey; n = 8) and D1-VTA-ChR2 (blue; n = 7). (**h**) Latency for the mouse to reach the pellet (in seconds), (**i**) latency for the beginning of a feeding episode (in seconds) and (**j**) food consumption (pellet, milligrams), measured 30 minutes after the end of the feeding episode for D2-VP-YFP (grey; n = 9) and D2-VP-ChR2 (green; n = 10). *p ≤ 0.05, **p ≤ 0.01. Data are represented as mean ± SEM.

### 4.1.2. Alterations in depressive-like phenotype by optogenetic activation of D1- and D2-MSN terminals

To evaluate the depressive-like phenotypes produced by stimulation of D1- or D2-MSN terminals in the VP, or D1-MSN terminals in the VTA, we performed the FST (**Figure 9**), TST (**Figure 10**) and SDT (**Figure 11**).

Optogenetic activation of D1-MSN terminals in the VP seems to increase the depressive-like behavior, since the time spent immobile in the FST significantly increased through time in D1-VP-ChR2 mice (**Figure 9b**, $p = 0.0607$, post hoc baseline *vs* post-stimulation $p = 0.0058$). Furthermore, when compared with the control group, during the stimulation period, activation of these neurons led to a significant increase in the time spent immobile (**Figure 9b**, $p = 0.0094$, post hoc ChR2 *vs* YFP $p = 0.0252$). These differences between groups remained even when stimulation ceased (**Figure 9b**, $p = 0.0094$, post hoc ChR2 *vs* YFP $p = 0.0044$). The latency until the first immobility episode for each epoch was not affected by optogenetic stimulation of D1-VP-ChR2 mice (**Figure 9c**, $p = 0.2146$).

In the TST, optogenetic stimulation of these terminals did not alter the time that mice spent immobile (**Figure 10b**, $p = 0.1771$), or the latency until the first immobility episode (**Figure 10c**, $p = 0.0057$, post hoc baseline *vs* stimulation $p = 0.5872$); however, there was a significant increase between baseline and post-stimulation periods regarding latency until the first immobility episode (**Figure 10c**, $p = 0.0057$, post hoc baseline *vs* post-stimulation $p = 0.0364$).

The anhedonia was measured by the SDT, showing no significant differences in preference for a sugar reward between stimulation and no stimulation sessions for D1-VP-ChR2 mice (**Figure 11b**, $p = 0.9356$).

Optogenetic activation of D1-MSN terminals in VTA showed a tendency to increase the time that mice spent immobile in the FST (**Figure 9d**, $p = 0.5725$, post hoc baseline *vs* stimulation $p = 0.2378$) and in TST (**Figure 10d**, $p = 0.0235$, post hoc baseline *vs* stimulation $p = 0.3020$), being statistically significant when the baseline was compared with the post-stimulation periods (**Figure 10d**, $p = 0.0235$, post hoc baseline *vs* post-stimulation $p = 0.0250$). Importantly, D1-VTA-YFP group showed a tendency to decrease the time immobile throughout the FST session (**Figure 9d**, $p = 0.5725$, post hoc baseline *vs* post-stimulation $p = 0.3862$). In both FST and TST, latency until the first immobility episode tended to increase with time (**Figure 9e**, $p = 0.0768$; **Figure 10e**, $p = 0.0580$).

In the SDT, no significant differences were found in preference for a sugar reward between stimulation and no stimulation sessions for D1-VTA-ChR2 mice (**Figure 11c**, $p = 0.9451$).

Optogenetic activation of D2-MSN terminals in VP did not change the time spent immobile in the FST (**Figure 9f**, $p = 0.7635$), which was consistent with the results of the TST (**Figure 10f**, $p = 0.0581$). In the FST, the latency until the first immobility episode had a tendency to increase with time, being statistically significant between baseline and post-stimulation (**Figure 9g**, $p = 0.2203$, post hoc baseline *vs* post-stimulation $p = 0.0200$). In the TST, optogenetic stimulation did not alter the latency until the first immobility episode; however, control group showed a significant increase between baseline and post-stimulation periods (**Figure 10g**, $p = 0.0413$, post hoc baseline *vs* post-stimulation $p = 0.0476$).

In SDT, stimulation of D2-VP-ChR2 led to a significant decrease in the preference for sugar (**Figure 11d**, $p = 0.0003$, post hoc stimulation *vs* no stimulation $p = 0.0041$), indicative of an effect in anhedonic behavior. However, this decrease was also present in the D2-VP-YFP group (**Figure 11d**, $p = 0.0003$, post hoc stimulation *vs* no stimulation $p = 0.0225$).

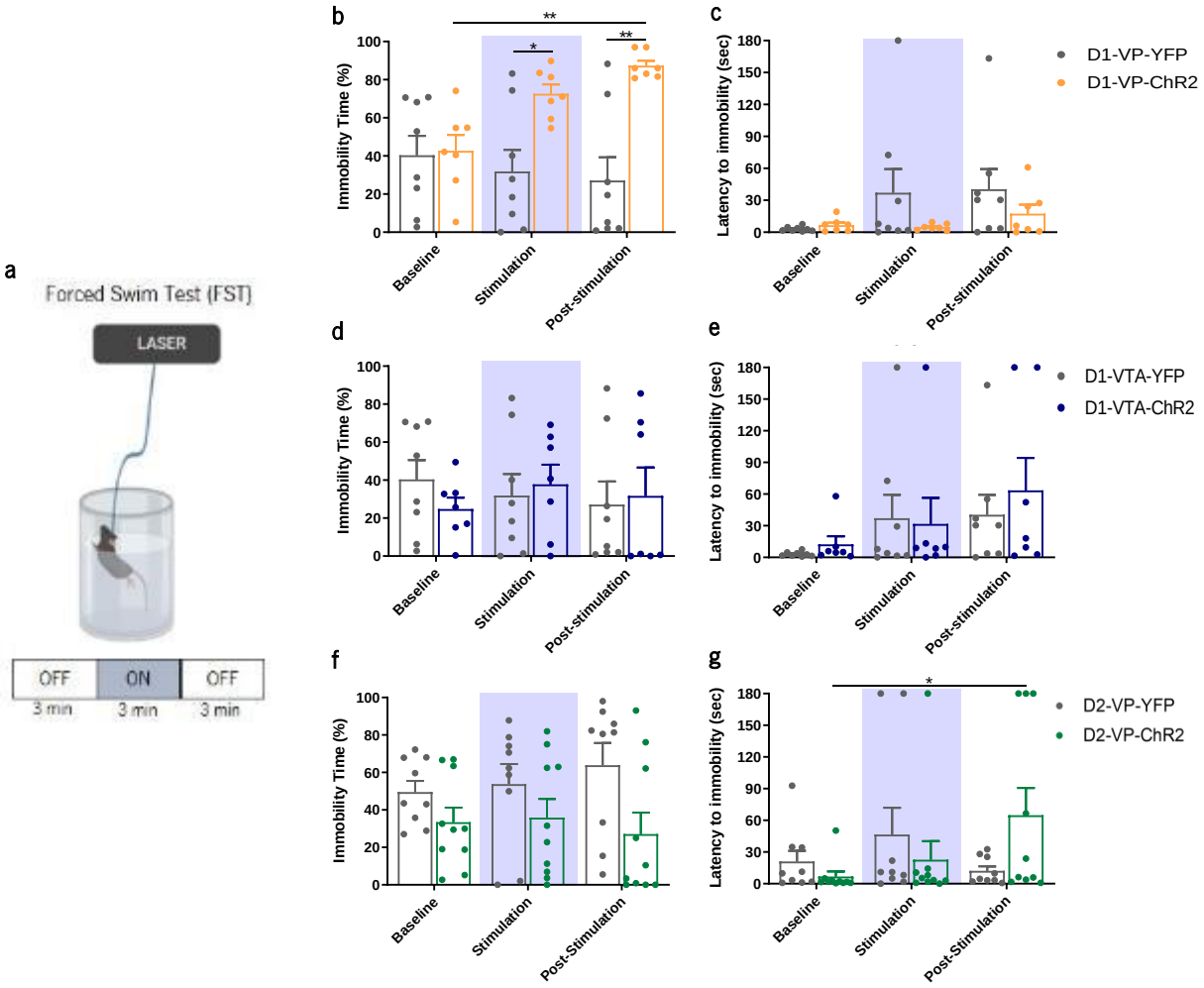


**Figure 9. Depressive-like behavior assessment - Forced Swim Test.** (**a**) Schematic representation of the Forced Swim Test (FST) with optogenetic stimulation protocol of 3-minute epochs: no stimulation (OFF), laser stimulation (ON), and no stimulation (OFF) (OFF-ON-OFF epochs). (**b**) Percentage of time spent immobile and (**c**) latency until first immobility episode (in seconds) for D1-VP-YFP (grey; n = 8) and D1-VP-ChR2 (orange; n = 7). (**d**) Percentage of time spent immobile and (**e**) latency until first immobility episode (in seconds) for D1-VTA-YFP (grey; n = 8) and D1-VTA-ChR2 (blue; n = 7). (**f**) Percentage of time spent immobile and (**g**) latency until first immobility episode (in seconds) for D2-VP-YFP (grey; n = 9) and D2-VP-ChR2 (green; n = 10). *p ≤ 0.05, **p ≤ 0.01. Data are represented as mean ± SEM.

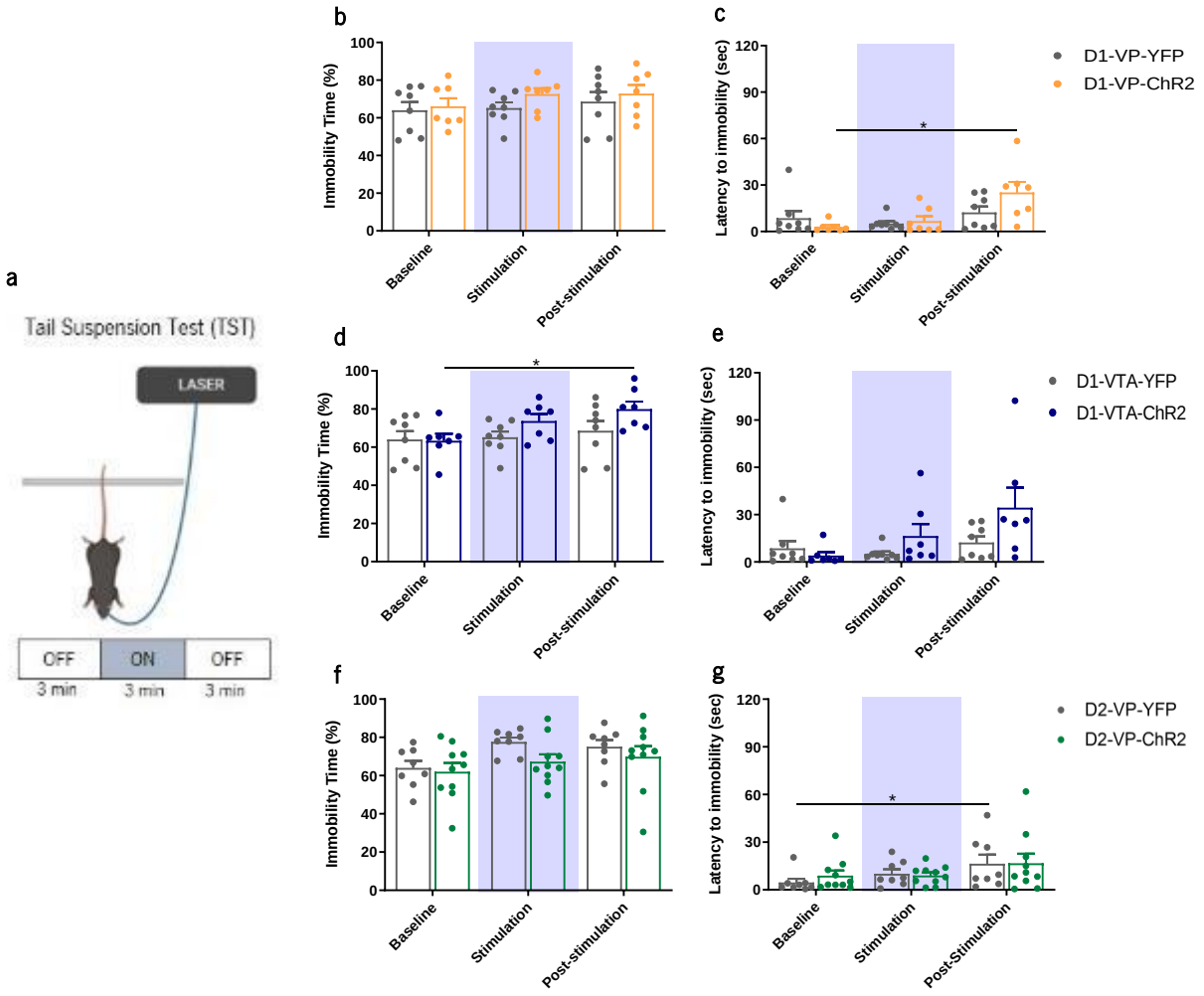


**Figure 10. Depressive- like behavior assessment - Tail Suspension Test.** (**a**) Schematic representation of the Tail Suspension Test (TST) with optogenetic stimulation protocol of 3-minute epochs: no stimulation (OFF), laser stimulation (ON), and no stimulation (OFF) (OFF-ON-OFF epochs). (**b**) Percentage of immobility time and (**c**) latency until first immobility episode (in seconds) for D1-VP-YFP (grey; n = 8) and D1-VP-ChR2 (orange; n = 7). (**d**) Percentage of immobility time and (**e**) latency until first immobility episode (in seconds) for D1-VTA-YFP (grey; n = 8) and D1-VTA-ChR2 (blue; n = 7). (**f**) Percentage of immobility time and (**g**) latency until first immobility episode (in seconds) for D2-VP-YFP (grey; n = 8) and D2-VP-ChR2 (green; n = 10). *p ≤ 0.05. Data are represented as mean ± SEM.

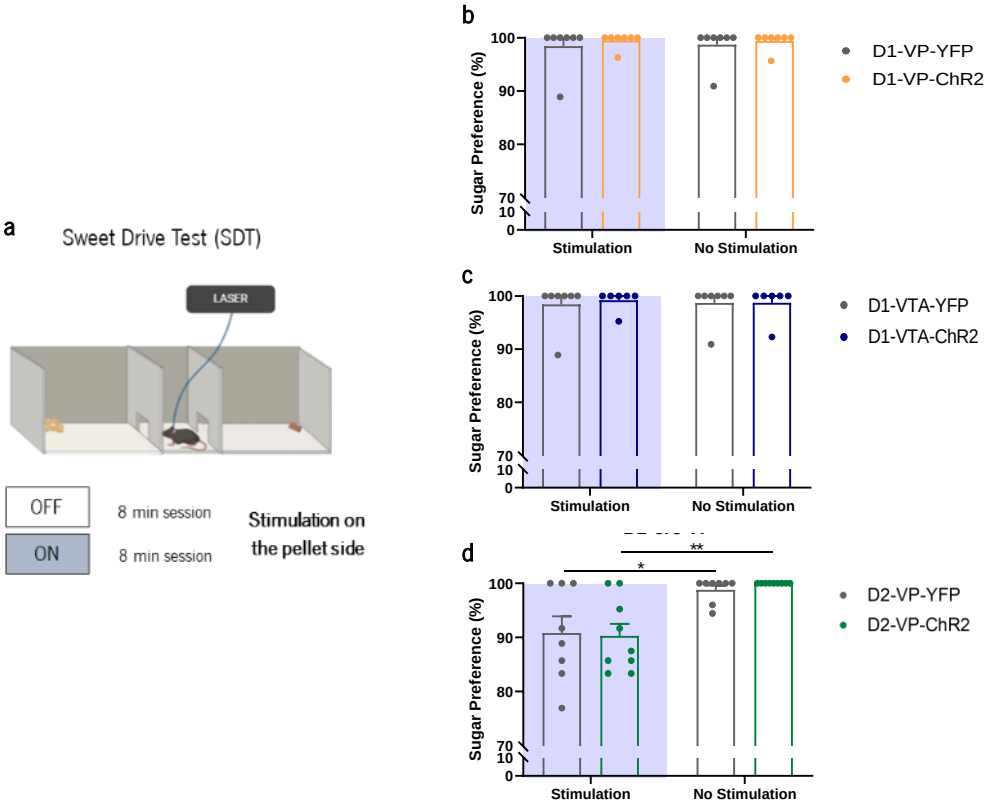


**Figure 11. Depressive- like behavior assessment – Sweet Drive Test.** (**a**) Schematic representation of the Sweet Drive Test (SDT). Optogenetic stimulation was performed each time the mouse crossed to the side of the chamber containing a sugar reward, during an 8-minute session. (**b**) Percentage of preference for sugar for D1-VP-YFP (grey; n = 7) and D1-VP-ChR2 (orange; n = 7). (**c**) Percentage of preference for sugar for D1-VTA-YFP (grey; n = 7) and D1-VTA-ChR2 (blue; n = 6). (**d**) Percentage of preference for sugar for D2-VP-YFP (grey; n = 8) and D2-VP-ChR2 (green; n = 9). *p ≤ 0.05, **p ≤ 0.01. Data are represented as mean ± SEM.

## 4.2. Electrophysiological activity

To understand the functional outcome of specific activation of D1- and D2-MSN projecting neurons, we performed *in vivo* electrophysiological recordings in the NAc (**Figure 12a**), VP (**Figure 13a**) and VTA (**Figure 14a**) of anesthetized mice, using the same optogenetic stimulation protocol of the one used in the behavioral tasks. Bregma coordinates used in recordings were also the same as the ones used for the implantation of the optic fiber in the animals that performed behavior. The electrode/optic fibers' locations were confirmed by hematoxylin-eosin coloration (**Figure 12c**, **Figure 13c** and **Figure 14c**).

### 4.2.1. Electrophysiological effects in NAc neurons in response to D1- and D2-MSN stimulation

In the NAc, putative MSNs (pMSN), putative cholinergic interneurons (pCIN), and putative fast-spiking GABAergic interneurons (pFS), were identified based on characteristic waveforms and basal firing rate[74,166] (**Figure 12b**).

In D1-cre mice, 64.29% of the NAc neurons recorded were identified as pMSNs and the remaining 35.71% as pCINs (**Figure 12e**). Optogenetic stimulation of D1-MSNs led to a tendency to decrease the firing rate of both type of cells (**Figure 12e'**, pMSNs, $p = 0.0430$; pCINs, $p = 0.0602$). Regarding pMSNs, 55.56% of the cells decreased their firing activity during the stimulation period, while the remaining 44.44% did not change their firing activity (**Figure 12e''**). 60% of pCINs also showed a decrease in their firing activity, while the remaining 40% did not change their activity (**Figure 12e''**).

In D2-cre mice, 83.33% of the NAc neurons recorded were identified as pMSNs and the remaining 16.67% as pCINs (**Figure 12e**). Optogenetic stimulation of D2-MSNs led to a tendency to decrease the firing rate of both type of cells (**Figure 12g'**, pMSNs, $p = 0.2902$). 20% of pMSNs showed an increase in firing activity, 60% of the cells decreased firing activity and the remaining 20% did not change firing activity (**Figure 12g''**) during stimulation. The only pCIN recorded showed a decrease in firing activity (**Figure 12g''**).

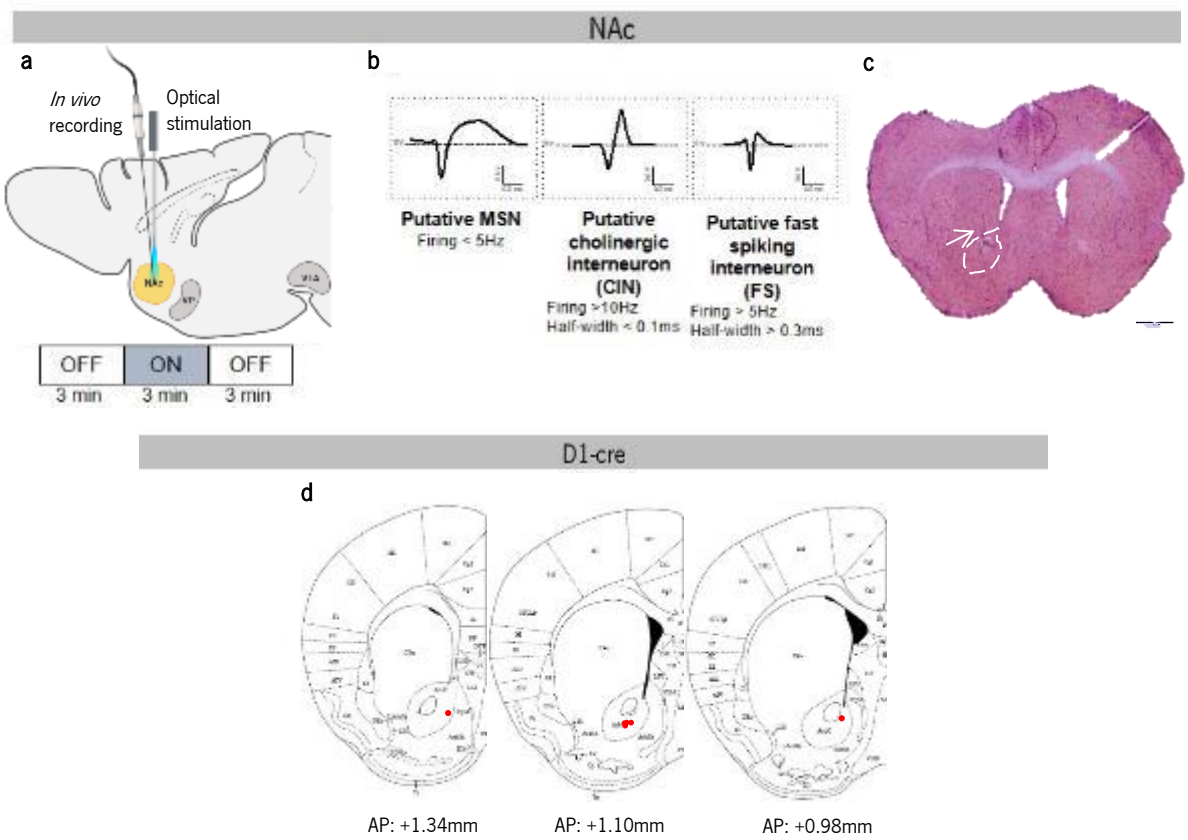

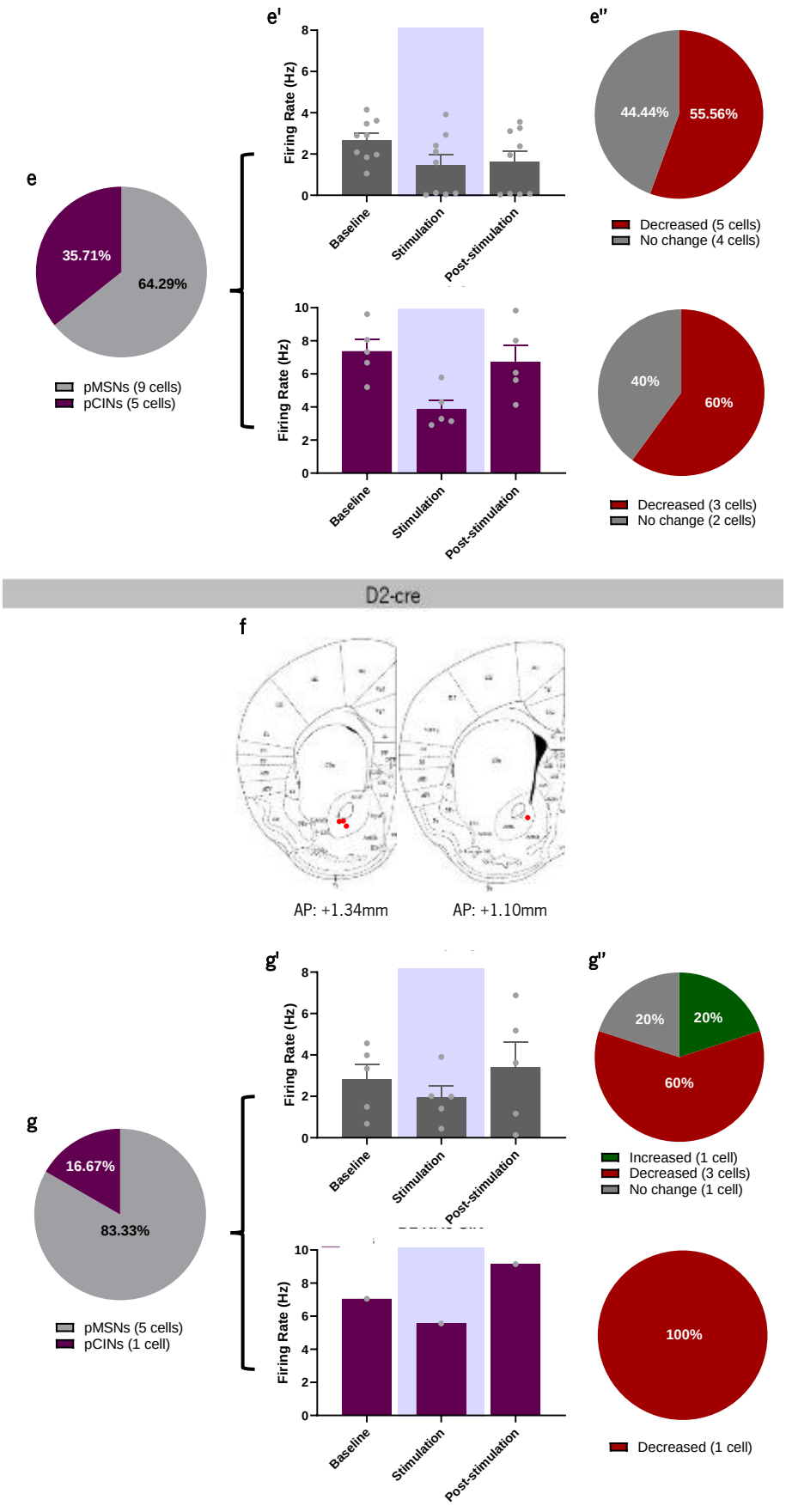
e
35.71%
64.29%
pMSNs (9 cells)
pCINs (5 cells)
e'
Firing Rate (Hz)
Baseline
Stimulation
Post-stimulation
e''
44.44%
55.56%
Decreased (5 cells)
No change (4 cells)
40%
60%
Decreased (3 cells)
No change (2 cells)
D2-cre
f
AP: +1.34mm
AP: +1.10mm
g
16.67%
83.33%
pMSNs (5 cells)
pCINs (1 cell)
g'
g''
20%
20%
60%
Increased (1 cell)
Decreased (3 cells)
No change (1 cell)
100%
Decreased (1 cell)

**Figure 12. Electrophysiological effects in NAc neurons in response to optogenetic stimulation.** (**a**) Schematic representation of NAc electrophysiological recordings during optogenetic stimulation protocol of 3-minute epochs: no stimulation (OFF), laser stimulation (ON), and no stimulation (OFF) (OFF-ON-OFF epochs). (**b**) NAc neurons were classified in three categories according to firing rate and waveform characteristics: putative medium spiny neurons (pMSNs), putative cholinergic interneurons (pCINs), and putative fast-spiking GABAergic interneurons (pFS). (**c**) Representative image of hematoxylin-eosin coloration confirming the recording location in NAc (NAcc is delineated by a white dashed line; white arrow indicates the cleft caused by the electrode + optic fiber). Scale bar 1mm. (**d**) Schematic representation of recording electrodes placement in NAc of D1-cre mice (red dots). (**e**) Percentage of pMSNs (grey) and pCINs (purple) recorded in D1-cre mice. (**e'**) Firing rate of pMSNs (grey; n = 9) and pCINs (purple; n = 5). (**e''**) Percentage of neurons that decreased (red; $n_{pMSNs}$ = 5; $n_{pCINs}$ = 3) and did not change (grey; $n_{pMSNs}$ = 4; $n_{pCINs}$ = 2) firing rate during the stimulation period. (**f**) Schematic representation of recording electrodes placement in NAc of D2-cre mice (red dots). (**g**) Percentage of pMSNs (grey) and pCINs (purple) recorded in D2-cre mice. (**g'**) Firing rate of pMSNs (grey; n = 5) and pCINs (purple; n = 1). (**g''**) Percentage of neurons that increased (green; $n_{pMSNs}$ = 1), decreased (red; $n_{pMSNs}$ = 3; $n_{pCINs}$ = 1) and did not change (grey; $n_{pMSNs}$ = 1) firing rate during the stimulation period. $^{*}p \leq 0.05$. Data are represented as mean ± SEM.

### 4.2.2. Electrophysiological effects in VP neurons in response to D1- and D2-MSN stimulation

*In vivo* electrophysiological recordings in the VP identified putative GABAergic neurons (pGABAergic) as those with a firing rate between 0.2Hz and 18.7Hz[74,167] (**Figure 13b**).

In D1-cre mice, 42 neurons recorded in the VP were identified as pGABAergic neurons. Optogenetic stimulation of D1-MSN terminals in the VP significantly decrease the firing activity of the neurons (**Figure 13e**, $p = 0.0054$, post hoc baseline *vs* stimulation $p = 0.0265$, post hoc baseline *vs* post-stimulation $p = 0.0097$). More specifically, optogenetic stimulation led to an increase in the firing activity of 11.91%, decrease of 57.14% and no change of the remaining 30.95% (**Figure 13e'**).

In D2-cre mice, 46 neurons recorded in the VP were identified as pGABAergic neurons. Optogenetic stimulation of D2-MSN terminals in the VP led to a significant decrease of their firing activity (**Figure 13g**, $p = 0.0002$, post hoc baseline *vs* stimulation $p < 0.0001$, post hoc baseline *vs* post-stimulation $p = 0.0495$). More specifically, optogenetic stimulation led to an increase in the firing activity of 10.87%, decrease of 63.04% and no change of the remaining 26.09% (**Figure 13g'**).

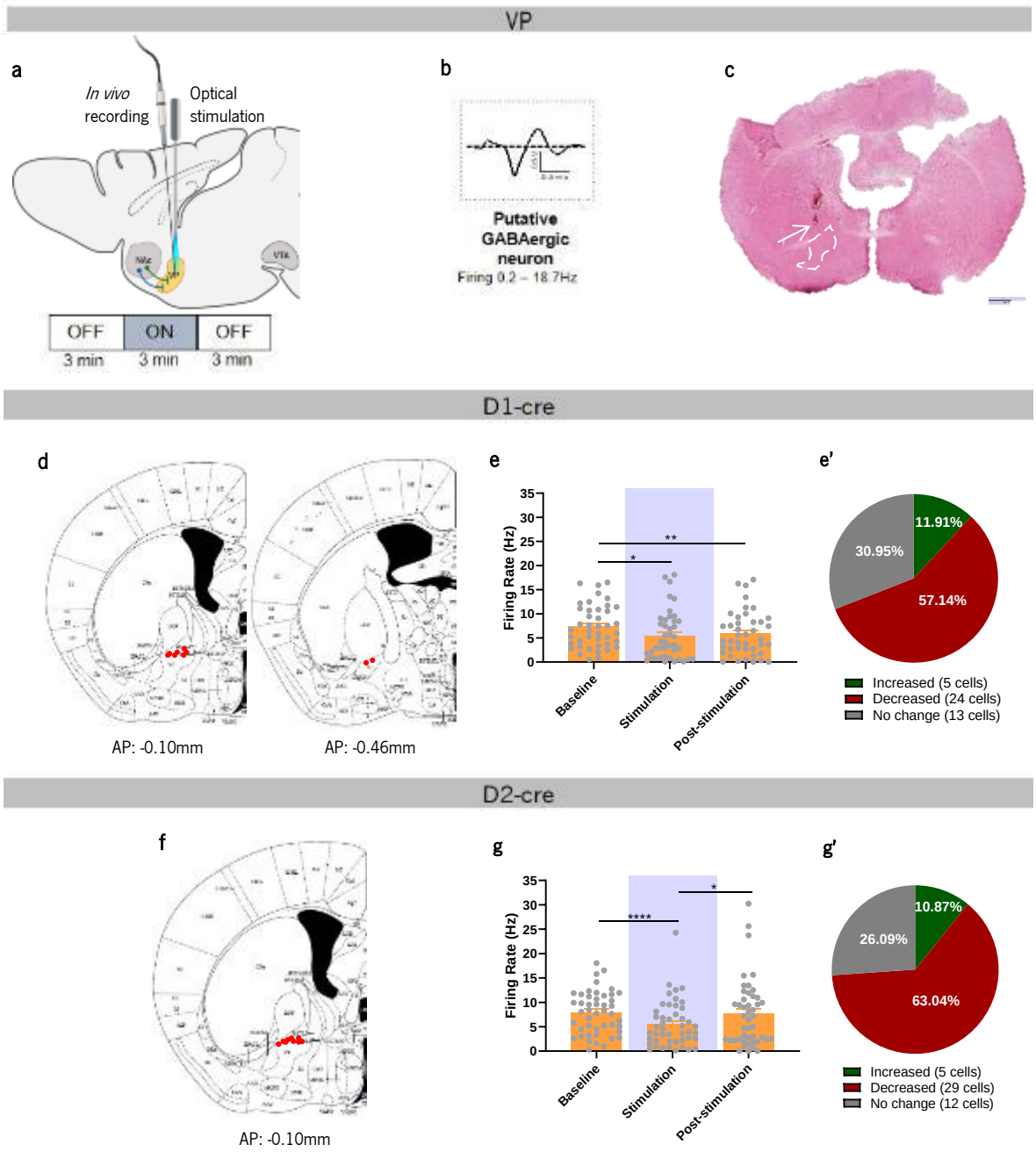


**Figure 13. Electrophysiological effects in VP neurons in response to optogenetic stimulation.** (**a**) Schematic representation of VP electrophysiological recordings during optogenetic stimulation protocol of 3-minute epochs: no stimulation (OFF), laser stimulation (ON), and no stimulation (OFF) (OFF-ON-OFF epochs). (**b**) VP neurons were classified as putative GABAergic neurons (pGABAergic) according to firing rate. (**c**) Representative image of hematoxylin-eosin coloration confirming the recording location in VP (VP is delineated by a white dashed line; white arrow indicates the cleft caused by the electrode + optic fiber). Scale bar 1mm. (**d**) Schematic representation of recording electrodes placement in VP of D1-cre mice (red dots). (**e**) Firing rate of pGABAergic neurons (orange; n = 42) in D1-cre mice. (**e'**) Percentage of neurons that increased (green; n = 5) decreased (red; n = 24) and did not change (grey; n = 13) firing rate during the stimulation period. (**f**) Schematic representation of recording electrodes placement in VP of D2-cre mice (red dots). (**g**) Firing rate of pGABAergic neurons (orange; n = 46) in D2-cre mice. (**g'**) Percentage of neurons that increased (green; n = 5), decreased (red; n = 29) and did not change (grey; n = 12) firing rate during the stimulation period. $^{*}p \leq 0.05$. Data are represented as mean ± SEM.

### 4.2.3. Electrophysiological effects in VTA neurons in response to D1-MSN stimulation

*In vivo* electrophysiological recordings in the VTA identified putative dopaminergic (pDAergic) and putative GABAergic neurons (pGABAergic) based on their basal firing rate and waveform half-width[74,168] (**Figure 14b**).

41.86% of the recorded VTA neurons were identified as pDAergic neurons and the remaining 58.14% were identified as pGABAergic neurons (**Figure 14e**). Optogenetic stimulation of D1-MSN terminals in the VTA did not alter the firing rate of pDAergic neurons, but significantly decrease the firing rate of pGABAergic neurons (**Figure 14e'**, pDAergic, $p = 0.1550$; pGABAergic, $p = 0.0033$, post hoc baseline *vs* stimulation $p = 0.0040$). 12% of pDAergic neurons increased their firing activity during the stimulation period, 56% of these neurons decreased their firing activity and 32% did not change their firing activity (**Figure 14e''**). Regarding pGABAergic neurons, 61.11% of the cells showed a decrease in their firing activity, and the remaining 38.89% did not change their activity (**Figure 14e''**).

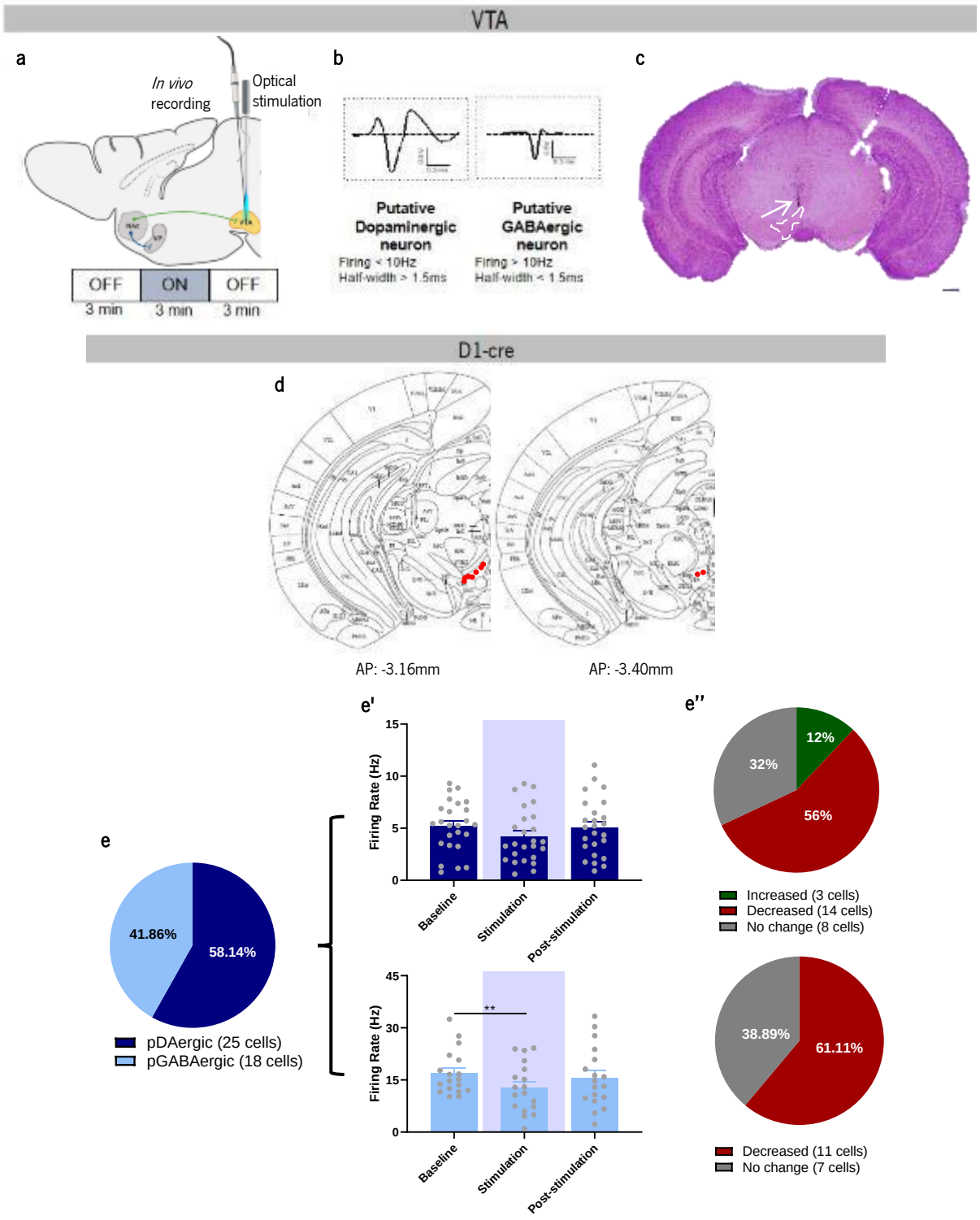


**Figure 14. Electrophysiological effects in VTA neurons in response to optogenetic stimulation.** (**a**) Schematic representation of VTA electrophysiological recordings during optogenetic stimulation protocol of 3-minute epochs: no stimulation (OFF), laser stimulation (ON), and no stimulation (OFF) (OFF-ON-OFF epochs). (**b**) VTA neurons were classified according to firing rate and waveform characteristics in putative dopaminergic neurons (pDAergic) and putative GABAergic neurons (pGABAergic). (**c**) Representative image of hematoxylin-eosin coloration confirming the recording location in VTA (VTA is delineated by a white dashed line; white arrow indicates the cleft caused by the electrode + optic fiber). Scale bar 1mm. (**d**) Schematic representation of recording electrodes placement in VTA of D1-cre mice (red dots). (**e**) Percentage of pDAergic (dark blue) and pGABAergic (light blue) neurons recorded in D1-cre mice. (**e'**) Firing rate of pDAergic (dark blue; n = 25) and pGABAergic (light blue; n = 18) neurons. (**e''**) Percentage of neurons that increased (green; $n_{pDAergic}$ = 3), decreased (red; $n_{pDAergic}$ = 14; $n_{pGABAergic}$ = 11) and did not change (grey; $n_{pDAergic}$ = 8; $n_{pGABAergic}$ = 7) firing rate during the stimulation period. Data are represented as mean ± SEM.

**Table 1.** Statistical analysis of the behavioral tests performed to evaluate anxiety- and depressive-like behaviors, and *in vivo* electrophysiological recordings. Data presented as MEAN ± SEM

*Statistics concerning interaction between time and ChR2/YFP factors (•), and within time (†) and ChR2/YFP (‡) factor*

| Figure | Mean ± SEM | Type of Test | Assume Sphericity? | Statistics |
|---|---|---|---|---|
| **5b** | YFP<br>Baseline: 40.70±12.23<br>Stimulation: 24.09±4.43<br>Post-stimulation: 27.17±3.33<br>ChR2<br>Baseline: 13.14±5.55<br>Stimulation: 9.33±4.17<br>Post-stimulation: 17.79±3.91 | Two-way ANOVA | No<br>Ɛ = 0.6549 | $\cdot F_{2,26} = 1.144$, $p = 0.3342$, $\eta^2_{partial} = 0.0809$<br>$^{\dagger}F_{1.310,17.03} = 1.376$, $p = 0.2679$, $\eta^2_{partial} = 0.0957$<br>$^{\ddagger}F_{1,13} = 8.064$, $p = 0.0139$, $\eta^2_{partial} = 0.3828$ |
| **5c** | YFP<br>Baseline: 4.00±0.63<br>Stimulation: 3.63±0.50<br>Post-stimulation: 2.88±0.30<br>ChR2<br>Baseline: 2.86±1.10<br>Stimulation: 1.86±0.74<br>Post-stimulation: 2.43±0.65 | Two-way ANOVA | No<br>Ɛ = 0.7870 | $\cdot F_{2,26} = 0.874$, $p = 0.4294$, $\eta^2_{partial} = 0.0630$<br>$^{\dagger}F_{1.574,20.46} = 1.445$, $p = 0.2557$, $\eta^2_{partial} = 0.1000$<br>$^{\ddagger}F_{1,13} = 2.180$, $p = 0.1636$, $\eta^2_{partial} = 0.1436$ |
| **5d** | YFP<br>Baseline: 40.70±12.23<br>Stimulation: 24.09±4.43<br>Post-stimulation: 27.17±3.33<br>ChR2<br>Baseline: 30.85±4.60<br>Stimulation: 27.83±3.93<br>Post-stimulation: 29.49±5.35 | Two-way ANOVA | No<br>Ɛ = 0.7082 | $\cdot F_{2,26} = 0.718$, $p = 0.4970$, $\eta^2_{partial} = 0.0524$<br>$^{\dagger}F_{1.416,18.41} = 1.351$, $p = 0.2740$, $\eta^2_{partial} = 0.0941$<br>$^{\ddagger}F_{1,13} = 0.044$, $p = 0.8375$, $\eta^2_{partial} = 0.0034$ |
| **5e** | YFP<br>Baseline: 4.00±0.63<br>Stimulation: 3.63±0.50<br>Post-stimulation: 2.88±0.30<br>ChR2<br>Baseline: 5.43±0.78<br>Stimulation: 5.00±0.54<br>Post-stimulation: 5.86±0.77 | Two-way ANOVA | No<br>Ɛ = 0.7383 | $\cdot F_{2,26} = 1.344$, $p = 0.278$, $\eta^2_{partial} = 0.0937$<br>$^{\dagger}F_{1.477,19.20} = 0.307$, $p = 0.6733$, $\eta^2_{partial} = 0.0231$<br>$^{\ddagger}F_{1,13} = 12.55$, $p = 0.0036$, $\eta^2_{partial} = 0.4912$<br>Sidak's post hoc:<br>D1-VTA-YFP Post-stimulation *vs* D1-VTA-ChR2 Post-stimulation: $p = 0.0213$ |
| **5f** | YFP<br>Baseline: 18.57±4.15<br>Stimulation: 25.54±4.97<br>Post-stimulation: 16.53±4.06<br>ChR2<br>Baseline: 41.16±9.07<br>Stimulation: 12.84±4.12<br>Post-stimulation: 8.76±2.09 | Two-way ANOVA | No<br>Ɛ = 0.7140 | $\cdot F_{2,30} = 9.707$, $p = 0.0006$, $\eta^2_{partial} = 0.3929$<br>$^{\dagger}F_{1.428,21.42} = 8.027$, $p = 0.0052$, $\eta^2_{partial} = 0.3486$<br>$^{\ddagger}F_{1,15} = 0.013$, $p = 0.9104$, $\eta^2_{partial} = 0.0009$<br>Tukey's post hoc:<br>D2-ChR2 Baseline *vs* D2-ChR2 Stimulation: $p = 0.0023$<br>D2-ChR2 Baseline *vs* D2-ChR2 Post-stimulation: $p = 0.0096$ |
| **5g** | YFP<br>Baseline: 3.71±0.61<br>Stimulation: 2.86±0.40<br>Post-stimulation: 2.71±0.71<br>ChR2<br>Baseline: 4.40±0.69<br>Stimulation: 1.80±0.44<br>Post-stimulation: 1.60±0.37 | Two-way ANOVA | No<br>Ɛ = 0.7784 | $\cdot F_{2,30} = 1.707$, $p = 0.1986$, $\eta^2_{partial} = 0.1022$<br>$^{\dagger}F_{1.557,23.35} = 7.203$, $p = 0.0062$, $\eta^2_{partial} = 0.3245$<br>$^{\ddagger}F_{1,15} = 1.126$, $p = 0.3053$, $\eta^2_{partial} = 0.0698$<br>Tukey's post hoc:<br>D2-ChR2 Baseline *vs* D2-ChR2 Stimulation: $p = 0.0322$<br>D2-ChR2 Baseline *vs* D2-ChR2 Post-stimulation: $p = 0.0216$ |

**Table 1.** (continuation)

| Figure | Mean ± SEM | Type of Test | Assume Sphericity? | Statistics |
|---|---|---|---|---|
| **6b** | YFP<br>Baseline: 2.42±0.54<br>Stimulation: 4.34±0.69<br>Post-stimulation: 4.45±0.98<br>ChR2<br>Baseline: 1.11±0.21<br>Stimulation: 1.58±0.58<br>Post-stimulation: 1.81±0.62 | Two-way ANOVA | No<br>Ɛ = 0.6247 | ·$F_{2,22}$ = 1.473, $p$ = 0.2511, $\eta^2_{partial}$ = 0.1181<br>†$F_{1.249,13.74}$ = 4.941, $p$ = 0.0370, $\eta^2_{partial}$ = 0.3099<br>‡$F_{1,11}$ = 10.200, $p$ = 0.0085, $\eta^2_{partial}$ = 0.4811<br>Sidak's post hoc:<br>D1-VP-YFP Stimulation *vs* D1-VP-ChR2 Stimulation: $p$ = 0.0347<br>D1-VP-ChR2 Baseline *vs* D1-VP-ChR2 Stimulation $p$ = 0.6284 |
| **6c** | YFP<br>Baseline: 0.64±0.12<br>Stimulation: 1.13±0.19<br>Post-stimulation: 0.66±0.07<br>ChR2<br>Baseline: 0.53±0.11<br>Stimulation: 0.50±0.12<br>Post-stimulation: 0.45±0.16 | Two-way ANOVA | No<br>Ɛ = 0.9346 | ·$F_{2,22}$ = 3.216, $p$ = 0.0596, $\eta^2_{partial}$ = 0.2262<br>†$F_{1.869,20.56}$ = 3.304, $p$ = 0.0598, $\eta^2_{partial}$ = 0.2310<br>‡$F_{1,11}$ = 5.035, $p$ = 0.0464, $\eta^2_{partial}$ = 0.3140<br>Tukey's post hoc:<br>D1-VP-YFP Stimulation *vs* D1-VP-YFP Post-stimulation: $p$ = 0.0384 |
| **6d** | YFP<br>Baseline: 12.33±3.05<br>Stimulation: 20.33±3.00<br>Post-stimulation: 14.00±3.79<br>ChR2<br>Baseline: 6.43±0.81<br>Stimulation: 10.43±2.78<br>Post-stimulation: 8.86±1.82 | Two-way ANOVA | No<br>Ɛ = 0.7867 | ·$F_{2,22}$ = 0.548, $p$ = 0.5856, $\eta^2_{partial}$ = 0.0475<br>†$F_{1.573,\ 17.31}$ = 3.119, $p$ = 0.0794, $\eta^2_{partial}$ = 0.2208<br>‡$F_{1,11}$ = 8.375, $p$ = 0.0146, $\eta^2_{partial}$ = 0.4323 |
| **6e** | YFP<br>Baseline: 176.04±41.29<br>Stimulation: 300.87±53.53<br>Post-stimulation: 188.17±30.44<br>ChR2<br>Baseline: 115.18±21.90<br>Stimulation: 116.05±37.61<br>Post-stimulation: 128.67±49.45 | Two-way ANOVA | No<br>Ɛ = 0.8788 | ·$F_{2,22}$ = 3.149, $p$ = 0.0627, $\eta^2_{partial}$ = 0.2226<br>†$F_{1.758,19.33}$ = 2.683, $p$ = 0.0991, $\eta^2_{partial}$ = 0.1961<br>‡$F_{1,11}$ = 4.791, $p$ = 0.0511, $\eta^2_{partial}$ = 0.3034 |
| **6f** | YFP<br>Baseline: 2.42±0.54<br>Stimulation: 4.34±0.69<br>Post-stimulation: 4.45±0.98<br>ChR2<br>Baseline: 2.22±0.49<br>Stimulation: 5.26±1.14<br>Post-stimulation: 3.82±0.89 | Two-way ANOVA | No<br>Ɛ = 0.7520 | ·$F_{2,20}$ = 0.472, $p$ = 0.6308, $\eta^2_{partial}$ = 0.0450<br>†$F_{1.504,15.04}$ = 4.865, $p$ = 0.0312, $\eta^2_{partial}$ = 0.3273<br>‡$F_{1,10}$ = 0.002, $p$ = 0.9657, $\eta^2_{partial}$ = 0.0002<br>Tukey's post hoc:<br>D1-VTA-ChR2 Baseline *vs* D1-VTA-ChR2 Stimulation: $p$ = 0.0413<br>D1-VTA-YFP Baseline *vs* D1-VTA-YFP Stimulation: $p$ = 0.0788 |
| **6g** | YFP<br>Baseline: 0.64±0.12<br>Stimulation: 1.13±0.19<br>Post-stimulation: 0.66±0.07<br>ChR2<br>Baseline: 1.01±0.21<br>Stimulation: 1.30±0.28<br>Post-stimulation: 0.70±0.10 | Two-way ANOVA | No<br>Ɛ = 0.9197 | ·$F_{2,20}$ = 0.454, $p$ = 0.6415, $\eta^2_{partial}$ = 0.0434<br>†$F_{1.839,18.39}$ = 5.590, $p$ = 0.0143, $\eta^2_{partial}$ = 0.3586<br>‡$F_{1,10}$ = 1.459, $p$ = 0.2549, $\eta^2_{partial}$ = 0.1273<br>Tukey's post hoc:<br>D1-VTA-ChR2 Baseline *vs* D1-VTA-ChR2 Stimulation: $p$ = 0.4762<br>D1-VTA-YFP Baseline *vs* D1-VTA-YFP Stimulation: $p$ = 0.1670<br>D1-VTA-YFP Stimulation *vs* D1-VTA-YFP Post-stimulation: $p$ = 0.0384 |

**Table 1.** (continuation)

| Figure | Mean ± SEM | Type of Test | Assume Sphericity? | Statistics |
|---|---|---|---|---|
| **6h** | YFP<br>Baseline: 12.33±3.05<br>Stimulation: 20.33±3.00<br>Post-stimulation: 14.00±3.79<br>ChR2<br>Baseline: 12.33±1.48<br>Stimulation: 25.17±3.08<br>Post-stimulation: 13.00±1.75 | Two-way ANOVA | No<br>Ɛ = 0.8053 | ·$F_{2,20}$ = 0.659, $p$ = 0.5282, $\eta^2_{partial}$ = 0.0618<br>†$F_{1.611,16.11}$ = 8.824, $p$ = 0.0040, $\eta^2_{partial}$ = 0.4688<br>‡$F_{1,10}$ = 0.2747, $p$ = 0.6116, $\eta^2_{partial}$ = 0.0267<br>Tukey's post hoc:<br>D1-VTA-ChR2 Baseline *vs* D1-VTA-ChR2 Stimulation: $p$ = 0.0157<br>Tukey's post hoc:<br>D1-VTA-ChR2 Stimulation *vs* D1-VTA-ChR2 Post-stimulation: $p$ = 0.0249<br>D1-VTA-YFP Stimulation *vs* D1-VTA-YFP Post-stimulation: $p$ = 0.2816 |
| **6i** | YFP<br>Baseline: 176.04±41.29<br>Stimulation: 300.87±53.53<br>Post-stimulation: 188.17±30.44<br>ChR2<br>Baseline: 246.11±52.70<br>Stimulation: 326.85±67.16<br>Post-stimulation: 201.59±33.57 | Two-way ANOVA | No<br>Ɛ = 0.8366 | ·$F_{2,20}$ = 0.231, $p$ = 0.7958, $\eta^2_{partial}$ = 0.0226<br>†$F_{1.673,16.73}$ = 4348, $p$ = 0.0357, $\eta^2_{partial}$ = 0.3030<br>‡$F_{1,10}$ = 0.639, $p$ = 0.4425, $\eta^2_{partial}$ = 0.1402<br>D1-VTA-ChR2 Baseline *vs* D1-VTA-ChR2 Stimulation: $p$ = 0.1572<br>D1-VTA-YFP Baseline *vs* D1-VTA-YFP Stimulation: $p$ = 0.1553 |
| **6j** | YFP<br>Baseline: 2.58±0.61<br>Stimulation: 2.78±0.57<br>Post-stimulation: 3.33±0.71<br>ChR2<br>Baseline: 1.72±0.32<br>Stimulation: 4.36±1.30<br>Post-stimulation: 3.49±0.99 | Two-way ANOVA | No<br>Ɛ = 0.8869 | ·$F_{2,30}$ = 2.377, $p$ = 0.1101, $\eta^2_{partial}$ = 0.1368<br>†$F_{1.774,26.61}$ = 3.814, $p$ = 0.0395, $\eta^2_{partial}$ = 0.2027<br>‡$F_{1,15}$ = 0.099, $p$ = 0.7570, $\eta^2_{partial}$ = 0.0066<br>D1-VP-ChR2 Baseline *vs* D1-VP-ChR2 Stimulation: $p$ = 0.1224 |
| **6k** | YFP<br>Baseline: 0.85±0.18<br>Stimulation: 0.86±0.14<br>Post-stimulation: 0.61±0.15<br>ChR2<br>Baseline: 0.73±0.19<br>Stimulation: 0.78±0.16<br>Post-stimulation: 0.41±0.09 | Two-way ANOVA | No<br>Ɛ = 0.7234 | ·$F_{2,30}$ = 0.092, $p$ = 0.9127, $\eta^2_{partial}$ = 0.0061<br>†$F_{1.447,21.70}$ = 3.497, $p$ = 0.0613, $\eta^2_{partial}$ = 0.1891<br>‡$F_{1,15}$ = 0.679, $p$ = 0.4227, $\eta^2_{partial}$ = 0.0433 |
| **6l** | YFP<br>Baseline: 15.33±3.35<br>Stimulation: 17.11±3.25<br>Post-stimulation: 14.33±2.73<br>ChR2<br>Baseline: 10.50±2.35<br>Stimulation: 11.25±2.64<br>Post-stimulation: 10.50±1.99 | Two-way ANOVA | No<br>Ɛ = 0.8608 | ·$F_{2,30}$ = 0.134, $p$ = 0.8749, $\eta^2_{partial}$ = 0.0089<br>†$F_{1.722,25.82}$ = 0.432, $p$ = 0.6244, $\eta^2_{partial}$ = 0.0280<br>‡$F_{1,15}$ = 2.174, $p$ = 0.1610, $\eta^2_{partial}$ = 0.1266 |
| **6m** | YFP<br>Baseline: 218.28±46.36<br>Stimulation: 230.21±40.38<br>Post-stimulation: 175.99±38.45<br>ChR2<br>Baseline: 169.92±40.27<br>Stimulation: 220.95±43.25<br>Post-stimulation: 136.92±24.78 | Two-way ANOVA | No<br>Ɛ = 0.6635 | ·$F_{2,30}$ = 0.260, $p$ = 0.7725, $\eta^2_{partial}$ = 0.0171<br>†$F_{1.327,19.91}$ = 2.989, $p$ = 0.0900, $\eta^2_{partial}$ = 0.1661<br>‡$F_{1,15}$ = 0.489, $p$ = 0.4951, $\eta^2_{partial}$ = 0.0316 |

**Table 1.** (continuation)

| Figure | Mean ± SEM | Type of Test | Assume Sphericity? | Statistics |
|---|---|---|---|---|
| **7b** | YFP<br>Baseline: 922.58±155.61<br>Stimulation: 940.31±139.76<br>Post-stimulation: 828.81±109.69<br>ChR2<br>Baseline: 755.971±95.59<br>Stimulation: 318.89±70.64<br>Post-stimulation: 398.64±110.41 | Two-way ANOVA | No<br>Ɛ = 0.9017 | ·$F_{2,28}$ = 2.804, $p$ = 0.0776, $\eta^2_{partial}$ = 1.1669<br>†$F_{1.803,25.25}$ = 3.409, $p$ = 0.0533, $\eta^2_{partial}$ = 0.1958<br>‡$F_{1,14}$ = 11.020, $p$ = 0.0051, $\eta^2_{partial}$ = 0.4404<br>Sidak's post hoc:<br>D1-VP-YFP Stimulation *vs* D1-VP-ChR2 Stimulation: $p$ = 0.0074<br>D1-VP-YFP Post-stimulation *vs* D1-VP-ChR2 Post-stimulation: $p$ = 0.0450<br>D1-VP-ChR2 Baseline *vs* D1-VP-ChR2 Stimulation: $p$ = 0.0132 |
| **7c** | YFP<br>Baseline: 28.73±5.23<br>Stimulation: 39.66±4.47<br>Post-stimulation: 37.45±5.58<br>ChR2<br>Baseline: 34.80±8.80<br>Stimulation: 12.46±3.83<br>Post-stimulation: 17.69±5.16 | Two-way ANOVA | No<br>Ɛ = 0.9255 | ·$F_{2,28}$ = 6.950, $p$ = 0.0035, $\eta^2_{partial}$ = 0.3317<br>†$F_{1.851,25.91}$ = 0.797, $p$ = 0.4526, $\eta^2_{partial}$ = 0.0539<br>‡$F_{1,14}$ = 5.087, $p$ = 0.0406, $\eta^2_{partial}$ = 0.2665<br>Sydak's post hoc:<br>D1-VP-YFP Stimulation *vs* D1-VP-ChR2 Stimulation: $p$ = 0.0013<br>Tukey's post hoc:<br>D1-VP-ChR2 Baseline *vs* D1-VP-ChR2 Stimulation: $p$ = 0.0499 |
| **7d** | YFP<br>Baseline: 3.81±0.58<br>Stimulation: 3.15±0.54<br>Post-stimulation: 2.77±0.39<br>ChR2<br>Baseline: 3.23±0.35<br>Stimulation: 1.33±0.31<br>Post-stimulation: 1.29±0.36 | Two-way ANOVA | No<br>Ɛ = 0.8177 | ·$F_{2,28}$ = 1.152, $p$ = 0.3304, $\eta^2_{partial}$ = 0.0760<br>†$F_{1.635,22.90}$ = 7.414, $p$ = 0.0051, $\eta^2_{partial}$ = 0.3461<br>‡$F_{1,14}$ = 12.090, $p$ = 0.0037, $\eta^2_{partial}$ = 0.4634<br>Sydak's post hoc:<br>D1-VP-YFP Stimulation *vs* D1-VP-ChR2 Stimulation: $p$ = 0.0400<br>D1-VP-YFP Post-stimulation *vs* D1-VP-ChR2 Post-stimulation: $p$ = 0.0414<br>Tukey's post hoc:<br>D1-VP-ChR2 Baseline *vs* D1-VP-ChR2 Stimulation: $p$ = 0.0245<br>D1-VP-ChR2 Baseline *vs* D1-VP-ChR2 Post-stimulation: $p$ = 0.0223 |
| **7e** | YFP<br>Baseline: 11.25±1.37<br>Stimulation: 7.50±1.00<br>Post-stimulation: 6.25±0.82<br>ChR2<br>Baseline: 6.63±0.78<br>Stimulation: 3.75±0.41<br>Post-stimulation: 3.50±1.05 | Two-way ANOVA | No<br>Ɛ = 0.7569 | ·$F_{2,28}$ = 0.475, $p$ = 0.6266, $\eta^2_{partial}$ = 0.0328<br>†$F_{1.514,21.19}$ = 10.090, $p$ = 0.0018, $\eta^2_{partial}$ = 0.4189<br>‡$F_{1,14}$ = 23.830, $p$ = 0.0002, $\eta^2_{partial}$ = 0.6299<br>Sidak's post hoc:<br>D1-VP-YFP Baseline *vs* D1-VP-ChR2 Baseline: $p$ = 0.0401<br>D1-VP-YFP Stimulation *vs* D1-VP-ChR2 Stimulation: $p$ = 0.0200<br>Tukey's post hoc:<br>D1-VP-ChR2 Baseline *vs* D1-VP-ChR2 Stimulation: $p$ = 0.0172<br>D1-VP-ChR2 Baseline *vs* D1-VP-ChR2 Post-stimulation: $p$ = 0.0266 |
| **7f** | YFP<br>Baseline: 922.58±155.61<br>Stimulation: 940.31±139.76<br>Post-stimulation: 828.81±109.69<br>ChR2<br>Baseline: 916.96±76.45<br>Stimulation: 575.63±116.98<br>Post-stimulation: 698.59±64.38 | Two-way ANOVA | No<br>Ɛ = 0.8203 | ·$F_{2,24}$ = 1.744, $p$ = 0.1963, $\eta^2_{partial}$ = 0.1269<br>†$F_{1.641,19.69}$ = 1.769, $p$ = 0.1994, $\eta^2_{partial}$ = 0.1285<br>‡$F_{1,12}$ = 1.517, $p$ = 0.2417, $\eta^2_{partial}$ = 0.1122 |

**Table 1.** (continuation)

| Figure | Mean ± SEM | Type of Test | Assume Sphericity? | Statistics |
|---|---|---|---|---|
| **7g** | YFP<br>Baseline: 28.73±5.23<br>Stimulation: 39.66±4.47<br>Post-stimulation: 37.45±5.58<br>ChR2<br>Baseline: 32.96±3.95<br>Stimulation: 28.98±6.50<br>Post-stimulation: 38.26±7.28 | Two-way ANOVA | No<br><br>Ɛ = 0.9332 | ·$F_{2,24}$ = 1.325, $p$ = 0.2845, $\eta^2_{partial}$ = 0.0994<br>†$F_{1.866,22.40}$ = 1.068, $p$ = 0.3565, $\eta^2_{partial}$ = 0.0817<br>‡$F_{1,12}$ = 0.111, $p$ = 0.7443, $\eta^2_{partial}$ = 0.0092 |
| **7h** | YFP<br>Baseline: 3.81±0.58<br>Stimulation: 3.15±0.54<br>Post-stimulation: 2.77±0.39<br>ChR2<br>Baseline: 3.92±0.38<br>Stimulation: 1.89±0.31<br>Post-stimulation: 2.21±0.24 | Two-way ANOVA | No<br><br>Ɛ = 0.6584 | ·$F_{2,24}$ = 1.485, $p$ = 0.2466, $\eta^2_{partial}$ = 0.1101<br>†$F_{1.317,15.80}$ = 7.836, $p$ = 0.0088, $\eta^2_{partial}$ = 0.3951<br>‡$F_{1,12}$ = 1.558, $p$ = 0.2358, $\eta^2_{partial}$ = 0.1149<br>Tukey's post hoc:<br>D1-VTA-ChR2 Baseline *vs* D1-VTA-ChR2 Stimulation: $p$ = 0.0038<br>D1-VTA-ChR2 Baseline *vs* D1-VTA-ChR2 Post-stimulation: $p$ = 0.0123 |
| **7i** | YFP<br>Baseline: 11.25±1.37<br>Stimulation: 7.50±1.00<br>Post-stimulation: 6.25±0.82<br>ChR2<br>Baseline:12.33±1.28<br>Stimulation: 5.50±0.99<br>Post-stimulation: 6.67±1.17 | Two-way ANOVA | No<br><br>Ɛ = 0.6663 | ·$F_{2,24}$ = 1.164, $p$ = 0.3291, $\eta^2_{partial}$ = 0.0884<br>†$F_{1.333,15.99}$ = 16.650, $p$ = 0.0004, $\eta^2_{partial}$ = 0.5812<br>‡$F_{1,12}$ = 0.026, $p$ = 0.8752, $\eta^2_{partial}$ = 0.0021<br>Tukey's post hoc:<br>D1-VTA-ChR2 Baseline *vs* D1-VTA-ChR2 Stimulation: $p$ = 0.0019<br>D1-VTA-ChR2 Baseline *vs* D1-VTA-ChR2 Post-stimulation: $p$ = 0.0021 |
| **7j** | YFP<br>Baseline: 987.62±168.30<br>Stimulation: 650.43±76.56<br>Post-stimulation: 539.39±77.03<br>ChR2<br>Baseline: 1095.36±111.84<br>Stimulation: 713.32±109.18<br>Post-stimulation: 683.52±69.86 | Two-way ANOVA | No<br><br>Ɛ = 0.7211 | ·$F_{2,34}$ = 0.135, $p$ = 0.8742, $\eta^2_{partial}$=0.0079<br>†$F_{1.442,24.52}$ = 17.340, $p$ < 0.0001, $\eta^2_{partial}$ = 0.5049<br>‡$F_{1,17}$ = 0.716, $p$ = 0.4094, $\eta^2_{partial}$ = 0.0404<br>Tukey's post hoc:<br>D2-VP-ChR2 Baseline *vs* D2-VP-ChR2 Stimulation: $p$ = 0.0368<br>D2-VP-ChR2 Baseline *vs* D2-VP-ChR2 Post-stimulation: $p$ = 0.0249<br>D2-VP-YFP Baseline *vs* D2-VP-YFP Post-stimulation: $p$ = 0.0114 |
| **7k** | YFP<br>Baseline: 33.85±6.46<br>Stimulation: 30.73±4.37<br>Post-stimulation: 24.61±4.41<br>ChR2<br>Baseline: 39.72±5.46<br>Stimulation: 33.31±4.01<br>Post-stimulation: 32.73±3.80 | Two-way ANOVA | No<br><br>Ɛ = 0.6873 | ·$F_{2,34}$ = 0.234, $p$ = 0.7924, $\eta^2_{partial}$ = 0.0136<br>†$F_{1.375,23.37}$ = 2.002, $p$ = 0.1672, $\eta^2_{partial}$ = 0.1054<br>‡$F_{1,17}$ = 1.261, $p$ = 0.2771, $\eta^2_{partial}$ = 0.0691 |
| **7l** | YFP<br>Baseline: 4.43±0.67<br>Stimulation: 2.22±0.23<br>Post-stimulation: 1.90±0.25<br>ChR2<br>Baseline: 4.72±0.56<br>Stimulation: 2.41±0.39<br>Post-stimulation: 2.32±0.21 | Two-way ANOVA | No<br><br>Ɛ = 0.6508 | ·$F_{2,34}$ = 0.056, $p$ = 0.9452, $\eta^2_{partial}$ = 0.0033<br>†$F_{1.302,22.13}$ = 33.110, $p$ < 0.0001, $\eta^2_{partial}$ = 0.6608<br>‡$F_{1,17}$ = 0.425, $p$ = 0.5231, $\eta^2_{partial}$ = 0.0244<br>Tukey's post hoc:<br>D2-VP-ChR2 Baseline *vs* D2-VP-ChR2 Stimulation: $p$ = 0.0030<br>D2-VP-ChR2 Baseline *vs* D2-VP-ChR2 Post-stimulation: $p$ = 0.0032<br>D2-VP-YFP Baseline *vs* D2-VP-YFP Stimulation: $p$ = 0.0198<br>D2-VP-YFP Baseline *vs* D2-VP-YFP Post-stimulation: $p$ = 0.0062 |

**Table 1.** (continuation)

| Figure | Mean ± SEM | Type of Test | Assume Sphericity? | Statistics |
|---|---|---|---|---|
| **7m** | YFP<br>Baseline: 9.22±1.49<br>Stimulation: 6.11±1.18<br>Post-stimulation: 5.33±0.90<br>ChR2<br>Baseline: 10.70±1.18<br>Stimulation: 7.70±0.79<br>Post-stimulation: 7.50±1.01 | Two-way ANOVA | No<br>ε = 0.9500 | ·$F_{2,34}$ = 0.084, $p$ = 0.9194, $\eta^2_{partial}$ = 0.0049<br>†$F_{1.900, 32.30}$ = 9.089, $p$ = 0.0009, $\eta^2_{partial}$ = 0.3484<br>‡$F_{1,17}$ = 2.217, $p$ = 0.1548, $\eta^2_{partial}$ = 0.1154<br>Tukey's post hoc:<br>D2-VP-YFP Baseline *vs* D2-VP-YFP Stimulation: $p$ = 0.0423<br>D2-VP-YFP Baseline *vs* D2-VP-YFP Post-stimulation: $p$ = 0.0294 |
| **8b** | YFP<br>Stimulation: 22.50±3.25<br>No Stimulation: 15.63±5.55<br>ChR2<br>Stimulation: 22.75±4.50<br>No Stimulation: 19.13±4.41 | Two-way ANOVA | Yes | ·$F_{1,14}$ = 0.104, $p$ = 0.7516, $\eta^2_{partial}$ = 0.0074<br>†$F_{1,14}$ = 1.088, $p$ = 0.3146, $\eta^2_{partial}$ = 0.0721<br>‡$F_{1,14}$ = 0.232, $p$ = 0.6378, $\eta^2_{partial}$ = 0.0163 |
| **8c** | YFP<br>Stimulation: 113.50±16.09<br>No Stimulation: 78.38±23.55<br>ChR2<br>Stimulation: 125.63±32.32<br>No Stimulation: 52.00±7.90 | Two-way ANOVA | Yes | ·$F_{1,14}$ = 0.811, $p$ = 0.3828, $\eta^2_{partial}$ = 0.0548<br>†$F_{1,14}$ = 6.478, $p$ = 0.0233, $\eta^2_{partial}$ = 0.3163<br>‡$F_{1,14}$ = 0.1008, $p$ = 0.7556, $\eta^2_{partial}$ = 0.0071<br>D1-VP-ChR2 Stimulation *vs* D1-VP-ChR2 No Stimulation $p$ = 0.0567 |
| **8d** | YFP<br>Stimulation: 182.50±27.82<br>No Stimulation: 250.00±28.35<br>ChR2<br>Stimulation: 241.25±23.26<br>No Stimulation: 240.00±22.15 | Mixed-effects analysis | Yes | ·$F_{1,13}$ = 5.993, $p$ = 0.0293, $\eta^2_{partial}$ = 0.3155<br>†$F_{1,13}$ = 5.524, $p$ = 0.0352, $\eta^2_{partial}$ = 0.2982<br>‡$F_{1,14}$ = 0.542, $p$ = 0.4738, $\eta^2_{partial}$ = 0.0373<br>Sydak's post hoc:<br>D1-VP-ChR2 Stimulation *vs* D1-VP-ChR2 No Stimulation $p$ = 0.9972<br>D1-VP-YFP No Stimulation *vs* D1-VP-YFP Stimulation: $p$ = 0.0079 |
| **8e** | YFP<br>Stimulation: 22.50±3.25<br>No Stimulation: 15.63±5.55<br>ChR2<br>Stimulation: 20.43±1.53<br>No Stimulation: 19.43±4.26 | Two-way ANOVA | Yes | ·$F_{1,13}$ = 0.449, $p$ = 0.5144, $\eta^2_{partial}$ = 0.0333<br>†$F_{1,13}$ = 0.807, $p$ = 0.3853, $\eta^2_{partial}$ = 0.0584<br>‡$F_{1,13}$ = 0.055, $p$ = 0.8175, $\eta^2_{partial}$ = 0.0042 |
| **8f** | YFP<br>Stimulation: 113.50±16.09<br>No Stimulation: 78.38±23.55<br>ChR2<br>Stimulation: 98.14±24.83<br>No Stimulation: 60.43±6.82 | Two-way ANOVA | Yes | ·$F_{1,13}$ = 0.005, $p$ = 0.9423, $\eta^2_{partial}$ = 0.0004<br>†$F_{1,13}$ = 4.302, $p$ = 0.0585, $\eta^2_{partial}$ = 0.2486<br>‡$F_{1,13}$ = 0.619, $p$ = 0.4455, $\eta^2_{partial}$ = 0.0455 |
| **8g** | YFP<br>Stimulation: 182.50±27.82<br>No Stimulation: 250.00±28.35<br>ChR2<br>Stimulation: 220.00±41.98<br>No Stimulation: 214.29±39.03 | Two-way ANOVA | Yes | ·$F_{1,13}$ = 9.058, $p$ = 0.0101, $\eta^2_{partial}$=0.4106<br>†$F_{1,13}$ = 6.451, $p$ = 0.0247, $\eta^2_{partial}$ = 0.3317<br>‡$F_{1,13}$ = 0.0004, $p$ = 0.9850, $\eta^2_{partial}$ = 0.00003<br>Sydak's post hoc:<br>D1-VTA-YFP No Stimulation *vs* D1-VTA-YFP Stimulation: $p$ = 0.0027 |
| **8h** | YFP<br>Stimulation: 29.22±4.45<br>No Stimulation: 23.11±4.70<br>ChR2<br>Stimulation: 37.10±5.45<br>No Stimulation: 15.50±3.63 | Two-way ANOVA | Yes | ·$F_{1,17}$ = 3.747, $p$ = 0.0697, $\eta^2_{partial}$ = 0.1806<br>†$F_{1,17}$ = 11.990, $p$ = 0.0030, $\eta^2_{partial}$ = 0.4136<br>‡$F_{1,17}$ = 0.0007, $p$ = 0.9797, $\eta^2_{partial}$ = 0.00004<br>Sydak's post hoc:<br>D2-VP-ChR2 No Stimulation *vs* D2-VP-ChR2 Stimulation: $p$ = 0.0022 |

**Table 1.** (continuation)

| Figure | Mean ± SEM | Type of Test | Assume Sphericity? | Statistics |
|---|---|---|---|---|
| **8i** | YFP<br>Stimulation: 86.56±9.66<br>No Stimulation: 87.44±10.67<br>ChR2<br>Stimulation: 140.20±6.19<br>No Stimulation: 85.90±24.90 | Two-way ANOVA | Yes | ·$F_{1,17}$ = 2.965, $p$ = 0.1032, $\eta^2_{partial}$ = 0.1485<br>†$F_{1,17}$ = 2.777, $p$ = 0.1139, $\eta^2_{partial}$ = 0.1404<br>‡$F_{1,17}$ = 3.331, $p$ = 0.0856, $\eta^2_{partial}$ = 0.1638<br>Sydak's post hoc:<br>D2-VP-ChR2 No Stimulation *vs* D2-VP-ChR2 Stimulation: $p$ = 0.0490<br>D2-VP-YFP No Stimulation *vs* D2-VP-ChR2 Stimulation: $p$ = 0.0345 |
| **8j** | YFP<br>Stimulation: 256.67±20.00<br>No Stimulation: 222.22±15.26<br>ChR2<br>Stimulation: 304.00±34.90<br>No Stimulation: 253.00±31.09 | Two-way ANOVA | Yes | ·$F_{1,17}$ = 0.261, $p$ = 0.6163, $\eta^2_{partial}$=0.0151<br>†$F_{1,17}$ = 6.940, $p$ = 0.0174, $\eta^2_{partial}$ = 0.2899<br>‡$F_{1,17}$ = 1.229, $p$ = 0.2830, $\eta^2_{partial}$ = 0.0674<br>D2-VP-ChR2 No Stimulation *vs* D2-VP-ChR2 Stimulation: $p$ = 0.0697 |
| **9b** | YFP<br>Baseline: 40.41±10.16<br>Stimulation: 31.87±11.31<br>Post-stimulation: 27.10±12.16<br>ChR2<br>Baseline: 42.68±8.33<br>Stimulation: 72.68±4.90<br>Post-stimulation: 87.37±2.60 | Two-way ANOVA | No<br>Ɛ = 0.6763 | ·$F_{2,26}$ = 12.50, $p$ = 0.0002, $\eta^2_{partial}$ = 0.4902<br>†$F_{1.353,17.58}$ = 3.688, $p$ = 0.0607, $\eta^2_{partial}$ = 0.2211<br>‡$F_{1,13}$ = 9.253, $p$ = 0.0094, $\eta^2_{partial}$ = 0.4158<br>Sydak's post hoc:<br>D1-VP-YFP Stimulation *vs* D1-VP-ChR2 Stimulation: $p$ = 0.0252<br>D1-VP-YFP Post-stimulation *vs* D1-VP-ChR2 Post-stimulation: $p$ = 0.0044<br>Tukey's post hoc:<br>D1-VP-ChR2 Baseline *vs* D1-VP-ChR2 Post-stimulation: $p$ = 0.0058 |
| **9c** | YFP<br>Baseline: 3.08±0.79<br>Stimulation: 37.14±22.19<br>Post-stimulation: 40.42±18.85<br>ChR2<br>Baseline: 6.72±2.43<br>Stimulation: 4.82±1.13<br>Post-stimulation: 17.50±8.40 | Two-way ANOVA | No<br>Ɛ = 0.7483 | ·$F_{2,26}$ = 0.970, $p$ = 0.3923, $\eta^2_{partial}$ = 0.0695<br>†$F_{1.497,19.46}$ = 1.676, $p$ = 0.2146, $\eta^2_{partial}$ = 0.1142<br>‡$F_{1,13}$ = 2.695, $p$ = 0.1246, $\eta^2_{partial}$ = 0.1717 |
| **9d** | YFP<br>Baseline: 40.41±10.16<br>Stimulation: 31.87±11.31<br>Post-stimulation: 27.10±12.16<br>ChR2<br>Baseline: 24.81±5.96<br>Stimulation: 37.81±10.35<br>Post-stimulation: 31.71±14.94 | Two-way ANOVA | No<br>Ɛ = 0.7053 | ·$F_{2,26}$ = 2.237, $p$ = 0.1269, $\eta^2_{partial}$ = 0.1468<br>†$F_{1.411,18.34}$ = 0.459, $p$ = 0.5725, $\eta^2_{partial}$ = 0.0341<br>‡$F_{1,13}$ = 0.014, $p$ = 0.9087, $\eta^2_{partial}$ = 0.0011<br>D1-VTA-ChR2 Baseline *vs* D1-VTA-ChR2 Stimulation $p$ = 0.2378<br>D1-VTA-YFP Baseline *vs* D1-VTA-YFP Post-stimulation $p$ = 0.3862 |
| **9e** | YFP<br>Baseline: 3.08±0.79<br>Stimulation: 37.14±22.19<br>Post-stimulation: 40.42±18.85<br>ChR2<br>Baseline: 12.41±7.67<br>Stimulation: 31.74±24.77<br>Post-stimulation: 63.45±30.77 | Two-way ANOVA | No<br>Ɛ = 0.9781 | ·$F_{2,26}$ = 0.290, $p$ = 0.751, $\eta^2_{partial}$ = 0.0218<br>†$F_{1.956,25.43}$ = 2.837, $p$ = 0.0768, $\eta^2_{partial}$ = 0.1791<br>‡$F_{1,13}$ = 0.247, $p$ = 0.6278, $\eta^2_{partial}$ = 0.0186 |

**Table 1.** (continuation)

| Figure | Mean ± SEM | Type of Test | Assume Sphericity? | Statistics |
|---|---|---|---|---|
| **9f** | YFP<br>Baseline: 49.58±5.89<br>Stimulation: 53.83±10.65<br>Post-stimulation: 63.89±11.84<br>ChR2<br>Baseline: 33.48±7.68<br>Stimulation: 35.86±10.03<br>Post-stimulation: 35.86±11.41 | Two-way ANOVA | No<br><br>Ɛ = 0.7872 | ·$F_{2,34}$ = 1.483, $p$ = 0.2413, $\eta^2_{partial}$ = 0.0802<br>†$F_{1.574,26.77}$ = 0.205, $p$ = 0.7635, $\eta^2_{partial}$ = 0.0119<br>‡$F_{1,17}$ = 4.132, $p$ = 0.0580, $\eta^2_{partial}$ = 0.1955 |
| **9g** | YFP<br>Baseline: 21.11±10.01<br>Stimulation: 46.55±25.31<br>Post-stimulation: 12.19±4.26<br>ChR2<br>Baseline: 6.77±4.85<br>Stimulation: 22.73±17.53<br>Post-stimulation: 64.88±25.86 | Two-way ANOVA | No<br><br>Ɛ = 0.9730 | ·$F_{2,34}$ = 3.945, $p$ = 0.0288, $\eta^2_{partial}$ = 0.1884<br>†$F_{1.946,33.08}$ = 1.586, $p$ = 0.2203, $\eta^2_{partial}$ = 0.0853<br>‡$F_{1,17}$ = 0.077, $p$ = 0.7847, $\eta^2_{partial}$ = 0.0045<br>Tukey's post hoc:<br>D2-VP-ChR2 Baseline *vs* D2-VP-ChR2 Post-stimulation: $p$ = 0.0200 |
| **10b** | YFP<br>Baseline: 64.01±4.36<br>Stimulation: 65.25±2.97<br>Post-stimulation: 68.65±5.06<br>ChR2<br>Baseline: 66.09±4.30<br>Stimulation: 72.60±3.14<br>Post-stimulation: 72.84±4.63 | Two-way ANOVA | No<br><br>Ɛ = 0.9514 | ·$F_{2,26}$ = 0.389, $p$ = 0.6815, $\eta^2_{partial}$ = 0.0291<br>†$F_{1.903,24.74}$ = 1.867, $p$ = 0.1771, $\eta^2_{partial}$ = 0.1256<br>‡$F_{1,13}$ = 0.905, $p$ = 0.3588, $\eta^2_{partial}$ = 0.0651 |
| **10c** | YFP<br>Baseline: 8.69±4.60<br>Stimulation: 5.14±1.52<br>Post-stimulation: 12.40±3.73<br>ChR2<br>Baseline: 2.94±1.17<br>Stimulation: 6.79±3.10<br>Post-stimulation: 25.22±6.80 | Two-way ANOVA | No<br><br>Ɛ = 0.8490 | ·$F_{2,26}$ = 2.796, $p$ = 0.0795, $\eta^2_{partial}$ = 1.1770<br>†$F_{1.698,22.07}$ = 7.121, $p$ = 0.0057, $\eta^2_{partial}$ = 0.3540<br>‡$F_{1,13}$ = 0.8397, $p$ = 0.3762, $\eta^2_{partial}$ = 0.0607<br>Tukey's post hoc:<br>D1-VP-ChR2 Baseline *vs* D1-VP-ChR2 Post-stimulation: $p$ = 0.0364<br>D1-VP-ChR2 Baseline *vs* D1-VP-ChR2 Stimulation: $p$ = 0.5872 |
| **10d** | YFP<br>Baseline: 64.01±4.36<br>Stimulation: 65.25±2.97<br>Post-stimulation: 68.65±5.06<br>ChR2<br>Baseline: 63.41±3.60<br>Stimulation: 73.69±3.68<br>Post-stimulation: 79.98±3.92 | Two-way ANOVA | No<br><br>Ɛ = 0.8053 | ·$F_{2,26}$ = 1.687, $p$ = 0.2047, $\eta^2_{partial}$ = 0.1149<br>†$F_{1.611,20.94}$ = 4.907, $p$ = 0.0235, $\eta^2_{partial}$ = 0.2741<br>‡$F_{1,13}$ = 2.360, $p$ = 0.1485, $\eta^2_{partial}$ = 0.1536<br>Tukey's post hoc:<br>D1-VTA-ChR2 Baseline *vs* D1-VTA-ChR2 Stimulation: $p$ = 0.3020<br>D1-VTA-ChR2 Baseline *vs* D1-VTA-ChR2 Post-stimulation: $p$ = 0.0250 |
| **10e** | YFP<br>Baseline: 8.69±4.60<br>Stimulation: 5.14±1.52<br>Post-stimulation: 12.40±3.73<br>ChR2<br>Baseline: 4.02±2.22<br>Stimulation: 16.46±7.58<br>Post-stimulation: 34.48±12.67 | Two-way ANOVA | No<br><br>Ɛ = 0.7161 | ·$F_{2,26}$ = 2.116, $p$ = 0.1408, $\eta^2_{partial}$ = 0.1400<br>†$F_{1.432,18.62}$ = 3.672, $p$ = 0.0580, $\eta^2_{partial}$ = 0.2202<br>‡$F_{1,13}$ = 4.253, $p$ = 0.0598, $\eta^2_{partial}$ = 0.2465 |

**Table 1.** (continuation)

| Figure | Mean ± SEM | Type of Test | Assume Sphericity? | Statistics |
|---|---|---|---|---|
| **10f** | YFP<br>Baseline: 64.01±3.68<br>Stimulation: 77.66±2.24<br>Post-stimulation: 75.14±3.50<br>ChR2<br>Baseline: 62.07±4.59<br>Stimulation: 67.31±3.81<br>Post-stimulation: 69.90±5.45 | Two-way ANOVA | No<br>Ɛ = 0.9719 | ·$F_{2,32}$ = 0.474, $p$ = 0.6268, $\eta^2_{partial}$ = 0.0288<br>†$F_{1.944,31.10}$ = 3.150, $p$ = 0.0581, $\eta^2_{partial}$ = 0.1645<br>‡$F_{2,16}$ = 3.301, $p$ = 0.0880, $\eta^2_{partial}$ = 0.1710 |
| **10g** | YFP<br>Baseline: 4.67±2.30<br>Stimulation: 10.15±2.78<br>Post-stimulation: 16.49±5.64<br>ChR2<br>Baseline: 8.98±3.20<br>Stimulation: 9.09±1.85<br>Post-stimulation: 16.75±5.96 | Two-way ANOVA | No<br>Ɛ = 0.7513 | ·$F_{2,32}$ = 0.310, $p$ = 0.7359, $\eta^2_{partial}$ = 0.0190<br>†$F_{1.503,24.04}$ = 4.025, $p$ = 0.0413, $\eta^2_{partial}$ = 0.2011<br>‡$F_{1,16}$ = 0.087, $p$ = 0.7712, $\eta^2_{partial}$ = 0.0054<br>Tukey's post hoc:<br>D2-VP-YFP Baseline *vs* D2-VP-YFP Post-stimulation: $p$ = 0.0476 |
| **11b** | YFP<br>Stimulation: 98.41±1.59<br>No Stimulation: 98.70±1.30<br>ChR2<br>Stimulation: 99.47±0.53<br>No Stimulation: 99.38±0.62 | Two-way ANOVA | Yes | ·$F_{1,12}$ = 0.026, $p$ = 0.8756, $\eta^2_{partial}$ = 0.0021<br>†$F_{1,12}$ = 0.007, $p$ = 0.9356, $\eta^2_{partial}$ = 0.0006<br>‡$F_{1,12}$ = 0.739, $p$ = 0.4067, $\eta^2_{partial}$ = 0.0580 |
| **11c** | YFP<br>Stimulation: 98.41±1.59<br>No Stimulation: 98.70±1.30<br>ChR2<br>Stimulation: 99.21±0.79<br>No Stimulation: 98.72±1.28 | Two-way ANOVA | Yes | ·$F_{1,11}$ = 0.075, $p$ = 0.7892, $\eta^2_{partial}$ = 0.0068<br>†$F_{1,11}$ = 0.005, $p$ = 0.9451, $\eta^2_{partial}$ = 0.0005<br>‡$F_{1,11}$ = 0.115, $p$ = 0.7415, $\eta^2_{partial}$ = 0.0103 |
| **11d** | YFP<br>Stimulation: 90.82±3.08<br>No Stimulation: 98.81±0.80<br>ChR2<br>Stimulation: 90.28±2.24<br>No Stimulation: 100.00±0.00 | Two-way ANOVA | Yes | ·$F_{1,15}$ = 0.207, $p$ = 0.6555, $\eta^2_{partial}$ = 0.0136<br>†$F_{1,15}$ = 21.66, $p$ = 0.0003, $\eta^2_{partial}$ = 0.5908<br>‡$F_{1,15}$ = 0.029, $p$ = 0.8667, $\eta^2_{partial}$ = 0.0019<br>Sidak's post hoc:<br>D2-VP-ChR2 No Stimulation *vs* D2-VP-ChR2 Stimulation: $p$ = 0.0041<br>D2-VP-YFP No Stimulation *vs* D2-VP-YFP Stimulation: $p$ = 0.0225 |
| **12e'** | pMSN<br>Baseline: 2.67±0.33<br>Stimulation:1.47±0.49<br>Post-stimulation:1.61±0.52<br>pCIN<br>Baseline: 7.38±0.73<br>Stimulation:3.89±0.53<br>Post-stimulation:6.74±0.99 | One-way ANOVA | No<br>pMSN<br>Ɛ = 0.6018<br>pCIN<br>Ɛ = 0.5161 | pMSN:<br>†$F_{1.204,9.629}$ = 5.140, $p$ = 0.0430, $\eta^2_{partial}$ = 0.3912<br>pCIN:<br>†$F_{1.032,4.129}$ = 6.569, $p$ = 0.0602, $\eta^2_{partial}$ = 0.6215 |
| **12g'** | pMSN<br>Baseline: 2.81±0.74<br>Stimulation: 1.95±0.57<br>Post-stimulation: 3.39±1.24<br>pCIN<br>Baseline: 7.055±0.00<br>Stimulation:5.56±0.00<br>Post-stimulation:9.14±0.00 | One-way ANOVA | No<br>pMSN<br>Ɛ = 0.5058 | pMSN:<br>†$F_{1.012,4.047}$ = 1.484, $p$ = 0.2902, $\eta^2_{partial}$ = 0.2707 |

**Table 1.** (continuation)

| Figure | Mean ± SEM | Type of Test | Assume Sphericity? | Statistics |
|---|---|---|---|---|
| **13e** | pGABAergic<br>Baseline: 7.34±0.68<br>Stimulation: 5.47±0.77<br>Post-stimulation: 5.84±0.71 | Friedman Test | – | $\chi^2 = 10.43$, $p = 0.0054$<br>Dunn's post hoc:<br>Baseline *vs* Stimulation: $p = 0.0265$<br>Baseline *vs* Post-stimulation: $p = 0.0097$ |
| **13g** | pGABAergic<br>Baseline: 7.94±0.64<br>Stimulation: 5.54±0.70<br>Post-stimulation: 7.62±1.01 | Friedman Test | – | $\chi^2 = 17.52$, $p = 0.0002$<br>Dunn's post hoc:<br>Baseline *vs* Stimulation: $p < 0.0001$<br>Baseline *vs* Post-stimulation: $p = 0.0495$ |
| **14e'** | pDAergic<br>Baseline: 5.22±0.49<br>Stimulation: 4.22±0.51<br>Post-stimulation: 5.07±0.55<br>pGABAergic<br>Baseline: 16.96±1.51<br>Stimulation: 12.72±1.68<br>Post-stimulation: 15.63±2.05 | One-way ANOVA | No<br><br>pDAergic<br>$\varepsilon = 0.9812$<br><br>pGABAergic<br>$\varepsilon = 0.8220$ | pDAergic:<br>$^{\dagger}F_{1.962,47.10} = 1.945$, $p = 0.1550$, $\eta^2_{partial} = 0.0749$<br>pGABAergic:<br>$^{\dagger}F_{1.644,27.95} = 7.835$, $p = 0.0033$, $\eta^2_{partial} = 0.3155$<br>Tukey's post hoc:<br>Baseline *vs* Stimulation: $p = 0.0040$ |

# Chapter 5 – Discussion

## 5. Discussion

In the last years, the development of sophisticated techniques to manipulate neuronal activity in a specific manner allowed researchers to better understand the neurobiological basis of behavior. Optogenetic approaches have been adopted as a core technique in neuroscience, because it allows bidirectional manipulation of specific neuronal circuits with anatomical, genetic and temporal precision[169]. Because of these advantages, this technique has been used to study the neural basis of psychiatric disorders such as depression and anxiety[170,171].

Increased vigilance, freezing, hypoactivity and suppressed food consumption (among others) are behavioral responses produced by anxiety. In rodents, anxiety-like behaviors are characterized as those elicited by aversive stimuli[131]. Thus, avoidance is a core feature of anxiety[132,133]. On the other hand, anhedonia, assessed as lack of pleasure, the loss of appetite and motivation towards everyday positive rewards, is a common symptom of depressive-like behavior, evidencing the involvement of the reward circuit in this mood disorder[3,5,114–117].

In order to unravel the relation between the function of the reward circuit and the emergence of mood disorders like depression and anxiety, optogenetic studies have been mainly performed in stress models, such as the chronic mild stress and the chronic social defeat stress[76,114,117,124–127,172,173]; however, the results are not clear, evidencing the complexity of the neuronal circuits involved.

### The role of NAc MSNs in behavior

Canonically, D1- and D2-MSNs have been demonstrated to have distinct roles in reward, being D1-MSNs responsible for positive rewarding events, and D2-MSNs responsible for the mediation of aversion[97]. Nonetheless, over the past years, studies have shown that this proposed opposing role is not so clear. Researchers showed that stimulation of D1-MSNs enhanced cocaine conditioning, whereas a decrease in cocaine effects was caused by D2-MSNs optogenetic stimulation[100], suggesting that D1-MSNs were pro-reward and D2-MSNs had an “aversive” role. However, stimulation of D2-MSNs per se did not lead to any preference or aversion whatsoever[100]. Nonetheless, recent studies from our team have shown that D1- and D2-MSNs can drive both reward and aversion, depending on their stimulation pattern[74,99,103]. A brief optogenetic stimulation of either MSN subtype induced positive reinforcement, while prolonged optogenetic stimulation of the same neuronal subpopulation induced aversion[74]. Also, others have shown that accumbal D1- and D2-MSN optical activation supports self-stimulation (positive reinforcement)[105].

In the present work, we went beyond the study of D1- and D2-MSNs in reward and took advantage of optogenetic strategies to attempt to dissect the role of these NAc MSN subtypes in anxiety- and depressive-like behaviors. We used animals injected with an AAV5 virus carrying a cre-dependent expression of ChR2, which allowed selective optogenetic stimulation of D1- or D2-MSNs that specifically project to VP or VTA. Optical manipulation of MSN terminals in VP or VTA was performed during the execution of a battery of validated behavioral tests to assess anxiety- and depressive-like behaviors.

Using this approach, we showed that both D1- and D2-MSNs are distinctly involved in anxiety- and depressive-like behaviors.

Role of NAc MSNs in anxious-like behavior

To assess anxiety-like behavior, we performed the EPM, OF, light/dark box and NSF tests. EPM, OF and light/dark box tests take advantage of natural preferences for dark spaces and aversions to illuminated, open, and elevated areas, traits that rodents naturally present. Thus, an anxious-like phenotype is considered when rodents present higher latencies to enter and/or lower amounts of time spent in a more exposed and illuminated area[131,174,175]. The NSF test measures anxiety levels by the amount of time that an animal takes to enter the center of the arena (anxiogenic environment) and starts food consumption. Animals with a longer latency to eat are described as anxious[176].

Our present data shows an anxious-like phenotype caused by stimulation of D1-MSN terminals in the VP and VTA, and by stimulation of D2-MSN terminals in the VP, although this phenotype is not observed in all behavioral tests.

Optogenetic stimulation of D1-MSN terminals in VP provoked an anxiety-like behavior measured by the light/dark box. This optogenetic manipulation led to a decrease in distance traveled, time spent, time in ambulation and number of entries in the light zone of the light/dark box (**Figure 7b**, **c**, **d** and **e**). Importantly, stimulation did not lead to behavioral changes in control animals. The NSF test showed a tendency to a higher latency to begin a feeding episode during stimulation session; however, control animals also presented similar results, so these changes were not a direct response to stimulation (**Figure 8c**). To note, stimulation of these terminals revealed a statistically significant difference in the time spent in the center portion of the OF arena when compared with the control group (**Figure 6b**); however, D1-VP-YFP animals slightly increased the time spent in the center of the arena between the third and the sixth minutes of the test that stabilized in the last 3-minute epoch. Thus, the stimulation was not the only factor that led to this decrease in time spent in the center arena.

Similarly, an anxious-like phenotype was observed in D1-VTA-ChR2 animals in the light/dark box test during stimulation. Specifically, time in ambulation and the number of entries were reduced with stimulation (**Figure 7h** and **i**). Since the distance traveled had a tendency to decrease (**Figure 7f**) and time spent in the light zone was not altered (**Figure 7g**), it is possible to conclude that these animals spent more time immobile in the anxious arena hinting to a freezing phenotype, characteristic of anxiety-like behavior. The NSF test also showed a tendency to a higher latency to begin a feeding episode during the stimulation session; however, control animals also presented similar results, so it remains unclear if these changes were due to stimulation itself (**Figure 8f**). Surprisingly, stimulation of D1-MSN terminals in the VTA led to a significant increase in time spent in the center of the OF arena (**Figure 6f**) and number of entries in such arena (**Figure 6h**). However, neither time in ambulation (**Figure 6g**) nor distance traveled (**Figure 6i**) in this anxious arena were affected. So, during stimulation, animals spent more time in transitions between center and periphery. This result can be interpreted as an anxious phenotype once the increased time in the center of the arena was not spent in movement, thus being a result of constant entries in the zone.

D2-VP-ChR2 group was the one showing anxiety-like behavior in all tests performed, except in the OF test. In EPM, the time spent and the number of entries in open arms decreased significantly with stimulation, and interestingly remained at lower levels after stimulation (**Figure 5f** and **g**). The absence of returning to basal levels after stimulation was not expected and could indicate a *delayed/carry-over* effect of the stimulation in VP activity, contributing for the anxious phenotype even after termination of stimulation. Results of light/dark box test demonstrated an anxious-like phenotype provoked by stimulation of such neurons, since both distance and time in ambulation in light zone decreased (**Figure 7j** and **l**). Importantly, the locomotor activity was not affected (**Figure 6j**, **k**, **l** and **m**), so these results are not a reflex of possible motor dysfunction. It is important to highlight that over time both groups tended to decrease the distance, time spent, time in ambulation and number of entries in the light zone, so this may not be necessarily a consequence of stimulation (**Figure 7j**, **k**, **l** and **m**). A possible explanation could be the familiarity with the apparatus once our protocol is more extensive than the standard one (test duration of 10 minutes versus 15 minutes), resulting in a decrease in exploratory behavior. Finally, the anxious-like phenotype was also evident in the NSF test, where the stimulation session led to a higher latency to reach the pellet in the center of the arena and to begin a feeding episode (**Figure 8h** and **i**). This is a measure of anxious-like phenotype because food consumption, measured immediately after the test, was not affected, meaning lack of anhedonia symptoms (**Figure 8j**).

It is of relevance to relate these results with previous ones from our team showing that both MSN subtypes can induce reward and aversion, depending on the stimulation protocol[74]. In the present work, we used a prolonged stimulation protocol, which previously was reported to induce aversion, which is highly related to anxiety. If the stimulation protocol used in the present study did in fact cause an increase in aversive behavior, it might have significantly accounted for the decreased mobility of the animals and overall aversion for anxiolytic spaces. Although we did not perform any behavioral test to directly measure fear/avoidance, by analyzing the video camera recordings of the anxiety-like behavioral tasks, no freezing was observed in any of the tasks and locomotor activity was not altered by optogenetic stimulation. One way to control for this would be to evaluate freezing behavior of animals, and to measure innate responses to aversive stimuli such as heart and respiratory rate[177].

Role of NAc MSNs in depressive-like behavior

Optogenetic activation of both NAc MSN subtypes in animals exposed to social stress has shown an opposing role in depressive-like behaviors[124,125]. Indeed, optogenetic stimulation of D1-MSNs ameliorates depressive-like phenotypes while stimulation of D2-MSNs increases depressive-like phenotypes[124,125]. Besides, D1-MSN activity was found as a predictive marker of depression susceptibility, since naïve animals performing a social interaction task presented increased D1-MSN activity[126].

To assess depressive-like behavior, we performed the FST, TST and lastly the SDT to measure anhedonia, an important feature of this disorder. The FST and TST are based on the measurement of the duration of immobility when rodents are exposed to an inescapable situation[178]. When rodents are forced to swim or climb in a tight space where there is no escape, they adopt an immobile posture. This characteristic indicates that animals learned that it is impossible to escape and so preserve energy as if they have hope of escaping from this stressful situation. Subsequently, it was found that immobility is reduced by a wide range of clinically active antidepressants[178]. So, the longer the immobility time, the greater the depressive-like behavior.

Here, we showed that optogenetic activation of D1-MSN terminals in the VP led to a depressive-like phenotype measured by the FST. Throughout the session, the time that D1-VP-ChR2 animals spent immobile increased. Nevertheless, not all animals behaved the same way since these values are very dispersed. Even so, statistical differences were observed during stimulation, when compared the stimulated group with the control group. Interestingly, this difference persisted after cessation of stimulation (**Figure 9b**).

Stimulation of D1-MSN terminals in the VTA did not show statistical differences neither in the FST nor in the TST (**Figure 9d** and **e**; **Figure 10d** and **e**). However, there was a tendency to increase the time spent immobile during the protocol of TST, being statistical different between baseline and post-stimulation periods (**Figure 10d**).

Stimulation of D2-MSN terminals in the VP did not provoke a depressive-like phenotype neither in the FST nor in the TST (**Figure 9f** and **g**; **Figure 10f** and **g**).

There are some differences in the experimental design that we used that need to be discussed. Typically, the FST and TST have a duration of 6 minutes, although just the last 4 minutes are analyzed in the FST since the immobility is more prominent in this period[178]. It is important to highlight that our protocols were more extensive than the original ones, and in the case of FST, we evaluated the time since the beginning, not just the last minutes. So, the lower values of time spent immobile during baseline may be because of this evaluation methodology. Furthermore, the fact that animals had a ferrule implanted in the skull, fixed with dental cement could also be a reason for the dispersion of the time spent immobile within each group. Some animals could have a higher amount of dental cement, resulting in a greater weight in their head, which conveyed in greater difficulty in staying immobile. Interestingly, TST did not show lower values for immobility time in the baseline. Furthermore, individual values were not so dispersed in the TST as in the FST, reinforcing the theory that the cement weight could influence the performance of each animal in the FST. One interesting approach that we could adopt would be the type of analyses performed in TST and FST. Specifically in the FST, time spent struggling should be discriminated into swimming and climbing activities. At least one study demonstrated that optogenetic manipulations can alter the swimming and climbing time, but not alter the immobility time[179].

Tye and colleagues showed that photoinhibition of VTA DA neurons during TST decrease the time that mice spent struggling[114]. Although we did not directly modulate VTA DA neurons, we excited D1-MSNs that project to VP GABAergic and VTA GABAergic neurons that, in turn, target VTA DA neurons[34,63–70]. Since MSN stimulation leads to a decrease in neuronal activity of these GABAergic neurons, it is expected that DAergic activity in the VTA would increase. Our TST results did not show differences caused by stimulation, however, D1-VP-ChR2 and D1-VTA-ChR2 groups showed a tendency to increase the time that mice spent immobile, a feature of depressive-like behavior. Thus, our present results may be in line with the previous ones reported.

Since anhedonia is one of the most important symptoms of depression, we performed the SDT to measure this symptom. Our strategy to evaluate the alterations caused by stimulation of both MSN subtypes in the VP or VTA was to associate the stimulation to the familiar pellet. In that way, we intended

to increase the value of a reward that by itself presents a lower value than the sugar pellet. Stimulation of D2-MSN terminals in the VP was the only one that resulted in a decrease for sugar preference, which is translated into an anhedonic phenotype, however, the control group also presented such decrease in preference for sugar (**Figure 11d**). So, this anhedonic phenotype was not a result of the stimulation itself and may be related to changes in the environment of the behavioral apparatus that were not detected by the experimenter. Another way to assess anhedonia would be the sucrose preference test (SPT). Tye and co-workers implemented this behavioral procedure combined with optogenetics, showing differences in preference for sucrose caused by photoinhibition of VTA DA neurons[114]. However, this protocol had a duration of 90 minutes, divided in three alternating 30-minute epochs (OFF-ON-OFF), which may be a stimulation protocol too extensive.

In general, the control groups did not show differences across time, which was expected since the virus injected in these animals did not contain any opsin.

Notably, some issues were identified after all behavioral task assessments, namely the lack of sensitivity to perform tests divided in two sessions in a counterbalanced manner (specifically in the NSF and SDT). That way, external factors that could influence our results would be eliminated (e.g., different conditions in the *vivarium*, namely more noise, which could lead to higher levels of stress experienced by the mice).

Since some behavioral results are not completely clear, being more complicated to conclude about the influence of the optogenetic stimulation in anxiety- and depressive-like behavior, one possible alternative would be to use a different optogenetic experimental design. Although we used an experimental design previously validated[114,139,161], other studies used different optogenetic timelines, such as a higher number of alternating epochs[139,180], or three alternating epochs with a higher duration[180] (for example 5-minute epochs instead of 3-minute epochs). Switching the epoch presentation (ON-OFF-ON instead of OFF-ON-OFF that we used) could also help to understand the influence of optogenetic stimulation in the behavioral phenotype and exclude some biased results.

Neuronal correlates of optical stimulation

We also performed electrophysiological recordings in order to understand the impact of MSN terminal stimulation in downstream regions. Our data showed a general decrease in the activity of VP and VTA neurons with stimulation of both D1- and D2-MSN terminals (**Figure 13** and **Figure 14**), which is consistent with the release of GABA by these neurons.

With the D1-MSN stimulation protocol we used, it appears that we directly inhibit VTA GABAergic neurons (**Figure 14e'** and **e''**), being the DAergic neurons activated later. Important to refer, a study using optogenetic stimulation of D1-MSN terminals in the VTA during *ex vivo* whole-cell recordings showed that D1-MSNs target non-dopaminergic neurons of the VTA[181]. Moreover, Kupchik and colleagues showed a preferential innervation of VTA GABAergic neurons by D1-MSNs from the NAc core region[64]. However, Yang and co-workers showed that different NAc shell subregions can preferentially innervate either VTA GABAergic or DAergic neurons[34]. Since we observed a decrease in the activity of VTA pGABAergic neurons, it is possible that we stimulated D1-MSN terminals from both NAc core and shell subregions, leading to both increase and decrease in activity of the same neuronal population.

Optogenetic stimulation of both MSN subtype terminals in the VP led to a decrease in pGABAergic neuronal activity (**Figure 13e**, **e'**, **g** and **g'**), which is an expected result since GABA is an inhibitory neurotransmitter that causes a delayed action potential of the target neurons.

Not so expected were the results obtained in the NAc: stimulation of both MSN subtypes in the NAc led to a tendency to decrease the neuronal activity of MSNs and CINs (**Figure 12e'**, **e''**, **g'** and **g''**). Since channelrhodopsin led to a depolarization of the target neurons, it was expected to see an increase in neuronal activity of MSNs. Nonetheless, our electrophysiological approach does not allow us to specifically determine if the recorded neurons expressed ChR2 or not, so it is possible that the neurons recorded were not those that were stimulated. Thus, the decreased activity observed in these neurons could be due to lateral inhibition caused by stimulation of neighboring MSNs[185]. CINs receive inhibitory inputs from MSNs[93], which could be observed in our electrophysiological data. It is important refer that the number of neurons recorded in the NAc is low, being the percentage of MSNs recorded below of the known 95% of NAc population, so these results might be biased towards a non-representative population.

Previous studies have shown alterations in morphology of NAc MSNs in animals exposed to chronic stress. In fact, anhedonia induced by CMS was associated with dendritic hypertrophy and increased spine density of MSNs[186]. Furthermore, animals exposed to CSDS presented NAcs MSN spines with lower synaptic responses[187] and reduced levels of neuroligin 2 – an inhibitory synapse-specific protein – specifically in D1-MSNs[188].

Our electrophysiological data reveal some flaws that harden the interpretation of the results. In order to reduce the number of animals used, each mouse was submitted to a maximum of 5 recordings of 10 minutes each (2 recordings in the VP and VTA, in 2 different AP coordinates, and 1 recording in the NAc, being this performed always last), which could lead to a carry-over effect caused by consecutive stimulations. This stimulation overload might alter the basal activity of the cells, so the firing patterns

observed may not correspond specifically to modulation by optogenetic stimulation. The best solution would be to increase the number of animals used in order to perform only one recording per animal. However, it is important to bear in mind that this option would require a very high number of animals, which could be considered unethical.

Until now, several studies have shown impairments in the VTA activity in anxiety- and depressive-related disorders. For example, it has been reported a decrease in the VTA DAergic activity in animals exhibiting anxiety-like behaviors[68,114]. Besides that, a recent study showed that photoactivation of VTA GABAergic neurons induce anxiety-like behaviors in mice[158]. These could indicate that the reduction of the VTA DAergic activity may be mediated by VTA GABAergic lateral disinhibition[34,65]. Less concordant are the depressive-like studies showing that phasic activation of VTA DAergic neurons could increase the depressive-like phenotype in animals exposed to social defeat stress[117], or decrease this phenotype in animals exposed to chronic mild stress[114]. Previously, it was shown that chronic social defeat stress causes an increase in the firing rate of VTA DAergic neurons[116,127,172,173] and no change in the firing rate of VTA non-dopaminergic neurons, being these alterations specific for chronic social defeat[116]. Furthermore, D1-MSNs were found as predictors of depression, once their activity increased during a social interaction task performed in mice before exposure to a stress protocol[126]. Also, it is known that active avoidance leads to an increased activity of the NAc that is related to an increase in anxiety[133]. A recent study showed that optical stimulation of glutamatergic projections from the hippocampus to the NAc increase depressive-like behavior[189]. Furthermore, anhedonia and active coping were found to be associated with increased synaptic strength of ventral hippocampus excitatory synapses onto D1-MSNs in the NAc medial shell (NAcmSh)[190]. Thus, optogenetic activation of NAc should also increase depressive-like behavior. Our results showed an increase of the anxiety-like behavior caused by stimulation of D1-MSN terminals in the VTA, and a decrease in the firing rate of VTA pGABAergic neurons. These results can be explained by the preference of D1-MSNs to target GABAergic neurons of the VTA[181]. Since MSNs are GABAergic neurons, excitation of their terminals provokes inhibition of VTA GABAergic neurons. Regarding DAergic activity in this brain region, it would be expected an increase in their firing rate, since VTA DAergic neurons receive GABAergic projections from VP and VTA. Once we stimulated D1-MSN terminals that project to VTA GABAergic neurons, and we observed a decrease in the firing rate of these cells, DAergic neurons should increase their firing rate, as seen in a recent study from our team[74]. However, such observation was not replicated in the present study. Important to refer, the stimulation protocol used was not the same: in the present study we stimulated MSN terminals for 3 minutes, while in the study referred the stimulation

was performed in the MSN somas for 60 seconds. The hyperactivity of VTA DAergic neurons has been shown as a hallmark for depressive-like behavior[114,117,127,172], that might be caused by the decrease of VTA GABAergic neuronal activity, that was observed in our electrophysiological data. Thus, our electrophysiological data in VTA neurons may reflect a depressive-like phenotype caused by stimulation.

Furthermore, stimulation of both D1- and D2-MSN terminals in the VP or VTA caused an anxious-like phenotype that is in accordance with a study showing increased activity of the NAc in anxiety[133], since optogenetic activation of MSNs is translated into increased neuronal activity.

Regarding the involvement of the VP in anxiety and depression, as far as we know, no studies have been performed to dissect the role of MSN projections from NAc to this brain region, highlighting the importance of performing additional studies in order to understand the relevance of these projections for depressive-like behaviors.

Our results highlight the distinct roles of D1- and D2-MSNs in mental disorders, being urgent a detailed anatomical and electrophysiological characterization of NAc-to-VP and NAc-to-VTA neurons in this context. The major results obtained from this work are summarized in Table 2.

**Table 2.** Summary of the results obtained by assessment of anxiety- and depressive-like behaviors and *in vivo* electrophysiological recordings with stimulation of D1- and D2-MSN terminals in the VP, and stimulation of D1-MSN terminals in the VTA.
*= - no changes observed; ↑ - anxious- or depressive-like phenotype observed; ↓ - decrease in the neuronal activity observed*

| | Behavioral Test | D1-VP-ChR2 | D1-VTA-ChR2 | | D2-VP-ChR2 |
|---|---|---|---|---|---|
| Anxiety-like behavior | EPM | = | = | | ↑ |
| | Light/Dark Box | ↑ | ↑ | | = |
| | NSF | = | = | | ↑ |
| Depressive-like behavior | FST | ↑ | = | | = |
| | TST | = | = | | = |
| | SDT | = | = | | = |
| | | pGABAergic | pDAergic | pGABAergic | pGABAergic |
| | Neuronal Activity | ↓ | = | ↓ | ↓ |

# Chapter 6 – Conclusion

## 6. Conclusion

Increasing evidence has shown the involvement of brain regions of the reward circuit, namely the NAc, VP and VTA, in mood disorders like anxiety and depression. Herein, we showed that optical stimulation of D1- and D2-MSNs provokes different phenotypes in mice exposed to behavioral tasks used to assess anxiety- and depressive-like behaviors. In fact, optical stimulation of D1-MSNs-to-VP and D1-MSNs-to-VTA caused an anxious-phenotype, measured by light/dark box, and a depressive-phenotype, measured by FST and TST, respectively.

Optical stimulation of D2-MSNs-to-VP neurons induced an anxious-phenotype, measured by EPM, light/dark box and NSF; however, it has no impact on depressive-like behavior, although the hedonic component, measured by SDT, was altered. Neuronal activity in NAc, VP and VTA generally decreased during stimulation, being more prominent for GABAergic VP neurons receiving inputs from D2-MSNs.

Altogether, our results suggest distinct, but in some cases partially overlapping, roles for D1- and D2-MSNs in anxiety- and depressive-like behaviors.

# Chapter 7 – Future Perspectives

## 7. Future Perspectives

Further studies are needed to deepen the knowledge about the role of the direct and indirect pathways of the reward system in anxiety and depression disorders. It is crucial to repeat all the experimental design to confirm this data. Since these are preliminary results, further studies are necessary to better understand the differences between these pathways in anxious and depressive phenotypes. Furthermore, I believe it would be very interesting to replicate these studies using a group of animals in which we optically inhibit either MSN subtype using halorhodopsin (eNpHR). Also, a freely-moving electrophysiological setup combined with an optogenetic approach will be interesting to deepen the knowledge about the electrophysiological alterations caused by optogenetic stimulation of specific MSN subtypes and how these alterations influence the behavioral performance of the animals. Another asset could be the real-time measurement of dopamine release upon stimulation of NAc MSNs using fast-scan cyclic voltammetry (FSCV) combined with optogenetics[17].

# Chapter 8 – References

## 8. References


1. James, S. L. *et al.* Global, regional, and national incidence, prevalence, and years lived with disability for 354 diseases and injuries for 195 countries and territories, 1990–2017: a systematic analysis for the Global Burden of Disease Study 2017. *The Lancet* **392**, 1789–1858 (2018).

2. Association, A. P. *Diagnostic and Statistical Manual of Mental Disorders (DSM-5®)*. (American Psychiatric Pub, 2013).

3. Nestler, E. J. & Carlezon, W. A. The Mesolimbic Dopamine Reward Circuit in Depression. *Biol. Psychiatry* **59**, 1151–1159 (2006).

4. Bewernick, B. H. *et al.* Nucleus Accumbens Deep Brain Stimulation Decreases Ratings of Depression and Anxiety in Treatment-Resistant Depression. *Biol. Psychiatry* **67**, 110–116 (2010).

5. Satterthwaite, T. D. *et al.* Common and Dissociable Dysfunction of the Reward System in Bipolar and Unipolar Depression. *Neuropsychopharmacology* **40**, 2258–2268 (2015).

6. Smoski, M. J. *et al.* Decision-Making and Risk Aversion among Depressive Adults. *J. Behav. Ther. Exp. Psychiatry* **39**, 567–576 (2008).

7. Kelley, A. E. & Berridge, K. C. The Neuroscience of Natural Rewards: Relevance to Addictive Drugs. *J. Neurosci.* **22**, 3306–3311 (2002).

8. Wise, R. A. Dopamine, learning and motivation. *Nat. Rev. Neurosci.* **5**, 483–494 (2004).

9. Schultz, W. Multiple reward signals in the brain. *Nat. Rev. Neurosci.* **1**, 199–207 (2000).

10. Russo, S. J. & Nestler, E. J. The brain reward circuitry in mood disorders. *Nat. Rev. Neurosci.* **14**, 609–625 (2013).

11. Lammel, S., Ion, D. I., Roeper, J. & Malenka, R. C. Projection-specific modulation of dopamine neuron synapses by aversive and rewarding stimuli. *Neuron* **70**, 855–862 (2011).

12. Lammel, S. *et al.* Input-specific control of reward and aversion in the ventral tegmental area. *Nature* **491**, 212–217 (2012).

13. Lammel, S., Lim, B. K. & Malenka, R. C. Reward and aversion in a heterogeneous midbrain dopamine system. *Neuropharmacology* **76**, (2014).

14. Wise, R. A. & Rompre, P. P. Brain Dopamine and Reward. *Annu. Rev. Psychol.* **40**, 191–225 (1989).

15. Salamone, J. D. & Correa, M. THE MYSTERIOUS MOTIVATIONAL FUNCTIONS OF MESOLIMBIC DOPAMINE. *Neuron* **76**, 470–485 (2012).

16. Cagniard, B., Balsam, P. D., Brunner, D. & Zhuang, X. Mice with Chronically Elevated Dopamine Exhibit Enhanced Motivation, but not Learning, for a Food Reward. *Neuropsychopharmacology* **31**, 1362–1370 (2006).

17. Tsai, H.-C. *et al.* Phasic Firing in Dopaminergic Neurons Is Sufficient for Behavioral Conditioning. *Science* **324**, 1080–1084 (2009).

18. Schultz, W. Dopamine signals for reward value and risk: basic and recent data. *Behav. Brain Funct. BBF* **6**, 24 (2010).

19. Zahm, D. S. & Heimer, L. Two transpallidal pathways originating in the rat nucleus accumbens. *J. Comp. Neurol.* **302**, 437–446 (1990).

20. Zahm, D. S. & Brog, J. S. On the significance of subterritories in the "accumbens" part of the rat ventral striatum. *Neuroscience* **50**, 751–767 (1992).

21. Wright, C. I. & Groenewegen, H. J. Patterns of overlap and segregation between insular cortical, intermediodorsal thalamic and basal amygdaloid afferents in the nucleus accumbens of the rat. *Neuroscience* **73**, 359–373 (1996).

22. Voorn, P., Gerfen, C. R. & Groenewegen, H. J. Compartmental organization of the ventral striatum of the rat: Immunohistochemical distribution of enkephalin, substance P, dopamine, and calcium-binding protein. *J. Comp. Neurol.* **289**, 189–201 (1989).

23. Prensa, L., Richard, S. & Parent, A. Chemical anatomy of the human ventral striatum and adjacent basal forebrain structures. *J. Comp. Neurol.* **460**, 345–367 (2003).

24. Caboche, J., Vernier, P., Rogard, M. & Besson, M.-J. Haloperidol increases PPE mRNA levels in the caudal part of the nucleus accumbens in the rat: *NeuroReport* **4**, 551–554 (1993).

25. Churchill, L. *et al.* Patterns of glucose use after bicuculline-induced convulsions in relationship to γ-aminobutyric acid and μ-opioid receptors in the ventral pallidum — functional markers for the ventral pallidum. *Brain Res.* **581**, 39–45 (1992).

26. Deutch, A. Y. & Cameron, D. S. Pharmacological characterization of dopamine systems in the nucleus accumbens core and shell. *Neuroscience* **46**, 49–56 (1992).

27. Patel, S., Roberts, J., Moorman, J. & Reavill, C. Localization of serotonin-4 receptors in the striatonigral pathway in rat brain. *Neuroscience* **69**, 1159–1167 (1995).

28. Deutch, A. Y., Lee, M. C. & Iadarola, M. J. Regionally specific effects of atypical antipsychotic drugs on striatal Fos expression: The nucleus accumbens shell as a locus of antipsychotic action. *Mol. Cell. Neurosci.* **3**, 332–341 (1992).

29. Semba, J. Differential effects of acute and chronic treatment with typical and atypical neuroleptics on c-fos mRNA expression in rat forebrain regions using non-radioactive in situ hybridization. *Neurochem. Int.* **34**, 269–277 (1999).

30. Pinna, A. Differential Induction of Fos-Like-Immunoreactivity in the Extended Amygdala after Haloperidol and Clozapine. *Neuropsychopharmacology* **21**, 93–100 (1999).

31. Oka, T. *et al.* Atypical properties of several classes of antipsychotic drugs on the basis of differential induction of Fos-like immunoreactivity in the rat brain. *Life Sci.* **76**, 225–237 (2004).

32. Natesan, S., Reckless, G. E., Nobrega, J. N., Fletcher, P. J. & Kapur, S. Dissociation between In Vivo Occupancy and Functional Antagonism of Dopamine D2 Receptors: Comparing Aripiprazole to Other Antipsychotics in Animal Models. *Neuropsychopharmacology* **31**, 1854–1863 (2006).

33. Mogenson, G., Jones, D. & Yim, C. From motivation to action: Functional interface between the limbic system and the motor system. *Prog. Neurobiol.* **14**, 69–97 (1980).

34. Yang, H. *et al.* Nucleus accumbens subnuclei regulate motivated behavior via direct inhibition and disinhibition of VTA dopamine subpopulations. *Neuron* **97**, 434-449.e4 (2018).

35. Maldonado-Irizarry, C. S. & Kelley, A. E. Excitatory amino acid receptors within nucleus accumbens subregions differentially mediate spatial learning in the rat: *Behav. Pharmacol.* **6**, 527???539 (1995).

36. Parkinson, J. A., Olmstead, M. C., Burns, L. H., Robbins, T. W. & Everitt, B. J. Dissociation in Effects of Lesions of the Nucleus Accumbens Core and Shell on Appetitive Pavlovian Approach Behavior and the Potentiation of Conditioned Reinforcement and Locomotor Activity byd-Amphetamine. *J. Neurosci.* **19**, 2401–2411 (1999).

37. Corbit, L. H., Muir, J. L. & Balleine, B. W. The Role of the Nucleus Accumbens in Instrumental Conditioning: Evidence of a Functional Dissociation between Accumbens Core and Shell. *J. Neurosci.* **21**, 3251–3260 (2001).

38. Parkinson, J. A., Willoughby, P. J., Robbins, T. W. & Everitt, B. J. Disconnection of the anterior cingulate cortex and nucleus accumbens core impairs Pavlovian approach behavior: Further evidence for limbic cortical–ventral striatopallidal systems. *Behav. Neurosci.* **114**, 42–63 (2000).

39. Hernandez, P. J., Sadeghian, K. & Kelley, A. E. Early consolidation of instrumental learning requires protein synthesis in the nucleus accumbens. *Nat. Neurosci.* **5**, 1327–1331 (2002).

40. Ito, R., Robbins, T. W. & Everitt, B. J. Differential control over cocaine-seeking behavior by nucleus accumbens core and shell. *Nat. Neurosci.* **7**, 389–397 (2004).

41. Cardinal, R. N. & Cheung, T. H. Nucleus accumbens core lesions retard instrumental learning and performance with delayed reinforcement in the rat. *BMC Neurosci.* **6**, 9 (2005).

42. Alderson, H. L., Parkinson, J. A., Robbins, T. W. & Everitt, B. J. The effects of excitotoxic lesions of the nucleus accumbens core or shell regions on intravenous heroin self-administration in rats. *Psychopharmacology (Berl.)* **153**, 455–463 (2001).

43. Bossert, J. M., Gray, S. M., Lu, L. & Shaham, Y. Activation of Group II Metabotropic Glutamate Receptors in the Nucleus Accumbens Shell Attenuates Context-Induced Relapse to Heroin Seeking. *Neuropsychopharmacology* **31**, 2197–2209 (2006).

44. Bossert, J. M., Poles, G. C., Wihbey, K. A., Koya, E. & Shaham, Y. Differential Effects of Blockade of Dopamine D1-Family Receptors in Nucleus Accumbens Core or Shell on Reinstatement of Heroin Seeking Induced by Contextual and Discrete Cues. *J. Neurosci.* **27**, 12655–12663 (2007).

45. van der Plasse, G., Schrama, R., van Seters, S. P., Vanderschuren, L. J. M. J. & Westenberg, H. G. M. Deep Brain Stimulation Reveals a Dissociation of Consummatory and Motivated Behaviour in the Medial and Lateral Nucleus Accumbens Shell of the Rat. *PLoS ONE* **7**, e33455 (2012).

46. Voorn, P., Vanderschuren, L. J. M. J., Groenewegen, H. J., Robbins, T. W. & Pennartz, C. M. A. Putting a spin on the dorsal–ventral divide of the striatum. *Trends Neurosci.* **27**, 468–474 (2004).

47. Lanciego, J. L. *et al.* Thalamic innervation of striatal and subthalamic neurons projecting to the rat entopeduncular nucleus. *Eur. J. Neurosci.* **19**, 1267–1277 (2004).

48. Yin, H. H. & Knowlton, B. J. The role of the basal ganglia in habit formation. *Nat. Rev. Neurosci.* **7**, 464–476 (2006).

49. Morgane, P., Galler, J. & Mokler, D. A review of systems and networks of the limbic forebrain/limbic midbrain. *Prog. Neurobiol.* **75**, 143–160 (2005).

50. Hnasko, T. S., Hjelmstad, G. O., Fields, H. L. & Edwards, R. H. Ventral Tegmental Area Glutamate Neurons: Electrophysiological Properties and Projections. *J. Neurosci.* **32**, 15076–15085 (2012).

51. Groenewegen, H. J., Room, P., Witter, M. P. & Lohman, A. H. M. Cortical afferents of the nucleus accumbens in the cat, studied with anterograde and retrograde transport techniques. *Neuroscience* **7**, 977–996 (1982).

52. Brog, J. S., Salyapongse, A., Deutch, A. Y. & Zahm, D. S. The patterns of afferent innervation of the core and shell in the 'Accumbens' part of the rat ventral striatum: Immunohistochemical detection of retrogradely transported fluoro-gold. *J. Comp. Neurol.* **338**, 255–278 (1993).

53. Bolam, J. P. *et al.* Group Report: Microcircuits, Molecules, and Motivated Behavior. in *Microcircuits: the interface between neurons and global brain function* (eds. Grillner, S. & Graybiel, A. M.) (Cambridge, MA: The MIT Press, 2006). doi:10.7551/mitpress/4596.003.0011.

54. Guzmán, J. N. *et al.* Dopaminergic Modulation of Axon Collaterals Interconnecting Spiny Neurons of the Rat Striatum. *J. Neurosci.* **23**, 8931–8940 (2003).

55. Heimer, L., Zahm, D. S., Churchill, L., Kalivas, P. W. & Wohltmann, C. Specificity in the projection patterns of accumbal core and shell in the rat. *Neuroscience* **41**, 89–125 (1991).

56. Lu, X.-Y., Behnam Ghasemzadeh, M. & Kalivas, P. W. Expression of D1 receptor, D2 receptor, substance P and enkephalin messenger RNAs in the neurons projecting from the nucleus accumbens. *Neuroscience* **82**, 767–780 (1997).

57. Zhou, L., Furuta, T. & Kaneko, T. Chemical organization of projection neurons in the rat accumbens nucleus and olfactory tubercle. *Neuroscience* **120**, 783–798 (2003).

58. Wolf, P., Olpe, H.-R., Avrith, D. & Haas, H. L. GABAergic inhibition of neurons in the ventral tegmental area. *Experientia* **34**, 73–74 (1978).

59. Swanson, L. W. & Cowan, W. M. A note on the connections and development of the nucleus accumbens. *Brain Res.* **92**, 324–330 (1975).

60. Conrad, L. C. A. & Pfaff, D. W. Autoradiographic tracing of nucleus accumbens efferents in the rat. *Brain Res.* **113**, 589–596 (1976).

61. Nauta, W. J. H., Smith, G. P., Faull, R. L. M. & Domesick, V. B. Efferent connections and nigral afferents of the nucleus accumbens septi in the rat. *Neuroscience* **3**, 385–401 (1978).

62. Zahm, D. S. & Heimer, L. Specificity in the efferent projections of the nucleus accumbens in the rat: Comparison of the rostral pole projection patterns with those of the core and shell. *J. Comp. Neurol.* **327**, 220–232 (1993).

63. Edwards, N. J. *et al.* Circuit specificity in the inhibitory architecture of the VTA regulates cocaine-induced behavior. *Nat. Neurosci.* **20**, 438–448 (2017).

64. Kupchik, Y. M. *et al.* Coding the direct/indirect pathways by D1 and D2 receptors is not valid for accumbens projections. *Nat. Neurosci.* **18**, 1230–1232 (2015).

65. Bocklisch, C. *et al.* Cocaine Disinhibits Dopamine Neurons by Potentiation of GABA Transmission in the Ventral Tegmental Area. *Science* **341**, 1521–1525 (2013).

66. Floresco, S. B., West, A. R., Ash, B., Moore, H. & Grace, A. A. Afferent modulation of dopamine neuron firing differentially regulates tonic and phasic dopamine transmission. *Nat. Neurosci.* **6**, 968–973 (2003).

67. Hjelmstad, G. O., Xia, Y., Margolis, E. B. & Fields, H. L. Opioid Modulation of Ventral Pallidal Afferents to Ventral Tegmental Area Neurons. *J. Neurosci.* **33**, 6454–6459 (2013).

68. Chang, C. & Grace, A. A. Amygdala-Ventral Pallidum Pathway Decreases Dopamine Activity After Chronic Mild Stress in Rats. *Biol. Psychiatry* **76**, 223–230 (2014).

69. Mahler, S. V. *et al.* Designer Receptors Show Role for Ventral Pallidum Input to Ventral Tegmental Area in Cocaine Seeking. *Nat. Neurosci.* **17**, 577–585 (2014).

70. Faget, L. *et al.* Afferent inputs to neurotransmitter-defined cell types in the ventral tegmental area. *Cell Rep.* **15**, 2796–2808 (2016).

71. Root, D. H., Melendez, R. I., Zaborszky, L. & Napier, T. C. The ventral pallidum: Subregion-specific functional anatomy and roles in motivated behaviors. *Prog. Neurobiol.* **130**, 29–70 (2015).

72. Gerfen, C. *et al.* D1 and D2 dopamine receptor-regulated gene expression of striatonigral and striatopallidal neurons. *Science* **250**, 1429–1432 (1990).

73. Pardo-Garcia, T. R. *et al.* Ventral Pallidum Is the Primary Target for Accumbens D1 Projections Driving Cocaine Seeking. *J. Neurosci.* **39**, 2041–2051 (2019).

74. Soares-Cunha, C. *et al.* Nucleus accumbens medium spiny neurons subtypes signal both reward and aversion. *Mol. Psychiatry* (2019) doi:10.1038/s41380-019-0484-3.

75. Robertson, G. S. & Jian, M. D1 and D2 dopamine receptors differentially increase fos-like immunoreactivity in accumbal projections to the ventral pallidum and midbrain. *Neuroscience* **64**, 1019–1034 (1995).

76. Knowland, D. *et al.* Distinct Ventral Pallidal Neural Populations Mediate Separate Symptoms of Depression. *Cell* **170**, 284-297.e18 (2017).

77. Graveland, G. A. & Difiglia, M. The frequency and distribution of medium-sized neurons with indented nuclei in the primate and rodent neostriatum. *Brain Res.* **327**, 307–311 (1985).

78. Berlanga, M. L. *et al.* Cholinergic interneurons of the nucleus accumbens and dorsal striatum are activated by the self-administration of cocaine. *Neuroscience* **120**, 1149–1156 (2003).

79. Tepper, J. M., Tecuapetla, F., Koós, T. & Ibáñez-Sandoval, O. Heterogeneity and Diversity of Striatal GABAergic Interneurons. *Front. Neuroanat.* **4**, (2010).

80. Schall, T. A., Wright, W. J. & Dong, Y. Nucleus accumbens fast-spiking interneurons in motivational and addictive behaviors. *Mol. Psychiatry* (2020) doi:10.1038/s41380-020-0683-y.

81. Ribeiro, E. A. *et al.* Viral labeling of neurons synaptically connected to nucleus accumbens somatostatin interneurons. *PLOS ONE* **14**, e0213476 (2019).

82. Pisansky, M. T. *et al.* Nucleus Accumbens Fast-Spiking Interneurons Constrain Impulsive Action. *Biol. Psychiatry* **86**, 836–847 (2019).

83. Vincent, S. R., Staines, W. A. & Fibiger, H. C. Histochemical demonstration of separate populations of somatostatin and cholinergic neurons in the rat striatum. *Neurosci. Lett.* **35**, 111–114 (1983).

84. Smith, Y. & Parent, A. Neuropeptide Y-immunoreactive neurons in the striatum of cat and monkey: Morphological characteristics, intrinsic organization and co-localization with somatostatin. *Brain Res.* **372**, 241–252 (1986).

85. Kawaguchi, Y., Wilson, C. J., Augood, S. J. & Emson, P. C. Striatal interneurones: chemical, physiological and morphological characterization. *Trends Neurosci.* **18**, 527–535 (1995).

86. Tepper, J. M. & Bolam, J. P. Functional diversity and specificity of neostriatal interneurons. *Curr. Opin. Neurol.* **14**, 8 (2004).

87. Tepper, J. M., Koós, T. & Wilson, C. J. GABAergic microcircuits in the neostriatum. *Trends Neurosci.* **27**, 662–669 (2004).

88. Tepper, J. M., Wilson, C. J. & Koós, T. Feedforward and feedback inhibition in neostriatal GABAergic spiny neurons. *Brain Res. Rev.* **58**, 272–281 (2008).

89. Rymar, V. V., Sasseville, R., Luk, K. C. & Sadikot, A. F. Neurogenesis and stereological morphometry of calretinin-immunoreactive GABAergic interneurons of the neostriatum. *J. Comp. Neurol.* **469**, 325–339 (2004).

90. Witten, I. B. *et al.* Cholinergic Interneurons Control Local Circuit Activity and Cocaine Conditioning. *Science* **330**, 1677–1681 (2010).

91. Threlfell, S. *et al.* Striatal Dopamine Release Is Triggered by Synchronized Activity in Cholinergic Interneurons. *Neuron* **75**, 58–64 (2012).

92. Cachope, R. *et al.* Selective activation of cholinergic interneurons enhances accumbal phasic dopamine release: setting the tone for reward processing. *Cell Rep.* **2**, 33–41 (2012).

93. Bolam, J. P. & Bennett, B. Microcircuitry of the neostriatum. in *Molecular and Cellular Mechanisms of Neostriatal Function* (eds. Ariano, M. & Surmeier, D.) 1–20 (Austin: RG Landes Company, 1995).

94. Soares-Cunha, C., Coimbra, B., Sousa, N. & Rodrigues, A. J. Reappraising striatal D1- and D2-neurons in reward and aversion. *Neurosci. Biobehav. Rev.* **68**, 370–386 (2016).

95. Lanciego, J. L., Luquin, N. & Obeso, J. A. Functional Neuroanatomy of the Basal Ganglia. *Cold Spring Harb. Perspect. Med.* **2**, (2012).

96. Kravitz, A. V. & Kreitzer, A. C. Striatal Mechanisms Underlying Movement, Reinforcement, and Punishment. *Physiol. Bethesda Md* **27**, (2012).

97. Kravitz, A. V., Tye, L. D. & Kreitzer, A. C. Distinct roles for direct and indirect pathway striatal neurons in reinforcement. *Nat. Neurosci.* **15**, 816–818 (2012).

98. Smith, R. J., Lobo, M. K., Spencer, S. & Kalivas, P. W. Cocaine-induced adaptations in D1 and D2 accumbens projection neurons (a dichotomy not necessarily synonymous with direct and indirect pathways). *Curr. Opin. Neurobiol.* **23**, 546–552 (2013).

99. Soares-Cunha, C. *et al.* Activation of D2 dopamine receptor-expressing neurons in the nucleus accumbens increases motivation. *Nat. Commun.* **7**, (2016).

100. Lobo, M. K. *et al.* Cell Type-Specific Loss of BDNF Signaling Mimics Optogenetic Control of Cocaine Reward. *Science* **330**, 385–390 (2010).

101. Chandra, R. *et al.* Optogenetic inhibition of D1R containing nucleus accumbens neurons alters cocaine-mediated regulation of Tiam1. *Front. Mol. Neurosci.* **6**, (2013).

102. Song, S. S. *et al.* Optogenetics reveals a role for accumbal medium spiny neurons expressing dopamine D2 receptors in cocaine-induced behavioral sensitization. *Front. Behav. Neurosci.* **8**, (2014).

103. Soares-Cunha, C. *et al.* Nucleus Accumbens Microcircuit Underlying D2-MSN-Driven Increase in Motivation. *eNeuro* **5**, 1–16 (2018).

104. Steinberg, E. E. *et al.* Positive Reinforcement Mediated by Midbrain Dopamine Neurons Requires D1 and D2 Receptor Activation in the Nucleus Accumbens. *PLoS ONE* **9**, e94771 (2014).

105. Cole, S. L., Robinson, M. J. F. & Berridge, K. C. Optogenetic self-stimulation in the nucleus accumbens: D1 reward versus D2 ambivalence. *PLoS ONE* **13**, (2018).

106. Boschen, S. L., Wietzikoski, E. C., Winn, P. & Cunha, C. D. The role of nucleus accumbens and dorsolateral striatal D2 receptors in active avoidance conditioning. *Neurobiol. Learn. Mem.* **96**, 254–262 (2011).

107. Wietzikoski, E. C. *et al.* Roles of D1-like dopamine receptors in the nucleus accumbens and dorsolateral striatum in conditioned avoidance responses. *Psychopharmacology (Berl.)* **219**, 159–169 (2012).

108. Manago, F., Castellano, C., Oliverio, A., Mele, A. & De Leonibus, E. Role of dopamine receptors subtypes, D1-like and D2-like, within the nucleus accumbens subregions, core and shell, on memory consolidation in the one-trial inhibitory avoidance task. *Learn. Mem.* **16**, 46–52 (2008).

109. Cannon, C. M., Scannell, C. A. & Palmiter, R. D. Mice lacking dopamine D1 receptors express normal lithium chloride-induced conditioned taste aversion for salt but not sucrose. *Eur. J. Neurosci.* **21**, 2600–2604 (2005).

110. Hikida, T. *et al.* Pathway-specific modulation of nucleus accumbens in reward and aversive behavior via selective transmitter receptors. *Proc. Natl. Acad. Sci. U. S. A.* **110**, 342–347 (2013).

111. Nestler, E. J. & Hyman, S. E. Animal Models of Neuropsychiatric Disorders. *Nat. Neurosci.* **13**, 1161–1169 (2010).

112. Mineur, Y. S., Belzung, C. & Crusio, W. E. Effects of unpredictable chronic mild stress on anxiety and depression-like behavior in mice. *Behav. Brain Res.* **175**, 43–50 (2006).

113. Knowland, D. & Lim, B. K. Circuit-based frameworks of depressive behaviors: The role of reward circuitry and beyond. *Pharmacol. Biochem. Behav.* **174**, 42–52 (2018).

114. Tye, K. M. *et al.* Dopamine neurons modulate neural encoding and expression of depression-related behaviour. *Nature* **493**, 537–541 (2012).

115. Berton, O. *et al.* Essential Role of BDNF in the Mesolimbic Dopamine Pathway in Social Defeat Stress. **311**, 5 (2006).

116. Krishnan, V. *et al.* Molecular Adaptations Underlying Susceptibility and Resistance to Social Defeat in Brain Reward Regions. *Cell* **131**, 391–404 (2007).

117. Chaudhury, D. *et al.* Rapid regulation of depression-related behaviours by control of midbrain dopamine neurons. *Nature* **493**, 532–536 (2012).

118. Lim, B. K., Huang, K. W., Grueter, B. A., Rothwell, P. E. & Malenka, R. C. Anhedonia requires MC4 receptor-mediated synaptic adaptations in nucleus accumbens. *Nature* **487**, 183–189 (2012).

119. Schlaepfer, T. E. *et al.* Deep Brain Stimulation to Reward Circuitry Alleviates Anhedonia in Refractory Major Depression. *Neuropsychopharmacology* **33**, 368–377 (2008).

120. Bewernick, B. H., Kayser, S., Sturm, V. & Schlaepfer, T. E. Long-Term Effects of Nucleus Accumbens Deep Brain Stimulation in Treatment-Resistant Depression: Evidence for Sustained Efficacy. *Neuropsychopharmacology* **37**, 1975–1985 (2012).

121. Peciña, M. *et al.* Striatal dopamine D2/3 receptor-mediated neurotransmission in major depression: Implications for anhedonia, anxiety and treatment response. *Eur. Neuropsychopharmacol.* **27**, 977–986 (2017).

122. Drevets, W. *et al.* A functional anatomical study of unipolar depression. *J. Neurosci.* **12**, 3628–3641 (1992).

123. Anacker, C. *et al.* Neuroanatomic Differences Associated With Stress Susceptibility and Resilience. *Biol. Psychiatry* **79**, 840–849 (2016).

124. Lobo, M. K. *et al.* ΔFosB Induction in Striatal Medium Spiny Neuron Subtypes in Response to Chronic Pharmacological, Emotional, and Optogenetic Stimuli. *J. Neurosci.* **33**, 18381–18395 (2013).

125. Francis, T. C. *et al.* Nucleus Accumbens Medium Spiny Neuron Subtypes Mediate Depression-Related Outcomes to Social Defeat Stress. *Biol. Psychiatry* **77**, 212–222 (2015).

126. Muir, J. *et al.* In Vivo Fiber Photometry Reveals Signature of Future Stress Susceptibility in Nucleus Accumbens. *Neuropsychopharmacology* **43**, 255–263 (2018).

127. Cao, J.-L. *et al.* Mesolimbic Dopamine Neurons in the Brain Reward Circuit Mediate Susceptibility to Social Defeat and Antidepressant Action. *J. Neurosci.* **30**, 16453–16458 (2010).

128. Zarrindast, M.-R. & Khakpai, F. The Modulatory Role of Dopamine in Anxiety-like Behavior. *Arch. Iran. Med.* **18**, 591–603 (2015).

129. Pêgo, J., Sousa, J., Almeida, O. & Sousa, N. Stress and the neuroendocrinology of anxiety disorders. in *Behavioral Neurobiology of Anxiety and Its Treatment* vol. 2 97–118 (Springer Berlin Heidelberg, 2009).

130. Shin, L. M. & Liberzon, I. The Neurocircuitry of Fear, Stress, and Anxiety Disorders. *Focus J. Lifelong Learn. Psychiatry* **9**, 24 (2011).

131. Lezak, K. R., Missig, G. & Carlezon Jr, W. A. Behavioral methods to study anxiety in rodents. *Dialogues Clin. Neurosci.* **19**, 181–191 (2017).

132. Krypotos, A.-M., Effting, M., Kindt, M. & Beckers, T. Avoidance learning: a review of theoretical models and recent developments. *Front. Behav. Neurosci.* **9**, (2015).

133. Levita, L., Hoskin, R. & Champi, S. Avoidance of harm and anxiety: A role for the nucleus accumbens. *NeuroImage* **62**, 189–198 (2012).

134. Durant, C., Christmas, D. & Nutt, D. The Pharmacology of Anxiety. in *Behavioral Neurobiology of Anxiety and Its Treatment* (eds. Stein, M. B. & Steckler, T.) vol. 2 303–330 (Springer Berlin Heidelberg, 2009).

135. Simon, P., Panissaud, C. & Constentin, J. Anxiogenic-like effects induced by stimulation of dopamine receptors. *Pharmacol. Biochem. Behav.* **45**, 685–690 (1993).

136. de la Mora, M. P., Gallegos-Cari, A., Arizmendi-García, Y., Marcellino, D. & Fuxe, K. Role of dopamine receptor mechanisms in the amygdaloid modulation of fear and anxiety: Structural and functional analysis. *Prog. Neurobiol.* **90**, 198–216 (2010).

137. Zweifel, L. S. *et al.* Activation of Dopamine Neurons is Critical for Aversive Conditioning and Prevention of Generalized Anxiety. *Nat. Neurosci.* **14**, 620–626 (2011).

138. Davis, M., Walker, D. L., Miles, L. & Grillon, C. Phasic vs Sustained Fear in Rats and Humans: Role of the Extended Amygdala in Fear vs Anxiety. *Neuropsychopharmacology* **35**, 105–135 (2010).

139. Kim, S.-Y. *et al.* Diverging neural pathways assemble a behavioural state from separable features in anxiety. *Nature* **496**, 219–223 (2013).

140. Jennings, J. H. *et al.* Distinct extended amygdala circuits for divergent motivational states. *Nature* **496**, 224–228 (2013).

141. Calhoon, G. G. & Tye, K. M. Resolving the neural circuits of anxiety. *Nat. Neurosci.* **18**, 1394–1404 (2015).

142. Clauss, J. A., Avery, S. N., Benningfield, M. M. & Blackford, J. U. Social anxiety is associated with BNST response to unpredictability. *Depress. Anxiety* **36**, 666–675 (2019).

143. Canteras, N. S., Resstel, L. B., Bertoglio, L. J., de Pádua Carobrez, A. & Guimarães, F. S. Neuroanatomy of Anxiety. in *Behavioral Neurobiology of Anxiety and Its Treatment* (eds. Stein, M. B. & Steckler, T.) vol. 2 77–96 (Springer Berlin Heidelberg, 2009).

144. Lim, L. W. *et al.* Electrical stimulation alleviates depressive-like behaviors of rats: investigation of brain targets and potential mechanisms. *Transl. Psychiatry* **5**, e535–e535 (2015).

145. Zarrindast, M.-R., Babapoor-Farrokhran, S., Babapoor-Farrokhran, S. & Rezayof, A. Involvement of opioidergic system of the ventral hippocampus, the nucleus accumbens or the central amygdala in anxiety-related behavior. *Life Sci.* **82**, 1175–1181 (2008).

146. Radke, A. K. & Gewirtz, J. C. Increased Dopamine Receptor Activity in the Nucleus Accumbens Shell Ameliorates Anxiety during Drug Withdrawal. *Neuropsychopharmacology* **37**, 2405–2415 (2012).

147. Nikolaus, S., Huston, J. P. & Hasenöhrl, R. U. Anxiolytic-like effects in rats produced by ventral pallidal injection of both N- and C-terminal fragments of substance P. *Neurosci. Lett.* **283**, 37–40 (2000).

148. Lüthi, A. & Lüscher, C. Pathological circuit function underlying addiction and anxiety disorders. *Nat. Neurosci.* **17**, 1635–1643 (2014).

149. Kessler, R. C., Chiu, W. T., Demler, O. & Walters, E. E. Prevalence, Severity, and Comorbidity of 12-Month DSM-IV Disorders in the National Comorbidity Survey Replication. *Arch. Gen. Psychiatry* **62**, 617 (2005).

150. Richey, J. A. *et al.* Spatiotemporal dissociation of brain activity underlying threat and reward in social anxiety disorder. *Soc. Cogn. Affect. Neurosci.* **12**, 81–94 (2016).

151. Kühn, S., Schubert, F. & Gallinat, J. Structural correlates of trait anxiety: Reduced thickness in medial orbitofrontal cortex accompanied by volume increase in nucleus accumbens. *J. Affect. Disord.* **134**, 315–319 (2011).

152. Günther, V. *et al.* Volumetric Associations Between Amygdala, Nucleus Accumbens, and Socially Anxious Tendencies in Healthy Women. *Neuroscience* **374**, 25–32 (2018).

153. Burkhouse, K. L. *et al.* Nucleus accumbens volume as a predictor of anxiety symptom improvement following CBT and SSRI treatment in two independent samples. *Neuropsychopharmacology* **45**, 561–569 (2020).

154. Hasenöhrl, R. U., Jentjens, O., De Souza Silva, M. A., Tomaz, C. & Huston, J. P. Anxiolytic-like action of neurokinin substance P administered systemically or into the nucleus basalis magnocellularis region. *Eur. J. Pharmacol.* **354**, 123–133 (1998).

155. Ollmann, T. *et al.* Anxiolytic effect of neurotensin microinjection into the ventral pallidum. *Behav. Brain Res.* **294**, 208–214 (2015).

156. Saga, Y. *et al.* Ventral Pallidum Encodes Contextual Information and Controls Aversive Behaviors. *Cereb. Cortex* bhw107 (2016) doi:10.1093/cercor/bhw107.

157. Small, K. M., Nunes, E., Hughley, S. & Addy, N. A. Ventral tegmental area muscarinic receptors modulate depression and anxiety-related behaviors in rats. *Neurosci. Lett.* **616**, 80–85 (2016).

158. Chen, L. *et al.* Ventral tegmental area GABAergic neurons induce anxiety-like behaviors and promote palatable food intake. *Neuropharmacology* **173**, 108114 (2020).

159. Carlson, J. M., DeDora, D. J., Greenberg, T., Proudfit, G. H. & Mujica-Parodi, L. R. Hyper-Reactive Human Ventral Tegmental Area and Aberrant Mesocorticolimbic Connectivity in Overgeneralization of Fear in Generalized Anxiety Disorder. *J. Neurosci.* **34**, 5855–5860 (2014).

160. G. Paxinos & K. B. J. Franklin. *The Mouse Brain in Stereotaxic Coordinates*. (Gulf Professional Publishing, 2004).

161. Felix-Ortiz, A. C. *et al.* BLA to vHPC Inputs Modulate Anxiety-Related Behaviors. *Neuron* **79**, 658–664 (2013).

162. Crawley, J. & Goodwin, F. K. Preliminary report of a simple animal behavior model for the anxiolytic effects of benzodiazepines. *Pharmacol. Biochem. Behav.* **13**, 167–170 (1980).

163. Can, A. *et al.* The Mouse Forced Swim Test. *J. Vis. Exp.* (2012) doi:10.3791/3638.

164. Mateus-Pinheiro, A. *et al.* The Sweet Drive Test: refining phenotypic characterization of anhedonic behavior in rodents. *Front. Behav. Neurosci.* **8**, (2014).

165. Benazzouz, A. *et al.* Effect of high-frequency stimulation of the subthalamic nucleus on the neuronal activities of the substantia nigra pars reticulata and ventrolateral nucleus of the thalamus in the rat. *Neuroscience* **99**, 289–295 (2000).

166. Jin, X., Tecuapetla, F. & Costa, R. M. Basal ganglia subcircuits distinctively encode the parsing and concatenation of action sequences. *Nat. Neurosci.* **17**, 423–430 (2014).

167. Richard, J. M., Ambroggi, F., Janak, P. H. & Fields, H. L. Ventral Pallidum Neurons Encode Incentive Value and Promote Cue-Elicited Instrumental Actions. *Neuron* **90**, 1165–1173 (2016).

168. Ungless, M. A. Uniform Inhibition of Dopamine Neurons in the Ventral Tegmental Area by Aversive Stimuli. *Science* **303**, 2040–2042 (2004).

169. Yizhar, O., Fenno, L. E., Davidson, T. J., Mogri, M. & Deisseroth, K. Optogenetics in Neural Systems. *Neuron* **71**, 9–34 (2011).

170. Lobo, M. K., Nestler, E. J. & Covington, H. E. Potential utility of optogenetics in the study of depression. *Biol. Psychiatry* **71**, 1068–1074 (2012).

171. Steinberg, E. E., Christoffel, D. J., Deisseroth, K. & Malenka, R. C. Illuminating circuitry relevant to psychiatric disorders with optogenetics. *Curr. Opin. Neurobiol.* **0**, 9–16 (2015).

172. Razzoli, M., Andreoli, M., Michielin, F., Quarta, D. & Sokal, D. M. Increased phasic activity of VTA dopamine neurons in mice 3 weeks after repeated social defeat. *Behav. Brain Res.* **218**, 253–257 (2011).

173. Friedman, A. K. *et al.* Enhancing Depression Mechanisms in Midbrain Dopamine Neurons Achieves Homeostatic Resilience. *Science* **344**, 313–319 (2014).

174. Lister, RichardG. The use of a plus-maze to measure anxiety in the mouse. *Psychopharmacology (Berl.)* **92**, (1987).

175. Bourin, M. & Hascoët, M. The mouse light/dark box test. *Eur. J. Pharmacol.* **463**, 55–65 (2003).

176. Samuels, B. A. & Hen, R. Novelty-Suppressed Feeding in the Mouse. in *Mood and Anxiety Related Phenotypes in Mice* (ed. Gould, T. D.) vol. 63 (Humana Press, 2011).

177. Gore, F. *et al.* Neural Representations of Unconditioned Stimuli in Basolateral Amygdala Mediate Innate and Learned Responses. *Cell* **162**, 134–145 (2015).

178. Castagné, V., Moser, P., Roux, S. & Porsolt, R. D. Rodent Models of Depression: Forced Swim and Tail Suspension Behavioral Despair Tests in Rats and Mice. *Curr. Protoc. Neurosci.* **55**, (2011).

179. Carreno, F. R. *et al.* Activation of a ventral hippocampus–medial prefrontal cortex pathway is both necessary and sufficient for an antidepressant response to ketamine. *Mol. Psychiatry* **21**, 1298–1308 (2016).

180. Tye, K. M. *et al.* Amygdala circuitry mediating reversible and bidirectional control of anxiety. *Nature* **471**, 358–362 (2011).

181. Xia, Y. *et al.* Nucleus Accumbens Medium Spiny Neurons Target Non-Dopaminergic Neurons in the Ventral Tegmental Area. *J. Neurosci.* **31**, 7811–7816 (2011).

182. Lee, K.-W. *et al.* Cocaine-induced dendritic spine formation in D1 and D2 dopamine receptor-containing medium spiny neurons in nucleus accumbens. *Proc. Natl. Acad. Sci.* **103**, 3399–3404 (2006).

183. Bertran-Gonzalez, J. *et al.* Opposing Patterns of Signaling Activation in Dopamine D1 and D2 Receptor-Expressing Striatal Neurons in Response to Cocaine and Haloperidol. *J. Neurosci.* **28**, 5671–5685 (2008).

184. Perreault, M. L. *et al.* The Dopamine D1-D2 Receptor Heteromer Localizes in Dynorphin/Enkephalin Neurons: INCREASED HIGH AFFINITY STATE FOLLOWING AMPHETAMINE AND IN SCHIZOPHRENIA. *J. Biol. Chem.* **285**, 36625–36634 (2010).

185. Kohnomi, S., Koshikawa, N. & Kobayashi, M. $D_2$-like dopamine receptors differentially regulate unitary IPSCs depending on presynaptic GABAergic neuron subtypes in rat nucleus accumbens shell. *J. Neurophysiol.* **107**, 692–703 (2012).

186. Bessa, J. M. *et al.* Stress-induced anhedonia is associated with hypertrophy of medium spiny neurons of the nucleus accumbens. *Transl. Psychiatry* **3**, e266 (2013).

187. Khibnik, L. A. *et al.* Stress and Cocaine Trigger Divergent and Cell Type-Specific Regulation of Synaptic Transmission at Single Spines in Nucleus Accumbens. *Biol. Psychiatry* **79**, 898–905 (2016).

188. Heshmati, M. *et al.* Cell-type-specific role for nucleus accumbens neuroligin-2 in depression and stress susceptibility. *Proc. Natl. Acad. Sci. U. S. A.* **115**, 1111–1116 (2018).

189. Bagot, R. C. *et al.* Ventral hippocampal afferents to the nucleus accumbens regulate susceptibility to depression. *Nat. Commun.* **6**, (2015).

190. Pignatelli, M. *et al.* Cooperative synaptic and intrinsic plasticity in a disynaptic limbic circuit drive stress-induced anhedonia and passive coping in mice. *Mol. Psychiatry* (2020) doi:10.1038/s41380-020-0686-8.